SYNTHESIS AND CHRACTERIZATION OF REPEATING SEQUENCE COPOLYMERS WITH ALKYLIDENE FLUORENE UNITS

by

Xiao Jin

Bachelor of Science, Anhui University, 2007

Master of Science, University of Pittsburgh, 2010

Submitted to the Graduate Faculty of

Arts and Sciences in partial fulfillment

of the requirements for the degree of

Master of Science in Chemistry

University of Pittsburgh

2010

UNIVERSITY OF PITTSBURGH

Department of Chemistry

This thesis was presented

by

Xiao Jin

It was defended on

December 10th, 2009

and approved by

Tara Meyer, Associate Professor, Department of Chemistry

Toby Chapman, Associate Professor, Department of Chemistry

Nathaniel Rosi, Assistant Professor, Department of Chemistry

Thesis Director: Tara Meyer, Associate Professor, Department of Chemistry

SYNTHESIS AND CHARACTERIZATION OF REPEATING SEQUENCE COPOLYMERS WITH ALKYLIDENE FLUORENE UNITS

Xiao Jin, M.S.

University of Pittsburgh, 2010

A series of repeating sequence copolymers with the general formula $[(AF)_x(CH_2)_4CH_2=CH_2(CH_2)_4]_n$ (AF = $(C_{10}H_{21})_2$-alkylidene fluorene; x = 1-6) were prepared by acyclic diene metathesis of preformed segmers. These well-defined polymers, which are soluble in common organic solvents, exhibited GPC molecular weights of 15.2 k to 55.6 k in THF and chloroform vs. polystyrene standards. Absorbance and emission wavelengths were relatively independent of the AF units per segmer. All segmers and polymers exhibit liquid crystalline behavior. Phase transitions for these polymers depend on sequence.

TABLE OF CONTENTS

LIST OF TABLES

LIST OF FIGURES

LIST OF SCHEMES

PREFACE

I would greatly thank my research supervisor, Dr. Meyer for accepting me into her group and giving me guidance on how to be a real scientist. From her I have learned how to think logically and solve research problems. My more than two years' research life in the Meyer group has been enjoyable and full of fun. It is an unforgetable time of my life.

I would also like to thank Ben Norris, Ryan Stayschich and Jian Li. They offered a lot help with teaching me how to use new instruments and synthesis. Talking with group members, including Ryan Weiss and Tianqi Pan made me feel that I am part of a big family not just a research group.

I would also thank my parents and fiancee for their support of my graduate study. I owe a lot to my fiancee for firmly supporting our fragile long distance love for three years.

LIST OF ABBREVIATIONS

RSCs	Repeating Sequence Copolymers
AF	Alkylidene Fluorene
M	Methylene groups
OLED	Organic Light Emitting Diode
PPV	poly (p-phenylene vinylene)
OFET	Organic Field Effect Transistor
MCLCPs	Main Chain Liquid Crystalline Polymers
ADMET	Acyclic Diene Metathesis
GPC	Gel Permeation Chromatography
LCD	Liquid Crystal Display
DSC	Differential Scanning Calorimetry
N-I	Nematic into Isotropic
POM	Polarized Optical Microscopy

1.0 INTRODUCTION

1.1 OVERVIEW AND RELATIONSHIP TO PREVIOUS WORK

Two complete series of dialkylfluorene-*co*-methylene repeating sequence copolymers (RSCs) with structures similar to the polymers synthesized and discussed in this work were previously prepared by former Meyer group members (James Copenhafer and Robert Walters).[1,2] These dialkylfluorene copolymers did not exhibit strongly correlated sequence-dependent liquid crystalline properties, as was originally postulated and desired.

The current work focuses on forming RSCs with alternative monomers that have an alkylidene fluorene structure (Figure 1) because we believe that these polymers will exhibit a superior correlation of liquid crystal phase formation and sequence.

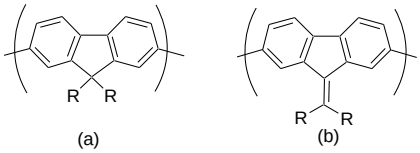

Figure 1. Chemical Structure of polyfluorene (a) and poly(alkylidene fluorene) (b) (where R = alkyl group).

1.2 ALKYLIDENE FLUORENES VS. DIALKYLFLUORENES

We have selected alkylidene fluorenes as component of a new series of alkylidene fluorenes because their structure is advantageous in comparison with dialkylfluorenes. Dialkylfluorenes have a sp^3-hybridized carbon at the 9-position, forcing the alkyl substituents to adopt orthorgonal disposition with respect to the aromatic system. This arrangement inhibits cofacial π-π stacking. Liquid crystalline phases formed in these systems arise primarily from the overlap of alkyl chains on adjacent "hairy rods" rather than from π stacking.[3,4] In contrast with dialkylfluorenes, alkylidene fluorenes have an sp^2-hybridized carbon at the 9-position, which should allow the alkyl chains to adopt a coplanar conformation relative to fluorene aromatic system. In support of this idea are the very small intermolecular distances that have been reported for the crystalline and liquid crystalline states of alkylidene fluorenes oligomers. The closeness of these interactions has been attributed to a cofacial, π–π stacking morphology.[4] Based on these observations, we hypothesized that alkylidene fluorene polymers would exhibit liquid crystalline properties that correlate more closely with sequence length than dialkylfluorene polymers and initiated the project of synthesizing alkylidene fluorene RSCs.

This report will focus on the synthesis of a new class of alkylidene fluorene RSCs (Figure 2) that have not yet been reported in the literature. The repeating sequence structure of these polymers was characterized by NMR spectroscopy and the photophysical properties and thermal properties were also investigated.

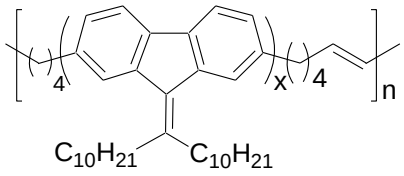

$P(AF)_XM_4=M_4$

Figure 2. General structure the alkylidene fluorene RSCs; (AF)x = alkylidene fluorene units and M = methylene groups.

1.3 SYNTHESIS CHALLENGES OF ALKYLIDENE FLUORENE OLIGOMERS

Synthesis of alkylidene fluorene-containing materials most frequently involves substitution at the 2-, 7-, and 9- positions. The numbering scheme for alkylidene fluorene is illustrate in Figure 3. Electrophilic aromatic substitution is most likely to occur at 2- and 7- positions. They are also often brominated or iodinated for further modification. Since the 9- and 10-positions, however, also react with nucleophiles and electrophiles, the use of the methodologies typically employed in the preparation of the more common dialkyl fluorene oligomers can be problematic.[5]

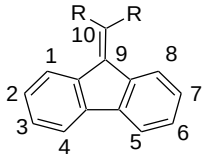

Figure 3. The numbering convention for alkylidene fluorene.

Since the ultimate synthetic objective of this project is to incorporate alkyl chains with terminal double bonds into the 2-, and 7-positions of preformed alkylidene fluorene oligomer units, with the objective of exploiting acyclic diene metathesis to produce repeating sequence copolymers, it is necessary to first synthesize fluorene oligomers with end groups, such as bromines, that are suitable for coupling to the olefin-terminated alkyl arm units. The most

relevant literature precedent for the synthesis of alkylidene fluorene oligomers of this type comes from Grisorio et al.[5] who succeeded in synthesizing the bis(boronate) oligo(fluorenylidene)s through Yamamoto[6] and Suzuki couplings. The disadvantages of this approach are modest yields of most oligo(alklidene fluorene)s and difficult separations. In addition, this approach does not address the exact control over the number of repeating units per oligomer. Therefore, the general synthetic methodology of Grisorio et al. was not employed. Instead we elected to develop an alternate route primarily based on Myaura-Suzuki couplings[7] to create well-defined alkylidene fluorene oligomers bearing substitutable bromines on the termini.

1.4 BACKGROUND: REPEATING SEQUENCE COPOLYMERS (RSCS)

The architecture of the alkylidene fluorene copolymers, whose synthesis and characterization are discussed herein, belong to a unique class of macromolecules known as repeating sequence copolymers (RSCs) (Figure 4). It is expected that the physical and photophysical properties of polymers can be better controlled than random polymers that are often made by changing the lengths of repeating units. The study of copolymers with exact lengths of repeating units is appealing methodology for designing polymers with desired properties and performance.[2]

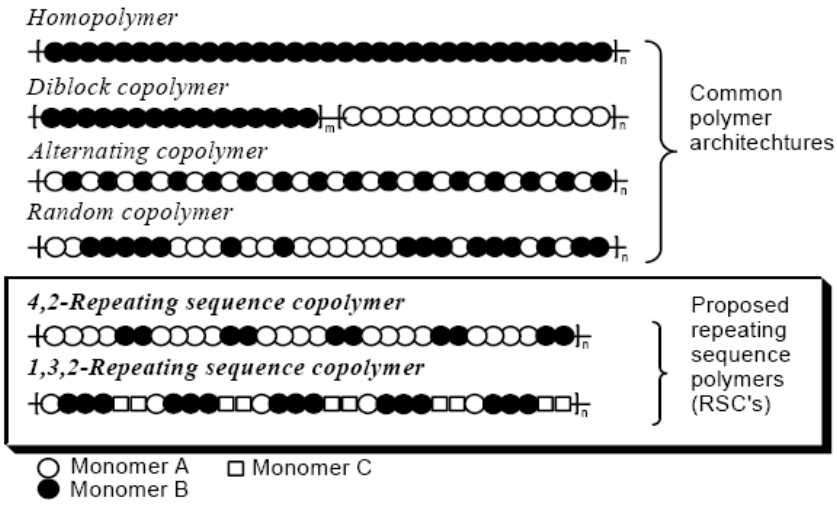

Figure 4. Examples of common architectures and comparison with the repeating sequence architecture.

1.5 ORGANIC ELECTRONICS AND LIGHT EMITTING DEVICES

Polyfluorenes have been shown to exhibit semiconductive and electron luminescence properties that enable them suitable for application in electronic and light emitting devices.[8,9] Poly(alkylidene fluorene)s, similar to poly(9,9-dialkylfluorene)s in that they exhibit semiconductive and luminescent properties, should also have potential application in organic light emitting devices (OLEDs).[4]

Organic electronics have attracted considerable attention from research groups. The attraction of this field has been the ability to modify chemical structure in ways that could directly influence the properties of the materials when deposited in thin film form. It is hoped that organic materials would ultimately have potential applications occupied by "traditional" semiconductors, but for a long time their ability and performance fell well short of those devices made from materials such as silicon or gallium arsenide.[10,11] The demonstration of efficient thin

film light emitting diode and a low voltage by Ching Tang and Steven Slyke[12,13] at Kodak changed the situation dramatically. Organic materials that are suitably modified are compatible with solution processing techniques, thereby eliminating the need for expensive lithography and vacuum deposition steps required for silicon based materials. The most successful application of organic thin film is the OLED, which is now employed in long-lived and highly efficient color displays. The first LED using conjugated polymer as emissive material were made in Cambridge 1989 using poly (p-phenylene vinylene) (PPV).[10]

Organic field effect transitors (OFETs) do not fall far behind OLEDs because of low cost and efficient solar cells. Alkylidene fluorenes have the potential for better performance than dialkyl fluorenes for some applications. Because the solid state polymers can only form two-dimensional lamellar structures to a limited extent, the out-of-plane conformation of substituents limited the charge-carrier mobility of the poly(9,9-dialkylfluorene)s, thereby impeding the intermolecular transport of the charge carriers and hence constricting the charge-carrier mobility. In order to bypass this constraint, Heeney et al. firstly synthesized and characterized poly(alkylidenefluorene)s with coplanar alkyl side chains. In OFETs, charge-carrier mobilities of up to 3×10^{-3} $cm^2V^{-1}s^{-1}$ at an on/off ratio of 10^6 were measured.[14,15]

1.6 LIQUID CRYSTALLINE POLYMERS

Liquid crystallinity is one of the properties that would be expected to respond strongly to changes in sequence in RSCs polymers. Many main chain liquid crystalline polymers (MCLCPs) have been reported to have interesting optical, thermal and physical properties. Mesogenic units, part of the backbone structure, can orient themselves into ordered phases that have both

properties of a liquid and a crystal, and such system are denoted main chain liquid crystal polymers. A template of MCLCPs is demonstrated in Figure 5, where red units represent mesogens and green lines indicate linking groups as spacers. The mesogenic monomer unit must be anisotropic and bifunctional to enable polymerization and generation of mesophases. Nematic and smectic liquid crystal phases have been found in MCLCPs. Rigid polymers, of different chain size, have difficulty packing in layer-like manner and so usually exhibit the nematic phase. However, polymers with flexible units between mesogenic moieties can easily arrange in a layer-like arrangement. The flexible spacer tends to play the same role as the terminal chains in low molar mass liquid crystals, and thus the longer the spacer units the greater the smectic tendency.[16]

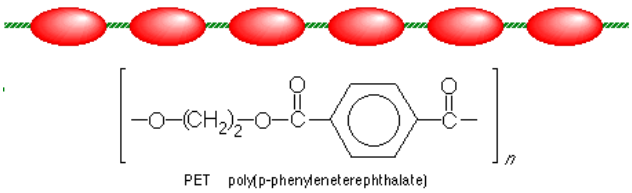

Figure 5. A general template for main chain liquid crystal polymers.

Figure 6 shows the three most common phases for liquid crystalline materials. As can been seen in Figure 6, the smectic A phase with only orientation in one direction has more order than nematic phase. Different phases of liquid crystalline polymers appear at different temperatures. Because of increasing disorder in the system, any crystal to smectic to nematic to isotropic phase transitions should appear at increasing temperatures.

Recently, the effects of spacer length and mesogen length on the formation of liquid crystalline phases have been reported by a previous member in Dr. Meyer group. Dr. Robert Walters, who studied RSCs of dialkylfluorene and methylene, demonstrated the nematic to isotropic transition temperature of RSCs increase as the length of mesogens, the dialkylfluorene

units, increases and a decrease in transition temperature as the length of spacer methylene groups increased.[2]

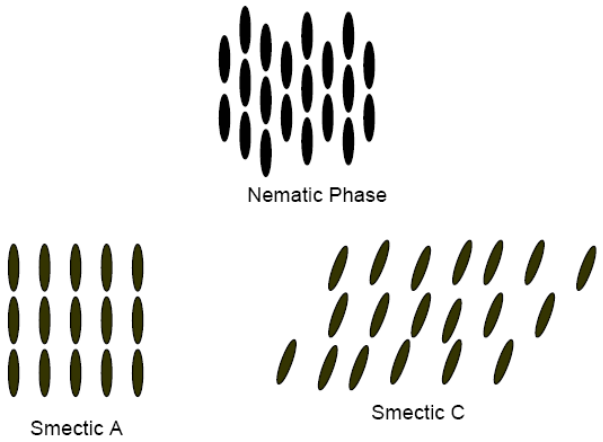

Figure 6. A visual representation of the alignment of mesogens in the three most common liquid crystalline phases.

2.0 RESULTS

2.1 NAMING CONVENTIONS

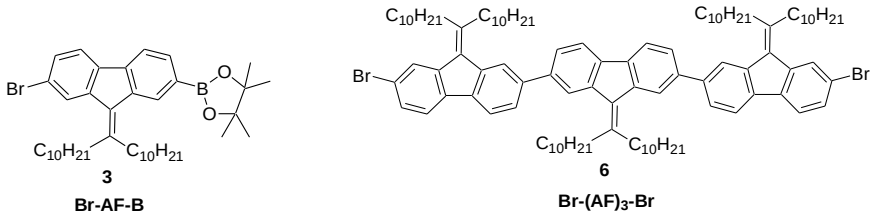

Figure 7. Examples of alkylidene fluorene units various substitution patterns provided to illustrate the naming convention.

Descriptive abbreviations for the intermediates, monomers, and final copolymers will be used throughout the whole thesis because of the complexity of the IUPAC names of such materials. Synthetic intermediates will be described by the number of alkylidene fluorene units and functional groups. For instance, the name **Br-(AF)$_3$-Br**, shown in Figure 7, indicates a tri-alkylidene fluorene unit with two bromines as end groups. For the name **Br-AF-B**, the Br represents a bromine group on the end of alkylidene fluorene unit, and the B indicates that the other end has one boronate functionality.

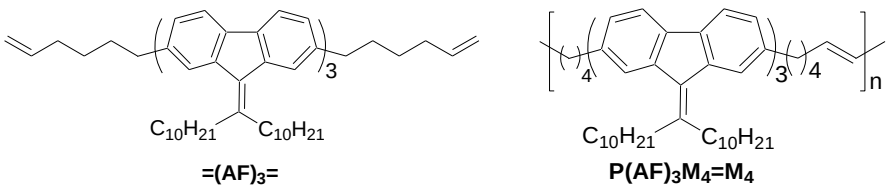

Figure 8. Structures of the tri-alkylidene fluorene monomer and polymers.

Monomers and polymers are represented by slightly different nomenclature (Figure 8). For example, =**(AF)$_3$=** represents a monomer with three alkylidene fluorene units and two, 6-carbon terminal alkene arms, while = indicates functionality of double bonds on the ends. This monomer is polymerized to yield the polymer **P(AF)$_3$M$_4$=M$_4$** using the ADMET[18-20] approach. "=" here indicates double bonds along the polymer chain, and M represents methylene group along the polymer backbone.

2.2 SYNTHETIC ROUTE

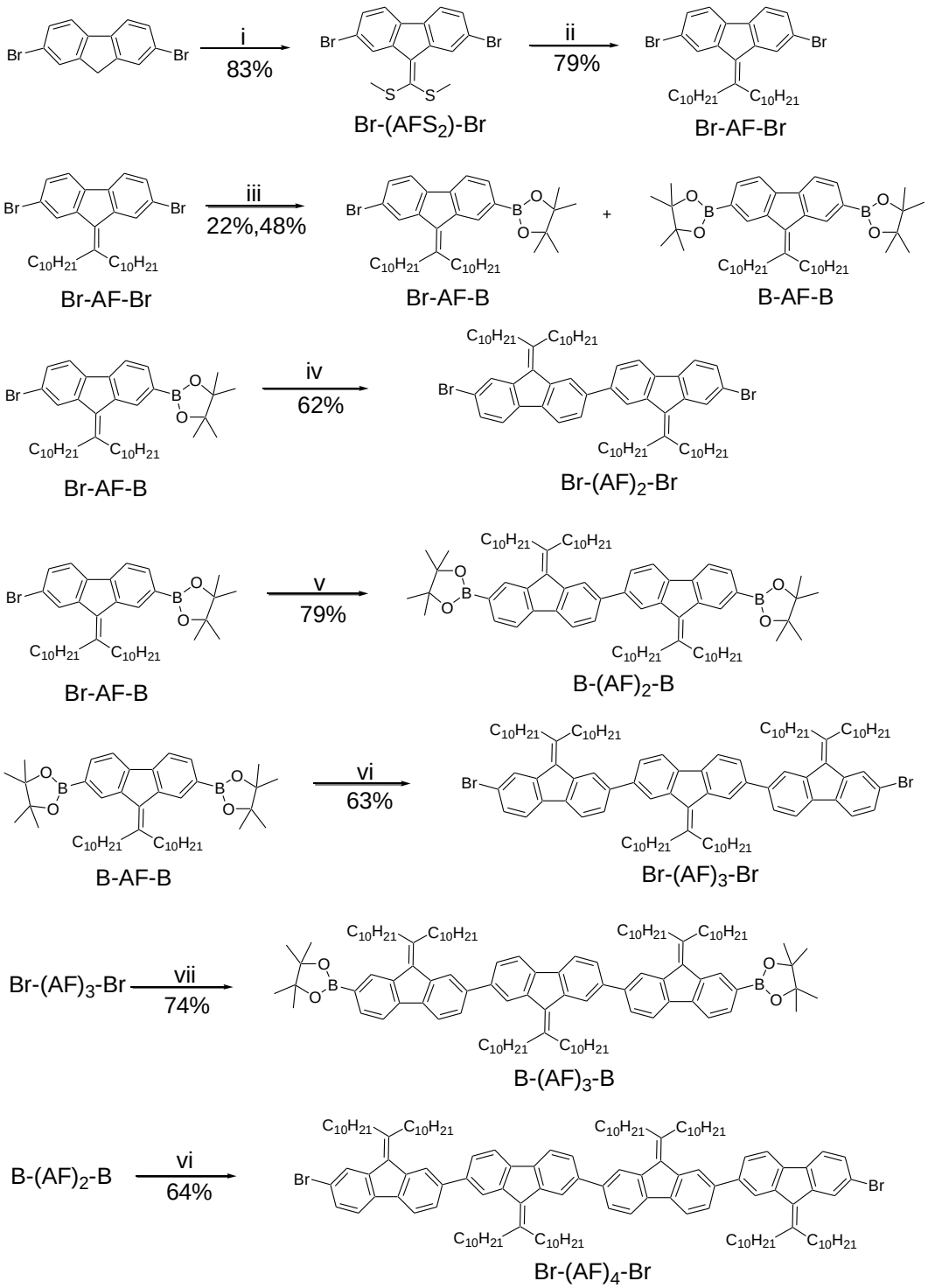

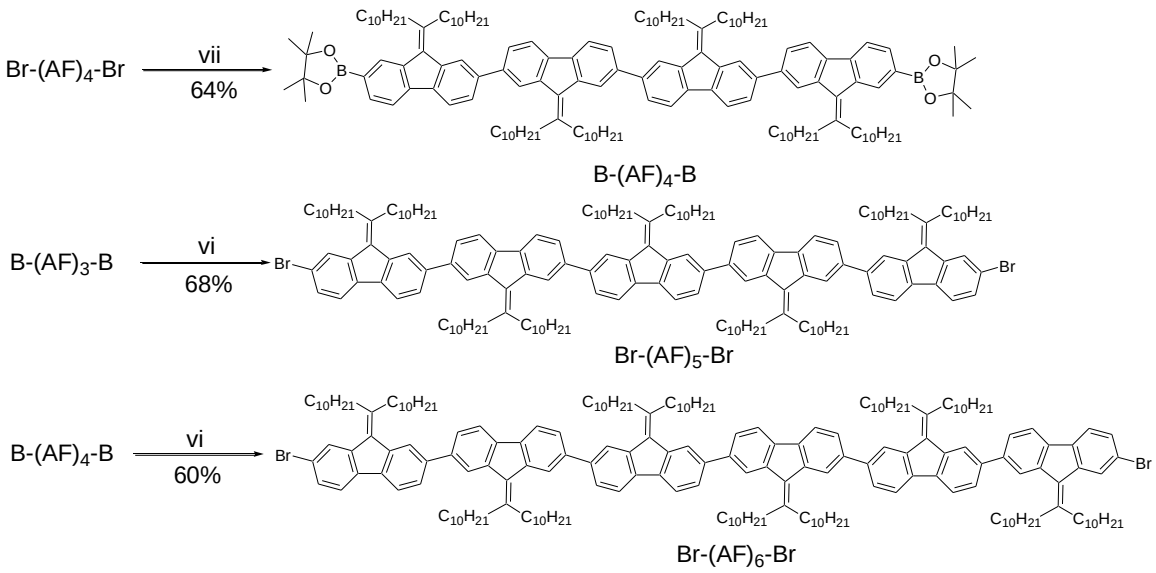

Scheme 1. Synthetic route of alkylidene fluorene oligomers and intermediates. (i) t-BuOK, CS_2, MeI, DMSO, rt; (ii) $LiCuCl_4$, $C_{10}H_{21}MgBr$, anhydrous ether; (iii) $PdCl_2$(dppf), bis(pinacolato) diboron, KOAc, 50 ℃; (iv) 2 equiv. Br-AF-Br, $Pd(PPh_3)_4$, K_2CO_3 (2M aqueous), toluene, ethanol; (v) $Ni(COD)_2$, 2,2'-bipyridine, COD, anhydrous toluene, 80 ℃; (vi) 4 equiv. Br-AF-Br, $Pd(PPh_3)_4$, K_2CO_3 (2M aqueous), toluene, ethanol; (vii) $PdCl_2$(dppf), bis(pinacolato) diboron, KOAc, 90 ℃

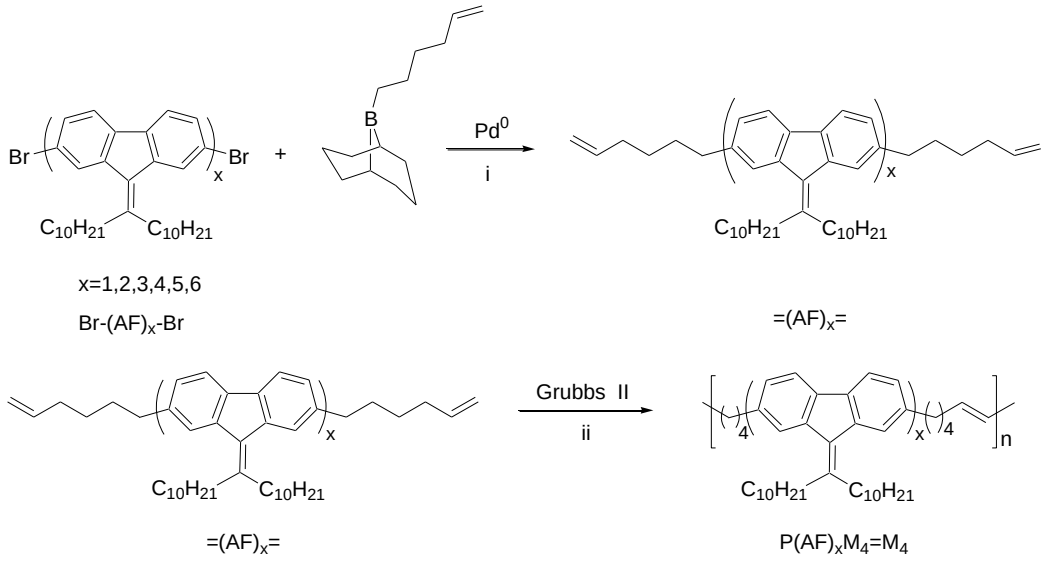

Scheme 2. Synthetic route to monomers and copolymers. (i) $PdCl_2(PPh_3)_4$, K_2CO_3 (2 M aqueous), THF, 45 ℃; (ii) Grubbs II, CH_2Cl_2, reflux.

2.3 SYNTHESIS OF ALKYLIDENE FLUORENE OLIGOMERS

The target alkylidene fluorene segmers were prepared through a convergent methodology, as outlined in Scheme I. We chose to use decyl alkyl chains to ensure good solubility of the segmers and polymers. **Br-AF-Br** was synthesized according to Heeney et al.'s procedure.[4] Starting from dibromofluorene, the initial step was the condensation of **Br-AF-Br** with carbon disulfide in the presence of potassium *tert*-butoxide, followed by a reaction with methyl iodide. The only difference in our preparation relative to Heeney's is that dimethylated thioacetal was not precipitated from cold water, because the dimethylated thioacetal precipitated directly from the reaction mixture. Hence, the product could simply isolated by filtration. In the subsequent step, the dimethylated thioacetal **Br-(AFS$_2$)-Br** was treated with 2 equiv of decylmagnesium bromide in the presence of a catalytic amount of Kuchi's salt to yield **Br-AF-Br** in a 79% yield. Using this approach we were able to produce the starting material on a 10 gram scale.

The oligomeric alkylidene fluorene units were assembled by the sequential coupling of monomers and dimers. To produce two key building blocks for this process, **Br-AF-Br** is first boronated by reaction with 2 equiv of bis(pinacolato)diboron. The reaction, which does not exhibit significant selectivity, produces both **Br-AF-B** and the diboronated alkylidene fluorene, **B-AF-B** in 22% and 48% yields, respectively. Since both are desired products and they can be easily separated by chromatography, no attempt was made to optimize the reaction for either single product.

The trimeric oligomer, **Br-(AF)$_3$-Br**, can be obtained through the Suzuki coupling of **B-AF-B** with **Br-AF-Br**, where the solvent system is a mixture of toluene and ethanol. To prevent polymerization, **Br-AF-Br** is used in a 4:1 excess over **B-AF-B**. The reaction proceeds to give the trimer in a 63% yield. Although **Br-AF-Br** is used in significant excess, the reaction still

gives a byproduct, which has more alkylidene fluorene units than the trimer. Fortunately, this material can be removed by column chromatography. Compared to boronation of **Br-AF-Br**, the boronation of the trimer is more difficult.

The tetramer, **Br-(AF)$_4$-Br**, is somewhat more challenging to prepare as it requires **Br-AF-B** as one of the starting materials. Despite many attempts we were unable to improve on the yield reported by Grisorio.[5] The yield for **Br-AF-B** is always modest, 45% at most, if it is produced separately from **B-AF-B**. Many factors were investigated to improve the yield, such as prolonging the reaction time and changing the amount of catalyst, base, and bis(pinacolato)diboron. The reaction always returns a large percent of the amount of starting material unreacted. These poor results are the reason behind our decision to exploit the reaction used to prepare **B-AF-B** to prepare both it and the mono-substituted by-product **Br-AF-B**. Although the yields for this reaction are still modest, 22% for **Br-AF-B**, the reaction is efficient in that two starting materials are produced simultaneously.

To produce the tetramer, **Br-AF-B** was subjected to Yamamoto coupling conditons[4] to yield **B-(AF)$_2$-B** in 79% yield. Instead of using the conventional solvent system, anhydrous toluene and DMF, for this Yamamoto coupling only anhydrous toluene is used to attain good solubility of **Br-AF-B**. **Br-(AF)$_4$-Br** is then obtained in 64% yield by the Suzuki coupling of **B-(AF)$_2$-B** with **Br-AF-Br** in a 1:4 ratio.

Both trimer and tetramer could be subsequently boronated to produce **B-(AF)$_3$-B** and **B-(AF)$_4$-B** in 74% and 64% yield, respectively. The reaction conditions for this step required a higher temperature (90 ℃) to guarantee diboronation than 50 ℃ used to produce both **Br-AF-B** and **B-AF-B**. To produce pentamer, **Br-(AF)$_5$-Br, B-(AF)$_3$-B** was reacted with 4 equiv of **Br-AF-Br** to give the 5-mer product in a 68% yield. The purification of **Br-(AF)$_5$-Br** is much easier

than that of **Br-(AF)$_3$-Br**, because there is no higher oligomeric by-product is formed in this reaction. **B-(AF)$_4$-B** was reacted with 4 equiv of **Br-AF-Br** to give the hexamer product, **Br-(AF)$_6$-Br,** in a 60% yield.

2.4 SYNTHESIS AND CHARACTERIZATION OF MONOMERS AND POLYMERS

The terminal olefin segmers, =**(AF)$_x$=** (x = 1-6), were conveniently prepared from the bis-bromo oligomers **Br-(AF)$_x$-Br** by Suzuki couplings with 9-hex-5-enyl-9-BBN (Scheme II). Yields ranged from 75% to 86%. This reaction is somewhat problematic in that it is difficult to separate the starting material, **Br-(AF)$_x$-Br**, from the mono-alkylated product or the dialkylated product =**(AF)$_x$=** by chromatography, because all have similar R_Fs. That being said, ^{13}C NMR data for the purified materials do not show significant contamination by mono-alkylated product (see discussion below).

The general synthetic approach to **P(AF)$_x$M$_4$=M$_4$** RSCs is also shown in Scheme II. The formation of **P(AF)$_x$M$_4$=M$_4$** with varying alkylidene fluorene oligomeric units was accomplished by ADMET polymerization of the bis terminal olefin monomers =**(AF)$_x$=**. This approach employed the methodology developed by Wagener el al.[17-19] and used Grubbs II as the catalyst and methylene chloride as the solvent system. The reaction was carried out in refluxing CH_2Cl_2. It was unnecessary to remove ethylene gas in the reaction, because Grubbs II is a very active catalyst. Ethyl vinyl ether was added to free catalyst from polymer chains. Polymers were purified by precipitation into cold methanol (3 x 30 mL). Originally, we planned to hydrogenate the ADMET-produced polymers, just as our group did with the dialkylfluorene copolymers.

However, we could not find out a selective way to hydrogenate double bond on the polymer chains while keeping double bonds on the alkylidene fluorene units.

Gel permeation chromatography (GPC) was employed to determine the relative molecular weights of the final copolymers using polystyrene standards for calibration. Molecular weights are summarized in Table 1. A typical GPC chromatograph of **P(AF)$_5$M$_4$=M$_4$** is shown in Figure 9. These copolymers have modest molecular weights (15.2 k to 55.6 k) and typically show polymodal character. The large segmer molecular weights mean that the degrees of polymerization for a given molecular weight are necessarily low. End group analysis by NMR spectroscopy did not prove useful. In spectra with resonances corresponding to end groups, the analysis by integration gave molecular weights greater than those determined by GPC for the same samples. As we would expect, based on the rigid-rod nature of the fluorene segments, that the GPC molecular weights would be greater than the actual values we hypothesize that cyclization is significant in these samples.

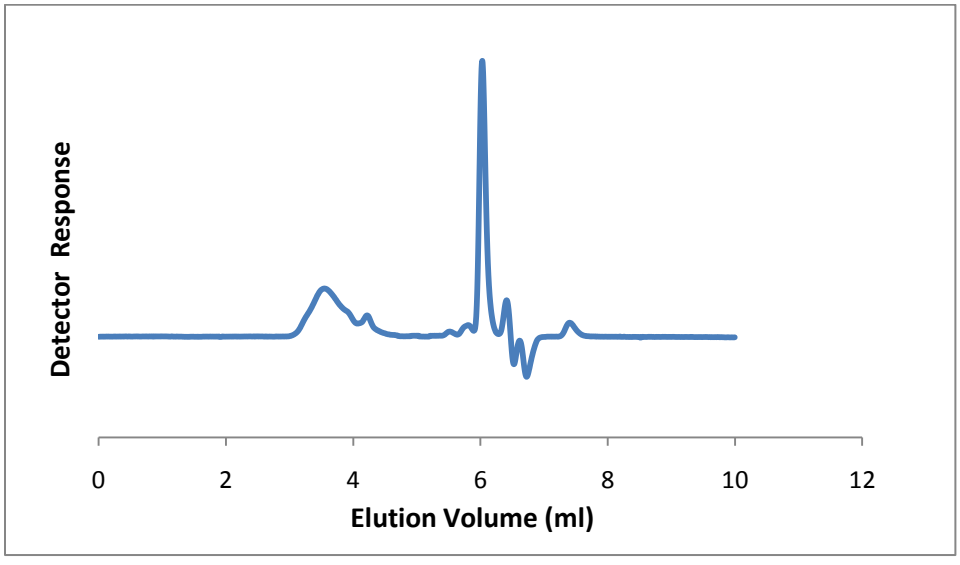

Figure 9. A typical GPC chromatograph of P(AF)5M4=M4 performed in THF at RT.

Table 1. Molecular weight data for the $P(AF)_xM_4=M_4$ series of RSCs.

Polymer	Mn[a] (kDa)	Mw[b] (kDa)	PDI[c]
$P(AF)_1M_4=M_4$	18.8	32.4	1.7 (Chloroform)
$P(AF)_2M_4=M_4$	16.7	27.0	1.6 (Chloroform)
$P(AF)_3M_4=M_4$	15.2	20.3	1.3 (THF)
$P(AF)_4M_4=M_4$	17.2	22.3	1.3 (THF)
	17.8	25.0	1.4 (Chloroform)
$P(AF)_5M_4=M_4$	24.6	33.0	1.3 (THF)
$P(AF)_6M_4=M_4$	55.6	65.6	1.2 (THF)

[a]The number of average molecular weight determined by GPC vs. polystyrene standards. [b]The weight average molecular weight determined by GPC vs. polystyrene standards. [c]Polydisperity M_w/M_n.

2.5 ^{1}H NMR AND ^{13}C NMR SPECTRAL CHARACTERIZATION OF SEGMERS AND POLYMERS

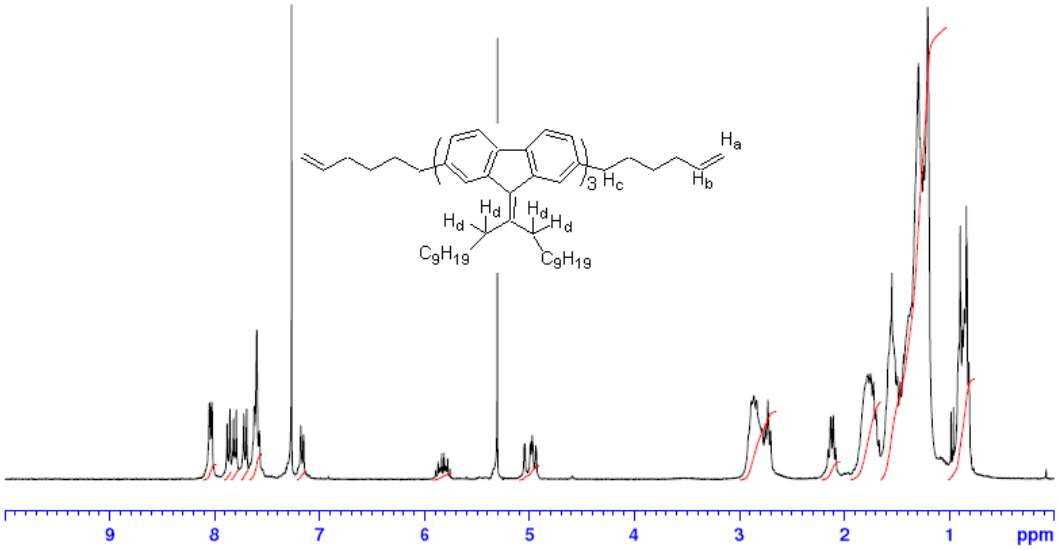

Figure 10. ^{1}H NMR spectrum of $=(AF)_3=$ ($CDCl_3$, 300 MHz).

Typical spectra for the trimeric segmer and polymer are shown in Figures 10 and 11. The protons of terminal double bonds (H_a and H_b) can be distinguished as multiplets at δ 4.98 and 5.7-5.9 ppm, respectively. The methylene groups (H_c) attached to the 2- and 7-positions of the terminal fluorenes can be observed as a triplet at δ 2.7 ppm that partially overlaps with the signal

for the methylene protons (H_d) of the alkyl chain attached the 9-position of the alkylidene fluorene. The signals in the complex aryl region from δ 7.15 to 8.05 ppm integrated with respect to the alkyl signals in ratios consistent with the proposed structure.

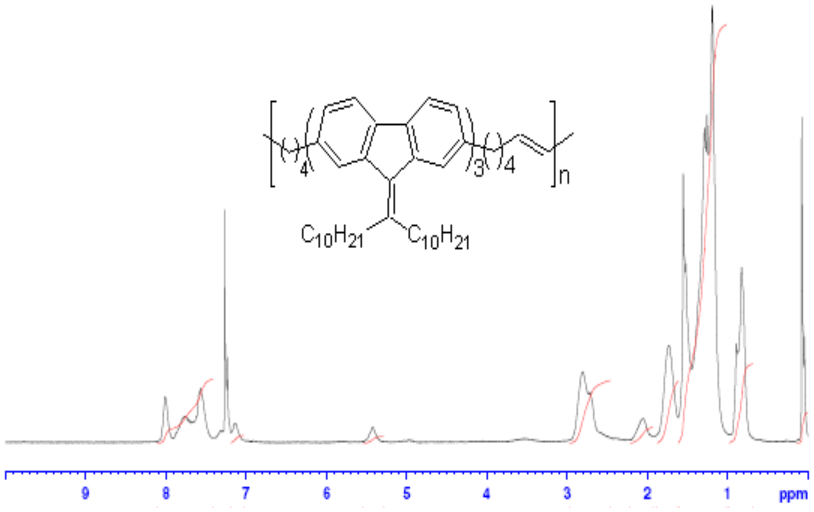

Figure 11. ^{1}H NMR spectrum of P(AF)$_3$M$_4$=M$_4$ (CDCl$_3$, 300 MHz).

The Suzuki coupling to produce copolymers was monitored by observation of the disappearance of signals for terminal double bonds and formation of new double bonds along polymer chain with significant chemical shift in ^{1}H NMR spectrum. The polymerization was terminated when signals for the termial oflefins centered at δ 5.0 and 5.8 ppm were replaced by those of the polymer's internal olefin at δ 5.4 ppm (a mixture of *cis/trans* in which *trans* predominates). The ratios are still consistent with the structure proposed.[1]

2.6 ^{13}C NMR STUDY TO DETERMINE PURITY OF MONOMERS

It is well known that impurities in monomers that terminate the metathesis polymerization may lead to the low degrees of polymerization. Mono-functional monomers were seen as a

particularly likely source of the relatively low molecular weights of the polymers that we isolated. These mono-functional species could be produced either by 1) accidental reduction of bromine end group 2) incomplete substitution of the dibromide with the olefin-terminated arms 3) reduction and/or isomerization of the olefin end groups. The problem is made worse by the relative difficulty of chromatographic separation of these mono-functional monomers from the desired difunctional ones. The low MWs could also be a result of incomplete reaction of the monomers.

To determine whether contamination by starting material and mono-alkylated by-product were significant problems, we examined the ^{13}C NMR spectra. The key in this approach was the identification of the signal for the carbon bearing a bromine terminus. In the spectrum of **Br-AF-Br** (Figure 12), by comparison with starting materials and related molecules we assign key carbons as follows: C-A and C-B at δ 120.44 and 121.15 ppm, C-C at δ 155.14 ppm, and peak C-D at δ 129.81 ppm.

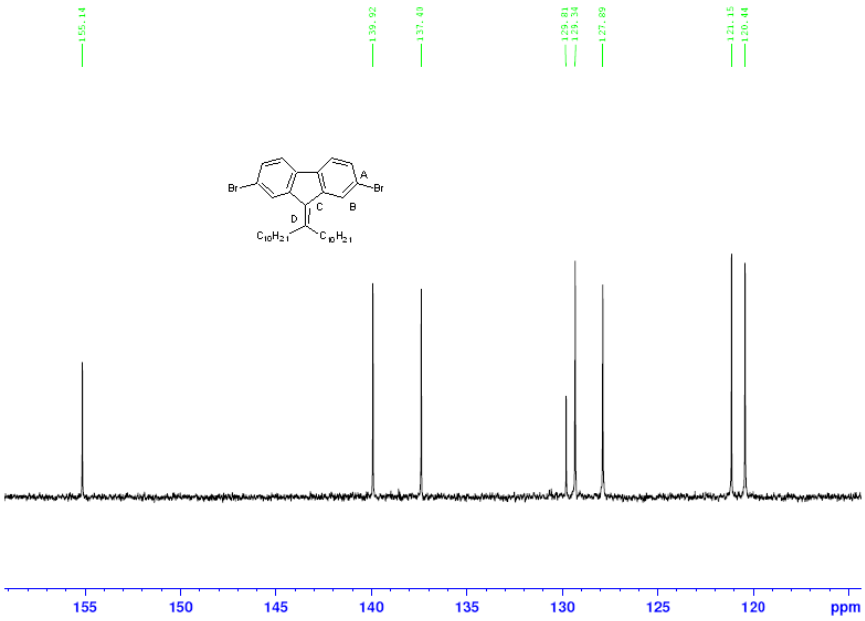

Figure 12. ^{13}C NMR spectrum of Br-AF-Br ($CDCl_3$, 75 MHz).

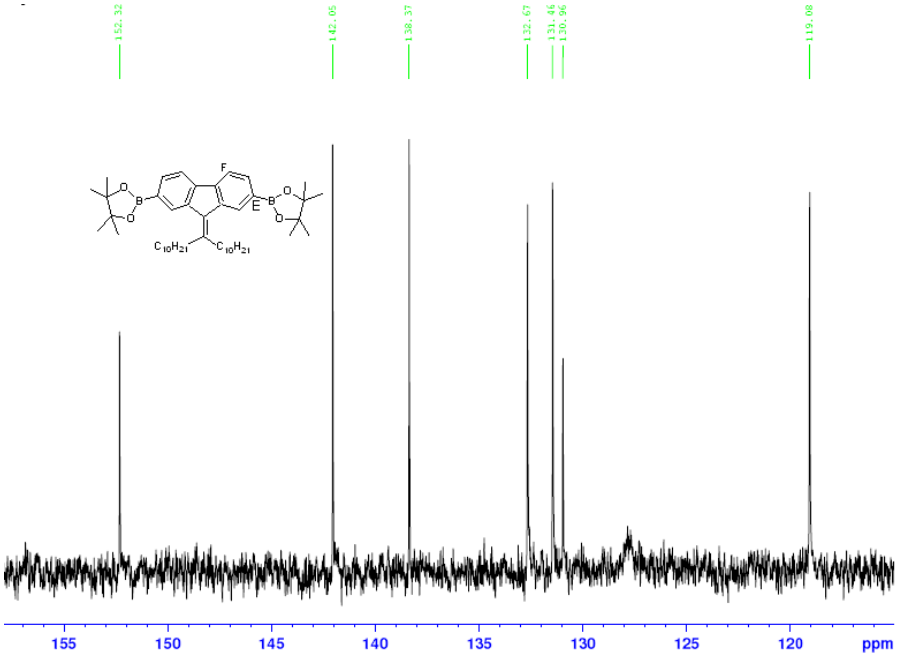

Figure 13. ^{13}C NMR spectrum of B-AF-B ($CDCl_3$, 75 MHz).

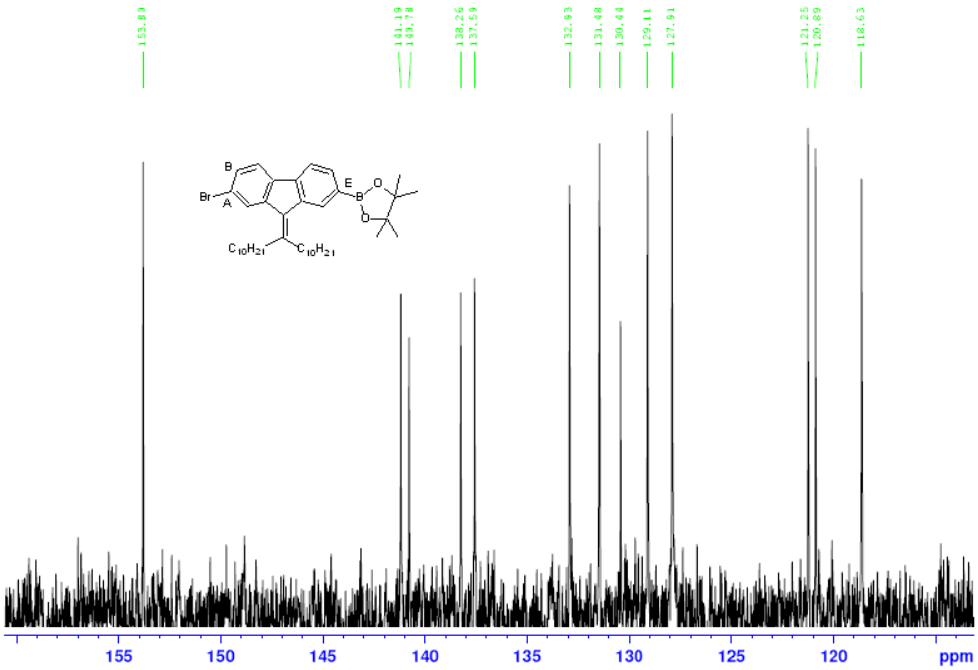

Figure 14. ^{13}C NMR spectrum of Br-AF-B ($CDCl_3$, 75 MHz).

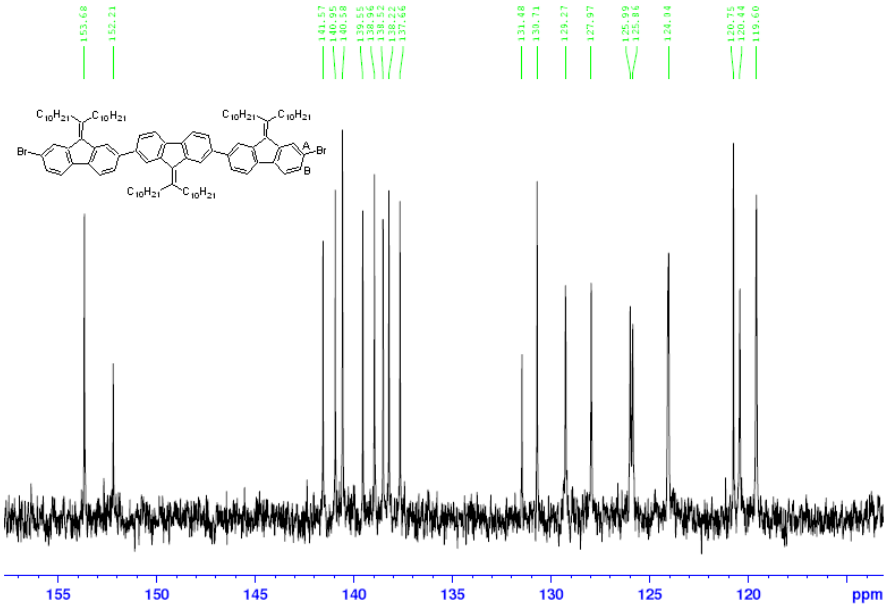

Figure 15. ^{13}C NMR spectrum of Br-(AF)$_3$-Br ($CDCl_3$, 75 MHz).

After **Br-AF-Br** is diboronated to produce **B-AF-B**, the spectrum of **B-AF-B** (Figure 13) no longer contains the signals identified as corresponding to carbon bearing the bromo substituent, C-A, nor the adjacent C-B carbon. This absence confirms that signals above δ 120 correspond to the presence of a terminal bromo group. Based on this analysis, the peak at δ 119.08 in the spectrum of **B-AF-B** must correspond to the presence of the terminal boronate.

The mono-brominated alkylidene fluorene, **Br-AF-B**, is electronically different from either of the symmetric species. Hence, the C-A and C-B signals associated with the terminal bromo group are slightly shifted from those of **Br-AF-Br**. Nonetheless, Figure 14 shows that the carbon, C-A, bearing the Br and C-B are clearly distinguishable as two very close peaks at δ 121.25 and 120.89 ppm. The peak at δ 118.63 can also be assigned as the boronate-bearing C-E.

Based on the analysis of these spectra, the conclusion can be reached that the fluorene-alkylidene unit bearing a terminal bromine in will exhibit two resonances slightly above δ 120

ppm, which is also confirmed by spectrum of **Br-(AF)$_3$-Br** (Figure 15). This dibromo trimer exhibits peaks at δ 120.75 and 120.44 ppm that correspond to C-A and C-B.

Using this information, we examined the ^{13}C NMR spectra for all monomers. We could not, however, see evidence for terminal bromines (to the limits of detection permitted by NMR). Hence this possible explanation for the low molecular weight could be eliminated.

For the possibility of accidental reduction of the terminal bromine group, we cannot find any direct evidence to prove it. But very small peaks appear in the aryl region on the ^{13}C NMR spectra of all monomers. So it is possible that accidental reduction (or other contamination) may be a contributing cause to the low molecular weight of the polymers.

The possibility of reduction or isomerization of the alkene groups on the segmers can be ruled out by examining the ^{1}H NMR spectra of monomers. New peaks will form in the ^{1}H NMR spectrum if terminal double bonds are reduced or isomerized. Since no such peak are visible, this explanation seems unlikely.

2.7 PHTOPHYSICAL PROPERTIES

2.7.1 UV-VIS Absorption Spectra

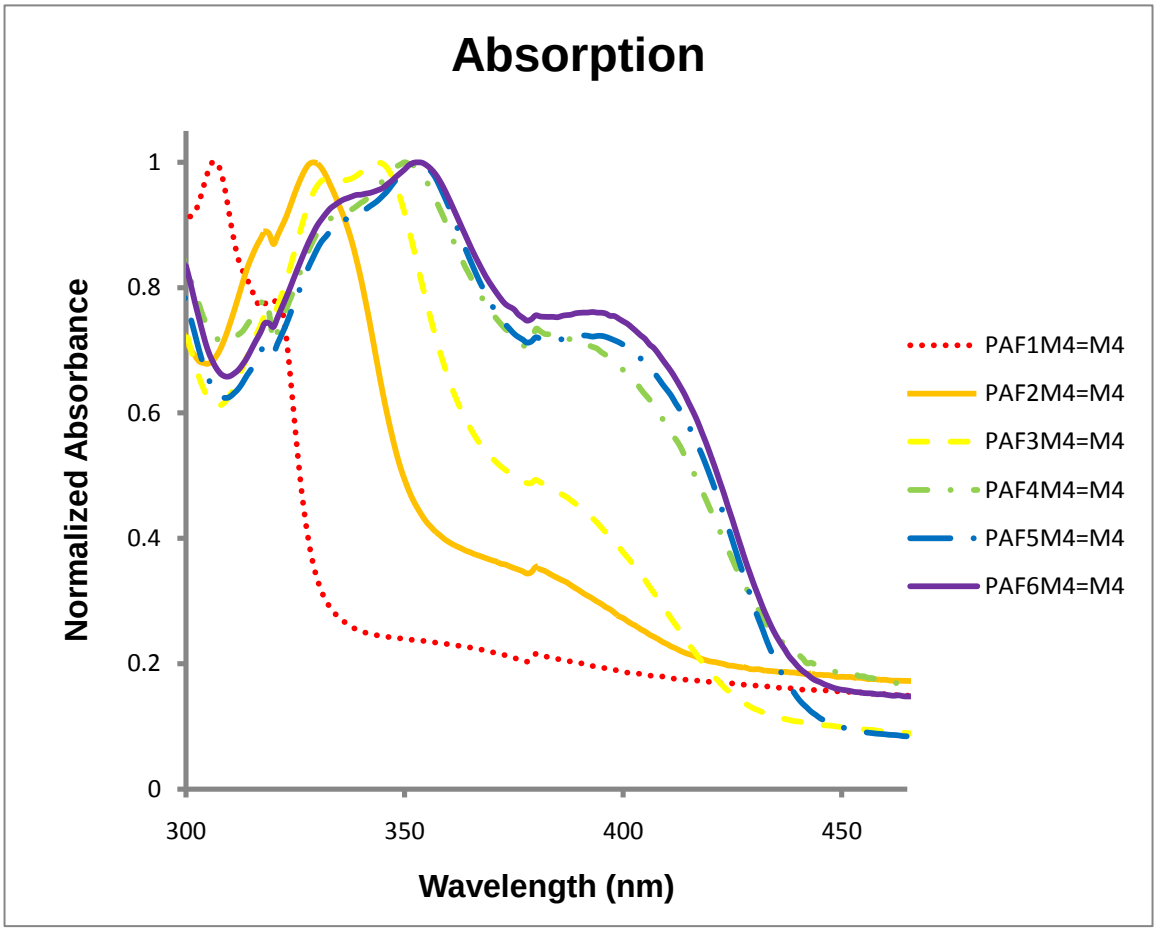

Figure 16. Normalized absorption spectra of $P(AF)_xM_4$=M_4 series of polymers at ~ 10^{-6} M in $CHCl_3$.

The absorption spectra of the **$P(AF)_xM_4$=M_4** series exhibited the expected trend of decreasing energy for the absorption maximum with increasing alkylidene fluorene units. Figure 16 shows the normalized absorption spectra and Table 2 lists the absorption maximums of polymers in $CHCl_3$. The shape of the absorption spectra, which exhibits a characteristic absorption at 300 nm to 353 nm and a shoulder at 350 nm to 400 nm, matches that previously reported in the literature for alkylidene fluorene oligomers by Grisorio and coworkers.[3]

Table 2. The absorption and emission maxima for $P(AF)_xM_4=M_4$ series.

Polymer	Absorption[a] Max (nm)	Emission[b] Max (nm)
$P(AF)_1M_4=M_4$	306	472
$P(AF)_2M_4=M_4$	329	465
$P(AF)_3M_4=M_4$	343	454
$P(AF)_4$ $M_4=M_4$	350	466
$P(AF)_5$ $M_4=M_4$	353	465
$P(AF)_6M_4=M_4$	353	465

[a]Absorption maximum measured in dilute $CHCl_3$ solution (~ 10^{-6} M). [b]The solution emission maximum measured in dilute $CHCl_3$ solution (~ 10^{-6} M).

2.7.2 UV-VIS Emission Spectra

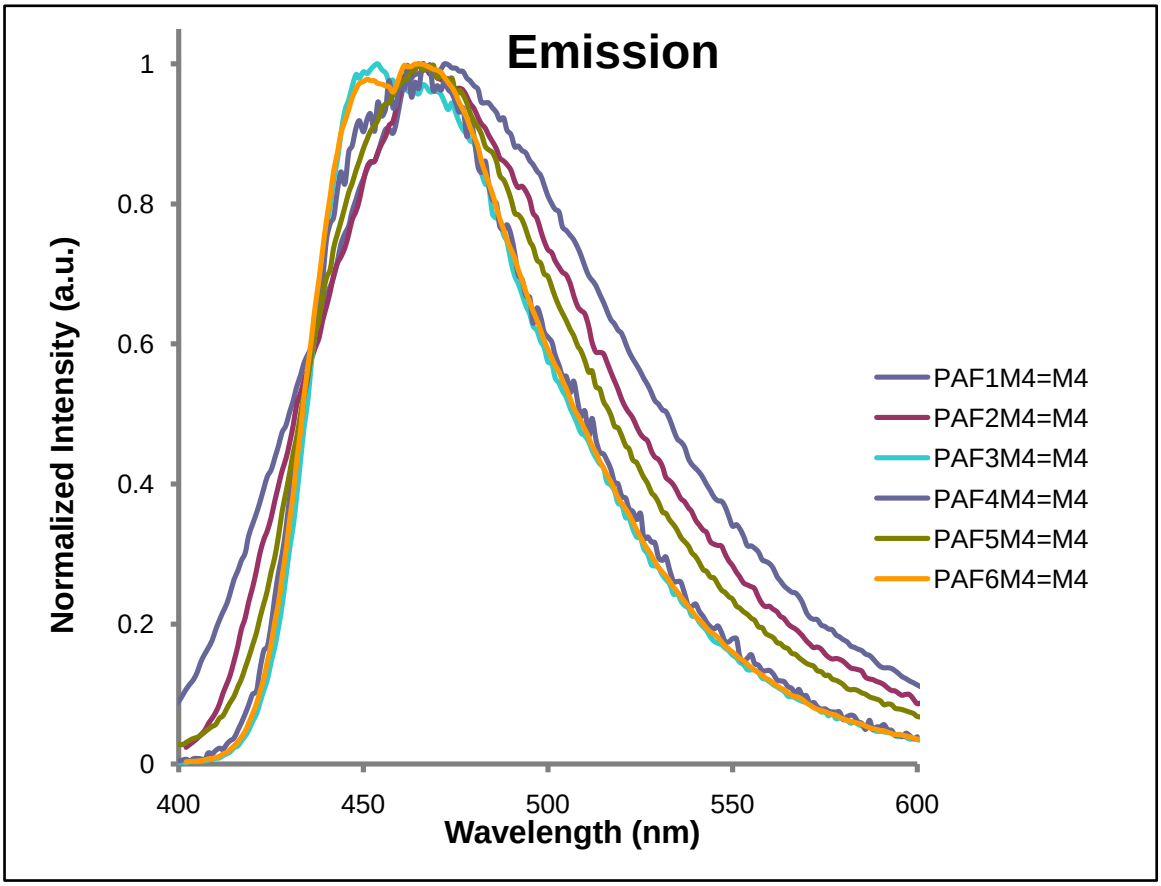

Figure 17. Normalized emission spectra of $P(AF)_xM_4=M_4$ series of polymers at ~ 10^{-6} M in $CHCl_3$.

The normalized emission spectra of **$P(AF)_xM_4=M_4$** series of polymers in $CHCl_3$ is shown in Figure 17 and tabulated in Table 2. The emission spectra are a little challenging to explain. It is

usual to expect that increasing the length of a conjugated chain will result in a red shift of the emission spectra. This trend was observed in our previous preparations of dialkylfluorene segmers.[1] However, all of the alkylidene fluorene polymers exhibit similar emission maxima. The fact that the maxima did not shift even in extremely dilute conditions ($<10^{-6}$ M) suggests that the phenomenon is not aggregation-based. Rather it seems likely that there is poor conjugation along the backbone due to twisting such that the emission is primarily from isolated alkylidene fluorene units.

2.8 THERMAL PROPERTIES

Alkylidene fluorene RSCs exhibit sequence dependent liquid crystal properties. The capability of alkylidene fluorene containing copolymers to be aligned and produce polarized emission is of great potential for making higher efficiency LCDs with OLEDs as back lights. There is previous evidence from the studies of specific mesogens that suggests that liquid phase transition temperatures should correlate with the sequence of repeating units.[2]

It should be noted that alkylidene fluorenes, unlike simple dialkylfluorenes, have an sp^2-hybridized carbon at the 9-position. This arrangement should facilitate the adoption of a coplanar conformation and therefore promote cofacial aggregation. Cofacial, π–π stacking morphology is very favorable to the formation of liquid crystalline phases.

The **P(AF)$_x$M$_4$=M$_4$** materials were investigated by polarized optical microscopy (POM). Using a hot stage, dropcast films on glass slides were heated and the thermal transitions were monitored. All polymers with x > 1 exhibited liquid crystalline phases. **P(AF)$_1$M$_4$=M$_4$** exhibited only a crystalline phase. The POM images observed for these liquid crystals were consistent with

nematic packing (Schlieren textures); the images are not suggestive of a smectic morphology. Although we have difficulty observing by POM the transitions from crystalline or amorphous to a liquid crystalline phase because the polymers form liquid crystals at room temperature when dropcast, we can identify the phase transition temperatures for the nematic to isotropic transition for all five liquid crystalline polymers (Table 3). Figure 18 shows the textures of **$P(AF)_xM_4=M_4$** (x = 1-6) polymers.

$P(AF)_1M_4=M_4$

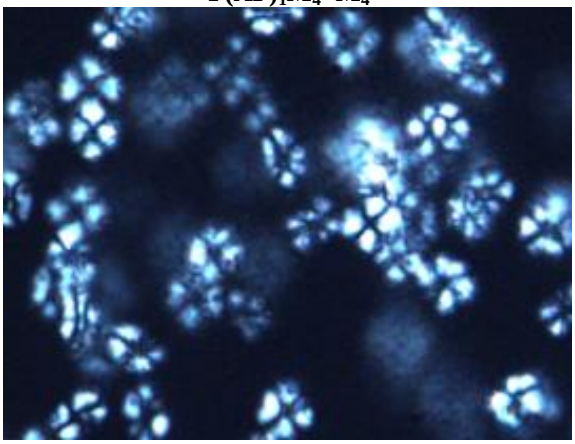

$P(AF)_2M_4=M_4$

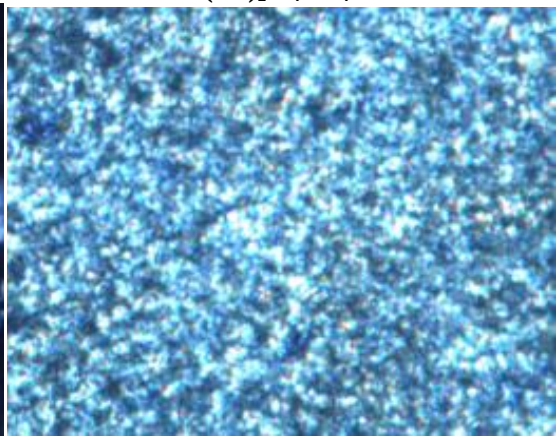

$P(AF)_3M_4=M_4$

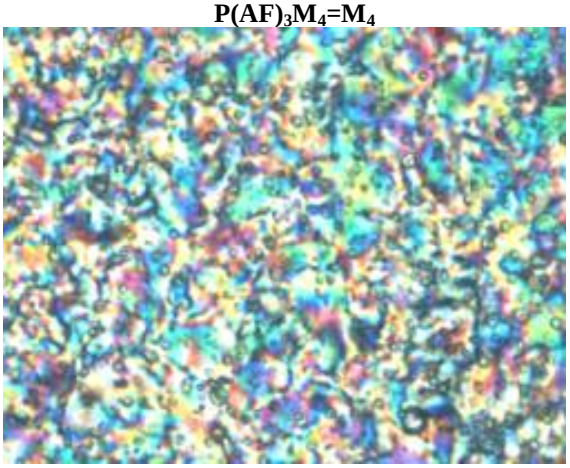

$P(AF)_4M_4=M_4$

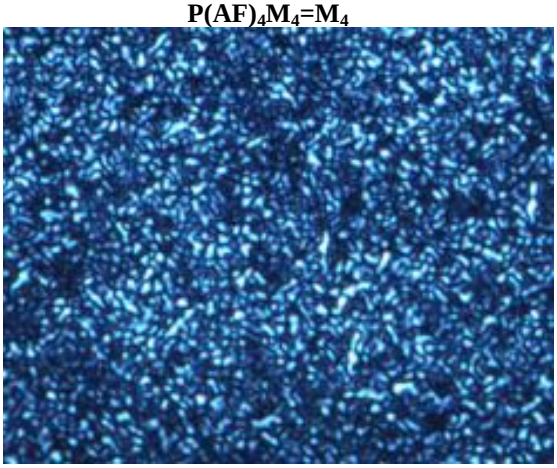

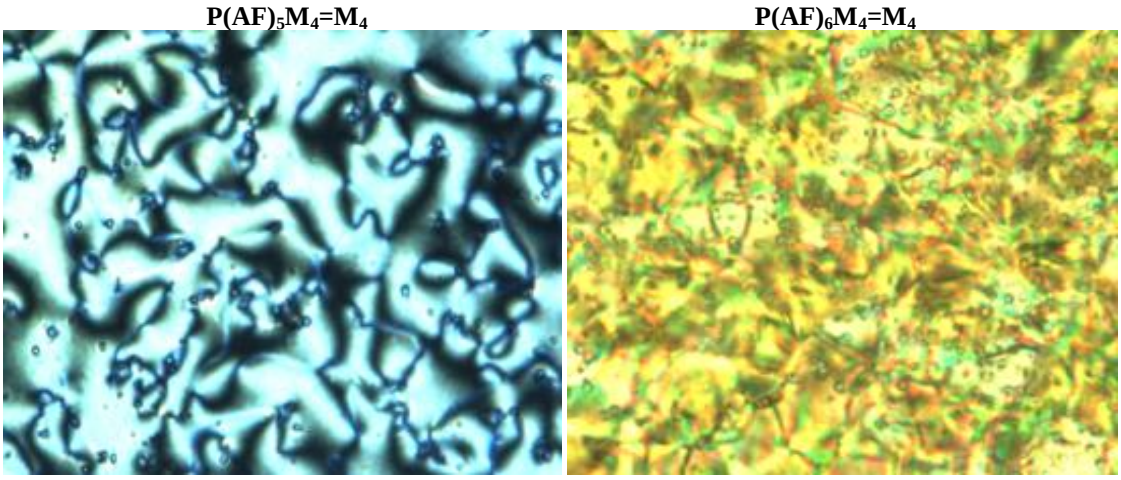

Figure 18. Polarized optical microscopy images of the nematic phase of $P(AF)_xM_4=M_4$ (x = 1-6).

Table 3. Phase transition temperatures determined by polarizing optical spectroscopy for the $P(AF)_xM_4=M_4$ series[a].

Polymer	T_{iso} (℃)	Transition
$P(AF)_1M_4=M_4$	45	(crystal → isotropic)
$P(AF)_2M_4=M_4$	99	(nematic → isotropic)
$P(AF)_3M_4=M_4$	107	(nematic → isotropic)
$P(AF)_4$ $M_4=M_4$	198	(nematic → isotropic)
$P(AF)_5$ $M_4=M_4$	222	(nematic → isotropic)
$P(AF)_6M_4=M_4$	230	(nematic → isotropic)

[a]Phase transitions were determined by polarized optical microscopy.

The same polymer samples were also characterized by differential scanning calorimetry (DSC) (Tables 4 and 5). The data were acquired on two separate instruments, a Perkin-Elmer Pyris 6 and a TA DSC Q200. The latter is equipped with a superior cooling system that made it possible to observe glass transition temperatures below 0 ℃. The data from the two data collections were complementary. The N-I transitions, for example, are easily identifiable from the Perkin-Elmer Pyris 6 data but not from the TA DSC Q200 data for some samples.

Table 4. DSC data for alkylidene fluorene RSCs (Trial 1)[a].

Polymer	Scan	T_{a-b}	T_{b-c}	T_{c-d}	T_{d-e}
$P(AF)_1M_4=M_4$	1st heating	37	47		
$P(AF)_2M_4=M_4$	1st heating	42	83	99	
	1st cooling	76			
	2nd heating	36	81	92	
	2nd cooling	75			
$P(AF)_3M_4=M_4$	1st heating	46	105		
$P(AF)_4M_4=M_4$	Not indentifiable				
$P(AF)_5M_4=M_4$	1st heating	54	224		
	1st cooling	112	224		
	2nd heating	222			
	2nd cooling	112	224		
$P(AF)_6M_4=M_4$	1st heating	105	238		
	1st cooling	67	240		
	2nd heating	96	233		
	2nd cooling	64	238		

[a]DSC data acquired with a Perkin-Elmer Pyris 6 instrument using ~ 10 mg samples. The samples were heated from 0 ℃ to typically 250 ℃, held for 5 min and then cooled back to 0 ℃ at 10 ℃/min. This same heat cycle was repeated and transition data is reported from both cycles.

Table 5. DSC data for alkylidene fluorene RSCs (Trial 2)[a].

Polymer	Scan	T_{a-b}	T_{b-c}	T_{c-d}	T_{d-e}
$P(AF)_1M_4=M_4$	1st heating	42	52		
	2nd heating	-25	-11	44	
$P(AF)_2M_4=M_4$	1st heating	53	89	102	
	1st cooling	76			
	2nd heating	13	33	87	100
	2nd cooling	81			
$P(AF)_3M_4=M_4$	1st heating	53	104		
	1st cooling	99			
	2nd heating	8	100		
	2nd cooling	99			
$P(AF)_4M_4=M_4$	1st heating	55	192		
	2nd heating	14			
$P(AF)_5M_4=M_4$	1st heating	55			
	2nd heating	62			
$P(AF)_6M_4=M_4$	1st heating	105			
	1st cooling	70			
	2nd heating	39	108		
	2nd cooling	68			

[a]DSC data were acquired with a TA DSC Q200 instrument equipped with a Refrigerated Cooling System 90 using 5 to 10 mg of sample. The samples were cooled to a temperature of -80 ℃ to -40 ℃ and heated to 160-250 ℃ at a rate of 10 ℃/min. This same heat cycle was repeated and transition data is reported from both cycles.

Table 6. Thermal data assignments for alkylidene fluorene RSCs.

Polymer	T_g[a]	T_m[b]	T_{cryst}[c]	$T_{cryst\ 1}$[d]	T_{nem}[e,h]	T_{iso}[f,h]
$P(AF)_1M_4=M_4$	-25	51	n/a[g]	n/a	n/a	42(45)
$P(AF)_2M_4=M_4$	n/a	53	76	33	87(72)	102(99)
$P(AF)_3M_4=M_4$	8	53	99	n/a	(45)	104(107)
$P(AF)_4M_4=M_4$	14	55	n/a	n/a	(45)	192(198)
$P(AF)_5M_4=M_4$	n/a	55	n/a	n/a	62(65)	224(222)
$P(AF)_6M_4=M_4$	39	n/a	70	n/a	105(91)	234(230)

[a]Glass transitions temperature calculated by Universal TA software from TA DSC Q200 data. [b]Taken from 1st heating cycle, assigned as m.p. of alkyl chain crystals. [c]Crystallization temperatures observed during the cooling process. [d]Crystallization temperatures observed during heating process. [e]Temperatures for the transition of polymers into a nematic phase. [f]Temperatures for the transition of polymers into isotropic liquids. [g]Not available. [h]Values in parentheses are obtained from POM.

The DSC scans were analyzed and the transitions from the DSC Q200 instrument were labeled using the Universal TA software. The data from both DSC acquisitions and POM were compared and tentative assignments have been made as shown in Table 6. A glass transition (T_g) was identified for most of our polymers (not identified for **$P(AF)_2M_4=M_4$** and **$P(AF)_5M_4=M_4$**). The T_g values generally increase with the number of alkylidene fluorene units per segmer.

All polymers except **$P(AF)_6M_4=M_4$**, exhibit an endothermic transition around 53 ℃ during the first heating cycle. The transition is not present, however, in the 2nd heating. Since the temperature does not depend on the length of the alkylidene fluorene block we think it is possible that it represents the melting of crystals formed primarily from the alkyl side chains and/or the flexible blocks. Side chain crystallization has been observed for rigid-rod oligomers and polymers bearing long alkyl side chains.[21]

The transition from glass/crystal to a nematic phase is difficult to identify for most samples. In the DSC intermediate transitions were only observed for **$P(AF)_2M_4=M_4$** and **$P(AF)_6M_4=M_4$**. The analysis of the POM images was complicated by the fact that dropcasting produced films that were already partly liquid crystalline. The nematic transition temperatures

were tentatively assigned by subtle changes in texture. The T_{nem} are sequence dependent but do not follow a simple trend.

Crystallization peaks were observed for some polymers. For **P(AF)$_2$M$_4$=M$_4$** and **P(AF)$_3$M$_4$=M$_4$**, we are quite sure that the crystallization process observed in the cooling cycle correlates with a change from the isotropic to the nematic phase. The crystallization peak observed for **P(AF)$_6$M$_4$=M$_4$** at 60-70 ℃ is not easily explained since we see no corresponding change in the POM. **P(AF)$_2$M$_4$=M$_4$** also shows an exothermic crystallization during the heating cycle. This transition could be related to the side chain crystallization discussed above.

The T_{iso} can be clearly observed by both DSC and POM and the data correlate well. Moreover, there is a clear trend in that T_{iso} increases with the number alkylidene fluorene units. It should be noted that **P(AF)$_1$M$_4$=M$_4$** is crystalline but not liquid crystalline so that T_{iso} is the simple melting point. Also, it is interesting that the difference in the T_{iso} is larger between dimer and trimer than between the higher segmers (Figure 19).

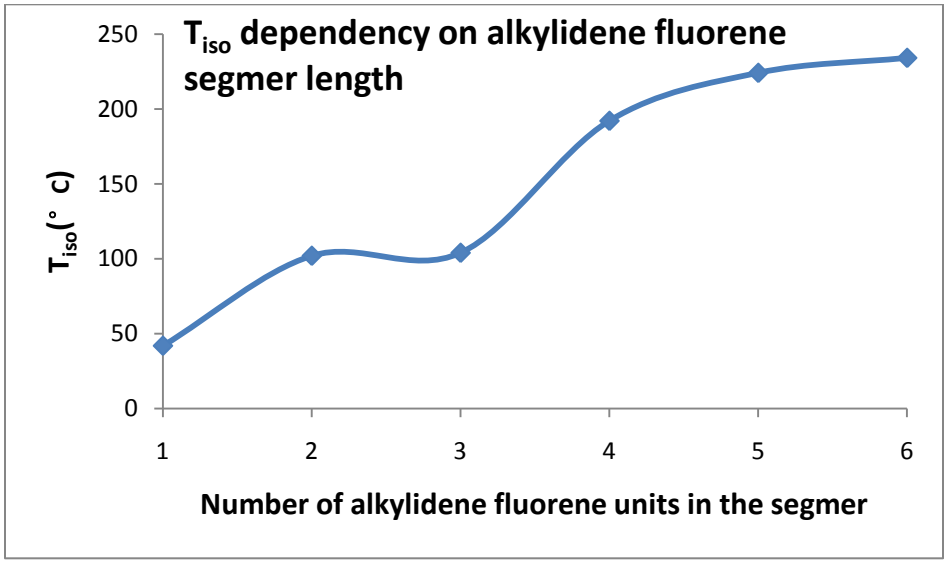

Figure 19. The isotropic transition temperature dependence on the number of alkylidene fluorene units.

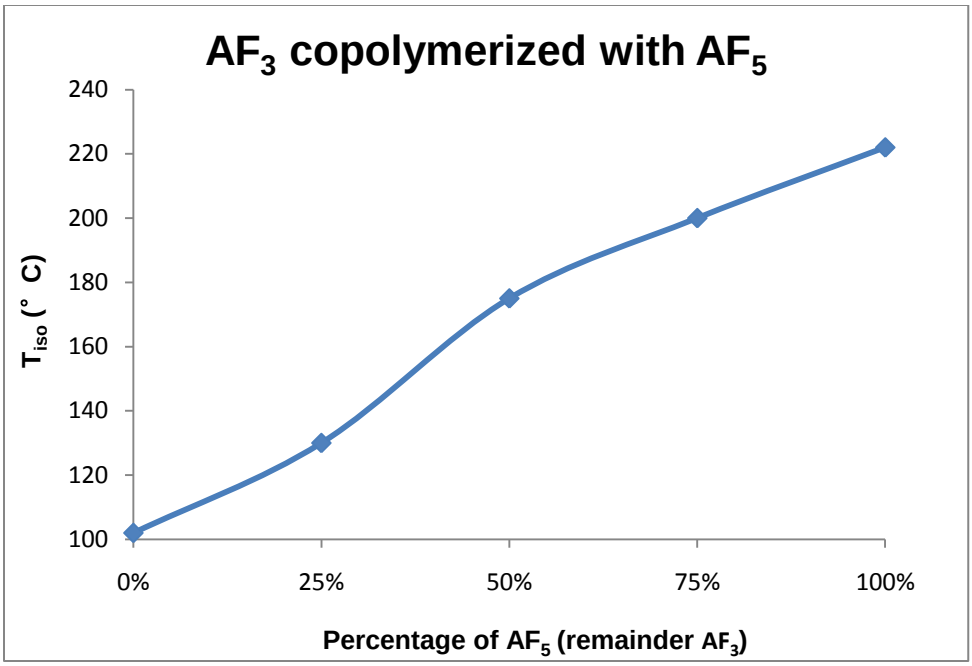

Figure 20. The N-I phase transition temperatures for P(AF)3M4=M4, P(25%AF3 : 75% AF5), P(50% AF3 : 50% AF5), P(75% AF3 : 25%AF5), P(AF)5M4=M4.

The thermal properties of copolymers prepared by mixing AF_5 and AF_3 segmers were also analyzed to determine if the thermal transitions were sequence specific. Figure 20 shows the plot of the N-I temperatures for both the pure homopolymers and the copolymers prepared by mixing the AF_5 and AF_3 segmers in different ratios: **P(25%AF_3 : 75% AF_5), P(50% AF_3 : 50% AF_5), P(75% AF_3 : 25%AF_5)**. The fact that there is a nearly linear increase of the N-I transition temperatures as the percentage of AF_5 increases suggests that there is no sequence specific behavior. As the liquid crystalline phases are nematic, it is not too surprising.

3.0 DISCUSSION

3.1 EXPLANATION OF BIMODAL PATTERN IN THE GPC

All six of our alkylidene fluorene copolymers exhibited a bimodal or polymodal pattern in the GPC. Heeney et al. also reported seeing bimodality for his analogous oligomers.[3] They proposed aggregation as an explanation and corroborated their hypothesis by showing that their GPC changed to favor the lower MW species at lower concentrations. For our polymers, however, we did not find that peak ratio changed dramatically on changing the concentration of polymer solutions. We found almost the same distribution of molecular weights by GPC independent of the concentrations of the polymer solutions. We hypothesize that our RSCs, which contain long, flexible spacers, are overall less rigid than pure poly(alkylidene fluorene)s, and hence they do not have as much propensity to aggregate in solution, even in a Θ solvent such as THF.

3.2 SYNTHETIC IMPROVEMENTS

Despite synthetic challenges involved in alkylidene fluorene discussed in introduction part, our group made several improvements in the synthesis. First, we able to exert control over the synthesis of well-defined alkylidene fluorene oligomers through a one-step reaction and second, the separation of products from unrelated starting materials and byproducts is much easier than

Grisorio's approach which employs a Yamamoto coupling to produce **B-(AF)$_3$-B** and **B-(AF)$_4$-B** in one reaction (Figure 3.1). **B-(AF)$_3$-B** and **B-(AF)$_4$-B** have similar R_fs, which affords a hard separation by column chromatography. Moreover, the Suzuki-Myaura reaction is less toxic than Yamamoto coupling, and yields of oligomer are decent. All oligomeric alkylidene fluorenes were obtained above 60% yields. Second, we achieve to create bifunctionality of alkylidene fluorene segmers, so that we can modify them to synthesize alkylidene fluorene RSCs. The target functionality in this project is different from that synthesized by Grisorio. We intend to synthesize bis halogenated oligomers, while Grisorio et al. Aimed to obtain bis boronated segmers. Third, excess **Br-AF-B**r is used to prevent potential and undesired polymerization involved. Although it is uncommon employed in organic synthesis, it is a creative idea for this project.

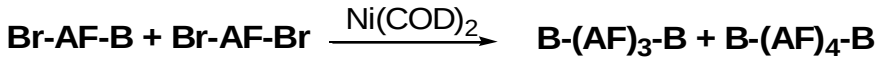

Figure 21. Representative synthetic strategy employed by Grisorio et al.

3.3 COMPARISON OF ALKYLIDENE FLUORENE SEGMERS AND POLYMERS WITH FLUORENE POLYMERS IN TERMS OF PHYSICAL PROPERTIES

Compared to the absorption spectra of copolymers of dialkylfluorene and methylene, **PF$_x$M$_y$**, investigated by our group previously, the changes in wavelength of the maximum absorption are relatively insensitive to oligomer length. When comparing **P(AF)$_3$M$_4$=M$_4$** to **P(AF)$_4$M$_4$=M$_4$**, for example, only a 7 nm increase in absorption maximum is observed. A 3 nm red shift exists from the change from **P(AF)$_4$M$_4$=M$_4$** to **P(AF)$_5$M$_4$=M$_4$** (Table 7). For the previously prepared dialkylfluorene copolymers, 12 nm and 5 nm increases correspond to the analogous change in

oligomer length. Moreover, the copolymers of the $\mathbf{PF_xM_y}$ series exhibit a larger red shift in wavelength of the maximum absorption than poly alkylidene fluorene series. For instance, for the polytrimer, λ_{max} is 343 nm for alkylidene fluorene copolymers, while λ_{max} is 354 nm for dialkylfluorene copolymers.

Table 7. Absorbance and emission maxima for fluorene containing polymers and oligomers.

Polymers or Oligomers	λ_{abs}(nm), $CHCl_3$	λ_{em}(nm), $CHCl_3$	Reference
PAF[a]	351	445 (529)[e]	4
$\mathbf{P(AF)_1M_4{=}M_4}$[b]	306	472	This work
$\mathbf{P(AF)_2M_4{=}M_4}$	329	465	This work
$\mathbf{P(AF)_3M_4{=}M_4}$	343	454	This work
$\mathbf{P(AF)_4M_4{=}M_4}$	350	466	This work
$\mathbf{P(AF)_5M_4{=}M_4}$	353	465	This work
$\mathbf{P(AF)_6M_4{=}M_4}$	353	465	This work
$\mathbf{OF_3}$[c]	338	414 (536)	5
$\mathbf{OF_4}$	348	414 (544)	5
$\mathbf{OF_5}$	352	415 (548)	5
$\mathbf{OF_6}$	354	415(548)	5
$\mathbf{PF_1M_{18}}$[d]	278	332	1
$\mathbf{PF_2M_{18}}$	335	372	1
$\mathbf{PF_3M_{18}}$	354	399	1
$\mathbf{PF_4M_{18}}$	366	408	1
$\mathbf{PF_5M_{18}}$	371	413	1
$\mathbf{PF_6M_{18}}$	374	415	1

[a]PDHF: poly(9,9-dihexylfluorene); [b]$P(AF)_5M_4{=}M_4$: polymers with alternating blocks of x units of alkylidene fluorene and olefins; [c]OF_x: oligomers with x units of alkylidene fluorene without any functionality on the terminus; [d]PF_xM_y: polymers with alternating blocks of x fluorenes units and y methylene units; [e]Values in parentheses are maximum emission wavelength in solid state.

Alkylidene fluorene series of polymers demonstrates a larger maximum emission wavelength, typically 450 nm, than corresponding wavelength of dialkylfluorene polymers, 408 nm, indicating poly(alkylidene fluorene) copolymers have more effective conjugation structure than dialkylfluorene copolymers. This finding is in accord with the hypothesis based on structure comparison that double bond on the alkylidene fluorene unit can enhance conjugation because the extra p orbitals on the double bonds can interact with those on the fluorene units, forming a

larger conjugated system. However, the effective conjugation for both alkylidene fluorene segmers and polymers is prone to reach saturation, as evidenced by the values of maximum emission wavelength, 465-466 nm for alkylidene fluorene polymers and 414-415 nm for alkylidene fluorene segmers.

By comparing alkylidene fluorene polymers data with segmers' data obtained by Grisorio et al., we found that the maximum absorbance wavelength of alkylidene fluorene polymers in solution match with that of segmers reported by Grisorio.OF3-6 all exhibit almost the same maximum wavelength of emission at 414-415 nm. Most of polymers in this work also show almost the same maximum wavelength of emission around 465 nm. It is likely that alkylidene fluorene has poor conjugation along the backbone because of twisting such that the emission is primarily from isolated alkylidene fluorene units. Furthermore, our emission spectra do not exhibit fine structures of polymers, which are supposed to appear on typical solution state emission spectra. The reasons for this discrepancy may arise from the relatively high concentration of our polymer solution and the rigidity of polymer structures, which could promote polymer aggregation. The aggregation may lead to disappearance of fines structures of polymers and make the maximum emission wavelength approach to the values in solid state. However, both our data and Grisorio's exhibit the same trend that the effective conjugation length reach maximum when the number of alkylidene fluorene units reaches 5.

3.4 OVERVIEW OF THERMAL PROPERTIES

Our polymers exhibit sequence dependence on the transition from liquid crystal phase into isotropic, concluded by both DSC and POM. However, we cannot conclude convincingly that the

transition from amorphous or crystal into nematic phase is also sequence dependent, because the polymers form liquid crystals at room temperature after preparation. Most of our polymers exhibit a segmer length independent thermal transition around 53 ℃, which we believe might be associated with the melting of crystals formed from the long alkyl side chains.

The textures of the liquid crystals do change as we progress through the series. **P(AF)$_1$M$_4$=M$_4$** crystallizes but does not exhibit a liquid crystalline phase. **P(AF)$_x$M$_4$=M$_4$** (x = 2-4) all have similar textures with a fairly fine grain. **P(AF)$_x$M$_4$=M$_4$** (x = 5-6) have a slightly different looking birefringence pattern. There is a similar but not identical pattern to the isotropization temperatures (Figure 19). Both the POM data and the T_{iso} trend suggest that there may be some change in morphology as the alkylidene fluorene segmer length increases.

The nature of the nematic phase of these polymers is not completely understood. It is known that polyfluorenes bearing branched substituents organize into nematic phases through the interaction of the alkyl side chains. We had hoped that π-stacking would dominate in the alkylidene fluorene versions shown here. The fact that we see side chain crystallization and that the isotropization temperatures scale with the number of fluorene units even in the mixed segmer polymers is more consistent, however, with a hairy rod model. The fact that we observe differences in behavior as we progress through the series could be as is posited above an indication that there is a change in morphology for the longer chain segmers. Further data (X-ray and modeling) would be required to determine accurately the packing of the RSCs in the liquid crystalline phases.

4.0 CONCLUSIONS

We have successfully prepared a series of alkylidene fluorene RSCs and examined photophysical and thermal properties, especially liquid crystal property, of these copolymers. Based on precursor's work, Heeney et al., Grisorio et al., we creatively developed an innovative methodology to synthesize well-defined oligomers with exact control over the segment lengths of the alkylidene fluorene. In addition, this methodology allows us to functionalize the oligomers to yield monomers with terminal double bonds. These monomers were polymerized via ADMET approach to produce target copolymers.

By investigating photophysical properties of alkylidene fluorene RSCs and comparing to those of dialkyfluorene RSCs, we learned that the conjugation length of alkylidene fluorene polymers does not increase significantly as the units of alkylidene fluorene are increased from 1 to 6 and that alkylidene fluorene RSCs are more conjugated than dialkylfluorene RSCs. All alkylidene fluorene RSCs have liquid crystal properties, and the phase transition temperatures from nematic to isotropic demonstrate sequence-dependent relationship with the alkylidene fluorene length.

5.0 EXPERIMENTAL SECTION

5.1 GENERAL

Toluene was distilled under nitrogen from sodium. 1,5-Hexadiene (98%, Acros) was distilled under nitrogen from calcium hydride. $Pd(PPh_3)_4$(Strem), $PdCl_2(PPh_3)_2$ (99.9+%, Strem), $Ni(COD)_2$(Strem), $PdCl_2$(dppf) (Aldrich), and Grubbs-II catalyst (Aldrich, Strem) were commercially obtained and stored in a nitrogen-filled glovebox. All other reagents were commercially obtained and used without further purification. ^{1}H NMR (300 MHz and 400 MHz) and ^{13}C NMR (75 MHz and 100 MHz) spectra were recorded with Bruker spectrometers. Chemical shifts were referenced to residual ^{1}H or ^{13}C signals in deuterated solvents. Column chromatography was performed using Sorbent 60 Å 40-63 μm standard grade silica. HRMS data were obtained on a Fison VG Autospec in the Mass Spectral Facility of the University of Pittsburgh. GPC data were acquired in THF (HPLC grade, Fisher) on a Waters system equipped with 510 pump, a U6K universal injector, and a 410 differential refractometer. GPC separation were achieved at 25 ℃ on Phenogel (500 and 1000 Å) or Jordi Gel DVD (500, 1000, and 10000 Å) eluting at 0.5 mL/min. Differential scanning calorimetry was performed on a Perkin Elmer Py 1096. Dibromo alkylidene fluorene was prepared according to the approach of Heeney et al. **9-BBN** was prepared according the approach of Chung.[21] **B-(AF)$_2$-B** was prepared according to the approach of Grisorio.[5]

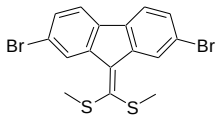

Br-(AFS_2)-Br xij11: According to the methods of Heeney et al.,[2] sodium *tert*-butoxide (15.6 g, 0.162 mol) was added in portions to a mechanically stirred solution of 2,7-dibromo fluorene (25 g, 0.077 mol) in anhydrous DMSO (500 mL) at RT under nitrogen. Carbon disulfide (6.47 g, 0.085 mol) was added via syringe and the reaction mixture was stirred for 10 min. Methyl iodide (23.0 g, 0.162 mol) was added via syringe over 5 min and reaction was stirred overnight. Concentrated ammonium hydroxide (25 mL) was added. The reaction mixture was filtered, washed with DMSO, dried, and the resultant solid was recrystallized from ethyl acetate:THF (2:1) to afford the product **Br-(AFS_2)-Br** as bright yellow needles (5.5 g, 83%). ^{1}H NMR (300 MHz, $CDCl_3$) δ 8.90 (s, 2 H), 7.51 (d, ^3J = 8.2 Hz, 2 H), 7.42 (d, ^3J = 8.2 Hz, 2 H), 2.57 (s, 6 H). ^{13}C NMR (75 MHz, $CDCl_3$) δ 147.3, 139.4, 137.5, 134.3, 130.3, 129.1, 121.2, 210.4, 19.1.

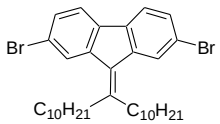

Br-AF-Br, xij12: To a stirred solution of **Br-(AFS_2)-Br** (5.0 g, 6.34 mmol) in anhydrous THF (100 mL) at -5 ℃ under nitrogen was added lithium tetrachlorocuprate (3 M of a 0.1M solution in THF, 0.3 mmol). Decylmagnesium bromide (26 mL of a 1.0 M solution in diethyl ether, 26 mmol) was then added over 30 min, keeping the temperature below 0 ℃ throughout. The reaction was stirred for a further 4 h at -5 ℃ and then quenched by the addition of 10% sodium hydroxide (50 mL). The reaction was stirred for 10 min and then filtered through Celite.

The filter cake was washed with ethyl acetate. The resulting layers were separated, and the aqueous layer further extracted with ethyl acetate. The combined organic extracts were washed with 10% aqueous solution of sodium hydroxide (50 mL), saturated sodium metabisulfite (50 mL), and brine (50 mL), and then dried over $MgSO_4$. The crude material was purified by column chromatography over silica (petroleum ether) to yield **Br-AF-Br** (pale yellow crystal, 5.6 g, 79%). ^{1}H NMR (300 MHz, $CDCl_3$) δ 7.87 (s, *J* = 1.2 Hz, 2 H), 7.59 (d, *J* = 8.1 Hz, 2 H), 7.44 (dd, 2 H), 2.73 (t, *J* = 8.3 Hz, 4 H), 1.72-1.67 (m, 4 H), 1.59-1.29 (m, 24 H), 0.91 (t, *J* = 6.7 Hz, 6 H). ^{13}C NMR (75 MHz, $CDCl_3$) δ155.1, 139.9, 137.4, 129.8, 129.3, 127.9, 121.2, 120.4, 37.5, 32.2, 32.0, 29.8, 29.7, 29.7, 29.5, 29.4, 27.8, 22.8, 22.8, 22.5, 14.2. MS (EI): m/z 618 (M^+, 12), 616 (M^+, 24), 614 (M^+, 12), 476 (M^+, -$C_{10}H_{21,}$ 7), 336 (M^+, - $C_{20}H_{42}$, 28).

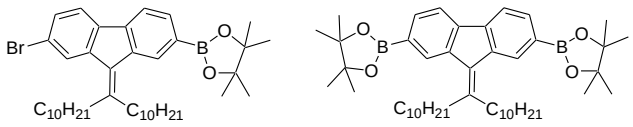

Br-AF-B, xij 31; **B-AF-B**, xij 21. To a 100 mL Schlenk flask under N_2 charged with **Br-AF-Br** (1.5 g, 2.4 mmol), $PdCl_2$(dppf) (100 mg, 0.123 mmol), and KOAc (1.3 g, 0.13 mol), *p*-dioxane (40 mL) was added. The reaction mixture was stirred at 60 ℃ for 24 h. After the mixture was cooled to RT, water (20 mL) was added and the organic layer was extracted with ethyl ether (2 x 40 mL). The organic layer was separated, washed with brine, and dried over $MgSO_4$. The residue was purified by column chromatography over silica (70:30 hexane:methylene chloride) to yield **Br-AF-B** (yellow solid, 0.35 g, 22%) and (40:60 hexane:methylene chloride) to yield **B-AF-B** (colorless crystalline solid, 0.8 g, 48 %). **Br-AF-B** ^{1}H NMR (300 MHz, $CDCl_3$) δ 8.23 (s, 1 H), 7.91 (s, 1 H), 7.79-7.73 (m, 2 H), 7.65 (d, *J* = 8.1 Hz, 1 H), 7.45 (d, *J* = 8.1 Hz, 1 H), 2.85-2.73 (m, 4 H), 2.80-1.22 (m, 44 H), 0.95-0.84 (m, 6 H).

^{13}C NMR (75 MHz, $CDCl_3$) δ 153.8, 141.2, 140.8, 138.3, 137.6, 132.3, 131.5, 130.4, 129.1, 129.1, 127.9, 118.6, 83.7, 38.0, 37.5, 31.9, 30.2, 30.1, 29.9, 29.7, 29.7, 29.6, 29.5, 29.4, 29.3, 28.2, 27.9, 25.0, 22.7, 14.1. **B-AF-B** ^{1}H NMR (300 MHz, $CDCl_3$) δ 8.25 (s, 2 H), 7.83-7.75 (q, 4 H), 2.85-2.80 (m, 4 H), 1.80-1.23 (m, 32 H), 0.92-0.85 (t, 6 H). ^{13}C NMR (75 MHz, $CDCl_3$) δ 152.3, 142.1, 138.4, 132.7, 131.5, 131.0, 119.1, 83.6, 37.9, 31.9, 30.3, 30.0, 29.9, 29.7, 29.7, 29.4, 28.3, 25.0, 22.7, 14.1.

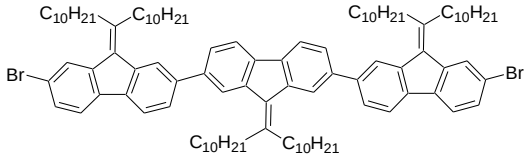

Br-(AF)$_3$-Br, xij 22. To a 50 mL Schlenk flask under N_2 charged with **Br-AF-Br** (1.7 g, 2.76 mmol), **B-AF-B** (0.50 g, 0.70 mmol), and $Pd(PPh_3)_4$ (60 mg, 0.052 mmol) a mixture of, toluene (20 mL), ethanol (4 mL) and 2.0 M K_2CO_3 (4 mL, 8.0 mmol) was added. The reaction mixture was stirred at 80 ℃ for 28 h. After cooling to RT, water (10 mL) was added and the aqueous layer was extracted with ether (50 mL). The organic layer was collected, washed with brine, and dried over $MgSO_4$. The residue was purified by column chromatography over silica (95:5 hexane:methylene chloride) to yield **Br-(AF)$_3$-Br** (yellow crystal, 0.65 g, 63%). ^{1}H NMR (300 MHz, $CDCl_3$) δ 8.03 (d, *J* = 2.7 Hz, 4H), 7.91-7.80 (m, 6 H), 7.70-7.58 (m, 6 H), 7.46 (d, 2 H, *J* = 9.3 Hz), 2.89-2.74 (m, 12 H), 1.86-1.15 (m, 108 H), 0.90-0.81 (m, 18 H). ^{13}C NMR (75 MHz, $CDCl_3$) δ 153.7, 152.2, 141.6, 141.0, 140.6, 139.6, 139.0, 138. 5, 138.2, 137.7, 131.5, 130.7, 129.3, 128.0, 126.0, 125.9, 124.0, 120.8, 120.4, 119.6, 37.8, 37.5, 32.0, 31.9, 30.5, 30.4, 30.1, 29.9, 29.8, 29.7, 29.7, 29.5, 29.4, 29.4, 28.1, 27.9, 22.7, 14.2, 14.1.

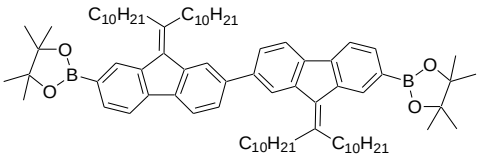

B-(AF)$_2$-B, xij 32. In the glove box, distilled toluene (20 mL) was added to a 50 mL Schlenk flask charged with Ni(COD)$_2$ (120 mg, 0.45 mmol), 2,2'-bipyridine (69 g, 0.45 mmol), and cyclooctadiene (48 mg, 0.45 mmol), and the mixture was stirred at 80 ℃ for 30 min. **Br-AF-B** (0.25 g, 0.38 mmol) in toluene (5 mL) was added in one portion. The reaction mixture was stirred at 80 ℃ for 24 h. After the mixture was cooled to RT, the solution was filtered through a Celite plug. The Celite was rinsed with petroleum ether (40-60 ℃). Purification by column chromatography over silica (50:50 hexane:methylene chloride) gave **B-(AF)$_2$-B** (yellow solid, 0.35 g, 79%). ^{1}H NMR (300 MHz, $CDCl_3$) δ 8.26 (s, 2 H), 8.04 (s, 2 H), 7.80 (d, *J* = 7.8 Hz, 2 H), 7.83-7.76 (m, 4 H), 7.60 (d, *J* = 8.1 Hz, 2 H), 2.86 (br-s, 8 H), 1.88-1.15 (m, 88 H), 0.95-0.79 (m, 12 H). ^{13}C NMR (75 MHz, $CDCl_3$) δ 152.4, 142.0, 141.6, 139.7 , 138.5, 138.1, 132.8, 131.5, 131.1, 127.3, 125.7, 124.0, 120.0, 118.7, 83.6, 37.9, 32.0, 31.9, 30.4, 30.3, 29.9, 29.8, 29.7, 29.7, 29.6, 29.5, 29.4, 28.3, 28.1, 22.7, 14.1.

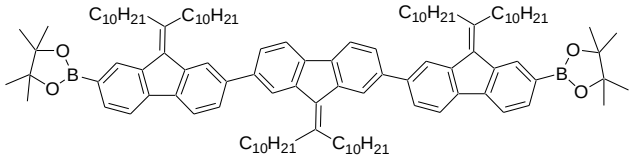

B-(AF)$_3$-B, xij 23. In a 50 mL Schlenk flask under N_2 charged with **Br-(AF)$_3$-Br** (0.65 g, 0.42 mmol), $PdCl_2$(dppf) (20 mg, 0.024 mmol), and KOAc (0.3 g, 3.1 mmol), p-dioxane (25 mL) was added. The reaction mixture was stirred at 80 ℃ for 24 h. After the mixture was cooled to RT, water (20 mL) was added and organic layer was extracted with ethyl ether (2 x 40 mL). The organic layer was separated, washed with brine, and dried over $MgSO_4$. The residue was purified

by column chromatography over silica (50:50 hexane:methylene chloride) to yield **B-(AF)$_3$-B** (yellow solid, 0.40 g, 56%). ^{1}H NMR (300 MHz, $CDCl_3$) δ 8.27 (s, 2 H), 8.07 (s, 4 H), 7.91-7.78 (m, 8 H), 7.67-7.60 (m, 4 H), 2.87 (br-s, 12 H), 1.88-1.15 (m, 120 H), 0.92-0.81 (m, 18 H). ^{13}C NMR (75 MHz, $CDCl_3$) δ 152.3, 142.0, 141.6, 141.1, 139.7, 139.5, 138.5, 138.1, 132.8, 132.8, 131.2, 125.9, 125.7, 124.1, 120.0, 119.6, 118.7, 83.6, 37.8, 31.9, 30.4, 30.3, 29.9, 29.8, 29.7, 29.4, 28.3, 28.1, 25.0, 22.7, 14.1.

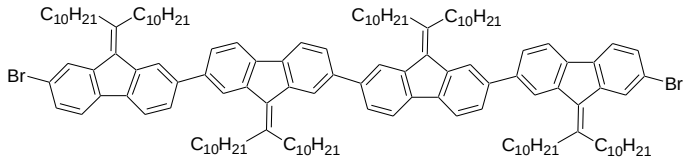

Br-(AF)$_4$-Br, xij 33. To a 50 mL Schlenk flask under N_2 charged with **Br-AF-Br** (1.0 g, 1.62 mmol), **B-(AF)$_2$-B** (0.50 g, 0.43 mmol), and $Pd(PPh_3)_4$ (30 mg, 0.026 mmol), toluene (20 mL), ethanol (6 mL) and 1.2 M K_2CO_3 (6 mL, 7.2 mmol) solution were added. The reaction mixture was stirred at 80 ℃ for 24 h. After the mixture was cooled to RT, water (10 mL) was added and organic layer was extracted with ethyl ether (2 x 20 mL). The organic layer was separated, washed with brine, and dried over $MgSO_4$. The residue was purified by column chromatography over silica (90:10 hexane:methylene chloride) to yield **Br-(AF)$_4$-Br** (yellow solid, 0.55 g, 64%). ^{1}H NMR (300MHz, $CDCl_3$) δ 8.05 (d, *J* = 11.1 Hz, 6 H), 7.91-7.80 (m, 8 H), 7.68-7.59 (m, 8 H), 7.46 (m, 2 H), 2.89-2.75 (m, 16 H), 1.88-1.15 (m, 128 H), 0.89-0.82 (m, 24 H). ^{13}C NMR (75 MHz, $CDCl_3$) δ 151.9, 141.6, 141.1, 140.8, 140.6, 139.6, 139.0, 138.6, 138.5, 138.4, 138.2, 137.6, 131.5, 130.7, 129.3, 128.0, 126.5, 126.0, 125.9, 124.7, 124.0, 120.7, 120.5, 119.6, 37.8, 37.5, 32.0, 31.7, 30.5, 30.4, 30.1, 29.9, 29.8, 29.7, 29.7, 29.5, 29.4, 29.4, 28.1, 27.9, 22.8, 14.2.

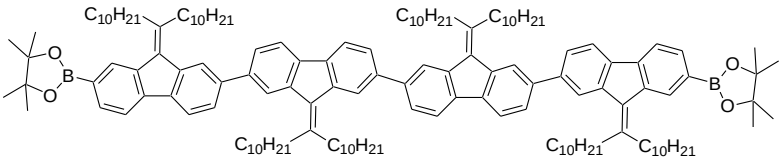

In a 50 mL Schlenk flask under N_2 charged with **Br-(AF)$_4$-Br** (0.60 g, 0.30 mmol), $PdCl_2$(dppf) (12 mg, 0.015 mmol), and KOAc (0.6 g, 6.0 mmol), p-dioxane (25 mL) was added. The reaction mixture was stirred at 85 ℃ for 24 h. After the mixture was cooled to RT, water (20 mL) was added and organic layer was extracted with ethyl ether (2 x 20 mL). The organic layer was separated, washed with brine, and dried over $MgSO_4$. The residue was purified by column chromatography over silica (70:30 hexane:methylene chloride) to yield **B-(AF)$_4$-B** (yellow solid, 0.40 g, 64%). ^{1}H NMR (300 MHz, $CDCl_3$) δ 8.28 (s, 2 H), 8.08 (s, 6 H), 7.91-7.78 (m, 10 H), 7.64-7.62 (m, 6 H), 2.90 (br-s, 16 H), 1.82-1.22 (m, 152 H), 0.92-0.89 (m, 24 H). ^{13}C NMR (75 MHz, $CDCl_3$) δ 152.2, 152.0, 142.1, 141.7, 141.1, 139.8, 139.6, 138.6, 138.5, 138.2, 133.0, 131.6, 131.3, 125.9, 125.8, 124.1, 124.0, 120.1, 119.7, 118.7, 83.6, 38.0, 37.9, 32.0, 30.5, 30.4, 30.0, 30.0, 29.9, 29.8, 29.8, 29.6, 29.5, 28.4, 28.2, 25.0, 22.8, 14.2.

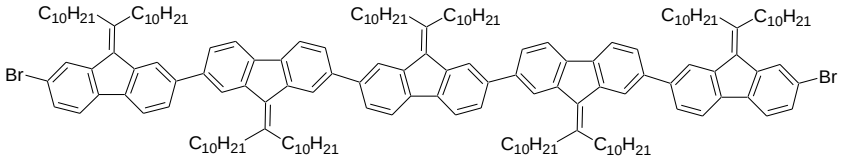

Br-(AF)$_5$-Br, xij 24. In a 50 mL Schlenk flask under N_2 charged with **Br-AF-Br** (0.67 g, 1.1 mmol), **B-(AF)$_3$-B** (0.44 g, 0.27 mmol), and $Pd(PPh_3)_4$ (16 mg, 0.014 mmol), toluene (20 mL), ethanol (4 mL) and 1.0 M K_2CO_3 (1 mL, 1.1 mmol) solution were added. The reaction mixture was stirred at 80 ℃ for 28 h. After the mixture was cooled to RT, water (10 mL) was added and organic layer was extracted with ethyl (2 x 20 mL). The organic layer was separated, washed with brine, and dried over $MgSO_4$. The residue was purified by column chromatography

over silica (85:15 hexane:methylene chloride) to yield **Br-(AF)$_5$-Br** (yellow solid, 0.45 g, 68%). ^{1}H NMR (300 MHz, $CDCl_3$) δ 8.09-8.05 (m, 8 H), 7.93-7.82 (m, 10 H), 7.69-7.63 (m, 10 H), 7.49-7.46 (m, 2 H), 2.91-2.76 (m, 20 H), 1.90-1.15 (m, 160 H), 0.93-0.87 (m, 30 H). ^{13}C NMR (75 MHz, $CDCl_3$) δ 153.6, 152.1, 152.0, 141.6, 141.1, 141.0, 140.8, 140.6, 139.6, 139.0, 138.6, 138.5, 138.4, 138.2, 137.6, 131.6, 131.5, 130.7, 129.3, 128.0, 125.9, 124.0, 120.7, 120.4, 119.6, 37.8, 37.5, 34.7, 32.0, 31.6, 30.5, 30.4, 30.2, 29.9, 29.8, 29.7, 29.5, 29.4, 28.1, 27.9, 25.3, 22.8, 14.2.

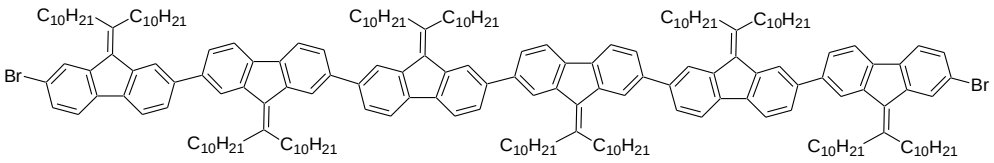

To a 50 mL Schlenk flask under N_2 charged with **Br-AF-Br** (344 mg, 0.56 mmol), **B-(AF)$_4$-B** (300 mg, 0.14 mmol), and $Pd(PPh_3)_4$ (8 mg, 0.007 mmol) a mixture of, toluene (20 mL), ethanol (4 mL) and 2.0 M K_2CO_3 (4 mL, 8.0 mmol) was added. The reaction mixture was stirred at 80 ℃ for 28 h. After cooling to RT, water (10 mL) was added and the aqueous layer was extracted with ether (50 mL). The organic layer was collected, washed with brine, and dried over $MgSO_4$. The residue was purified by column chromatography over silica (90:10 hexane:methylene chloride) to yield **Br-(AF)$_6$-Br** (yellow solid, 250 mg, 60%). ^{1}H NMR (300 MHz, $CDCl_3$) δ 8.09-8.05 (m, 10 H), 7.93-7.81 (m, 12 H), 7.68-7.61 (m, 12 H), 7.47 (d, *J* = 8.1 Hz, 2 H), 2.91-2.80 (m, 24 H), 1.83-1.22 (m, 192 H), 0.91-0.85 (m, 36 H). ^{13}C NMR (75 MHz, $CDCl_3$) δ 153.5, 151.9, 151.7, 141.4, 141.1, 140.9, 140.6, 139.6, 139.2, 139.0, 138.7, 138.5, 138.4, 138.3, 137.6, 131.7, 131.5, 125.9, 123.9, 120.7, 119.7, 37.8, 32.1, 32.1, 30.6, 30.4, 30.2, 30.1, 30.0, 29.9, 29.8, 29.6, 29.5, 29.5, 28.0, 22.9, 14.2.

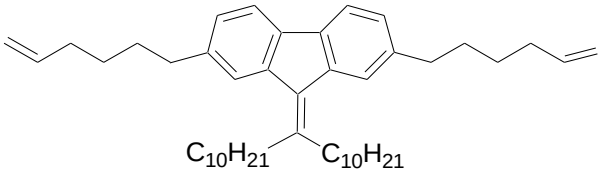

9-BBN was prepared according to the method of Chung et al.[20] In a N_2-atmosphere glovebox, a 50 mL flame-dried Schlenk flask was charged with **Br-AF-Br** (500 mg, 0.81 mmol), **9-BBN** (660 mg, 3.24 mmol), $PdCl_2(PPh_3)_2$ (28 mg, 0.04 mmol), and tetrahydrofuran (20 mL). Outside the glovebox, K_2CO_3 (8.1 mL x 2 M, 16.2 mmol) was added by syringe and the reaction mixture was stirred at 45 ℃ for 24 h. After cooling to RT, ethyl ether (20 mL) was added. The organic layer was separated, washed with the brine, and dried over $MgSO_4$. The residue was purified by column chromatography on silica gel with hexane: methylene chloride (90:10) as the eluent to yield =**AF=** (400 mg, 79%) as white crystals. ^{1}H NMR (300 MHz, $CDCl_3$) δ 7.62 (d, *J* = 7.8 Hz, 2 H), 7.54 (s, 1 H), 7.11 (d, *J* = 7.5 Hz, 2 H), 5.88-5.75 (m, 2 H), 5.05-4.98 (m, 4 H), 2.78-2.67 (m. 8 H), 2.10 (q, 4 H), 1.74-1.64 (m, 8 H), 1.58-1.29 (m, 36 H), 0.96-0.84 (m, 6 H). ^{13}C NMR (75 MHz, $CDCl_3$) δ150.8, 140.9, 138.9, 138.8, 137.6, 131.4, 126.7, 124.9, 118.7, 114.4, 37.6, 36.5, 33.7, 31.9, 31.6, 31.3, 29.8, 29.7, 29.4, 28.5, 28.0, 22.7, 14.1.

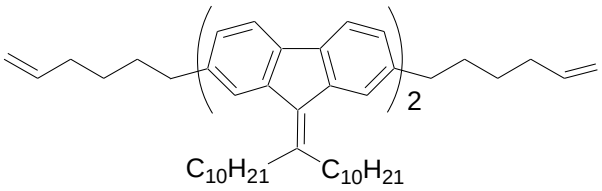

The procedure for the synthesis of =**AF=** was followed to prepare =**$(AF)_2$=**. In a N_2-atmosphere glovebox, a 25 mL flame-dried Schlenk flask was charged with **Br-$(AF)_2$-Br** (200 mg, 0.19 mmol), **9-BBN** (228 mg, 1.12 mmol), $PdCl_2(PPh_3)_2$ (7 mg, 0.04 mmol), and tetrahydrofuran (10 mL). Outside the glovebox, K_2CO_3 (1.9 mL x 2 M, 3.8 mmol) was added by

syringe and the reaction mixture was stirred at 45 ℃ for 24 h. After cooling to RT, ethyl ether (10 mL) was added. The organic layer was separated, washed with the brine, and dried over $MgSO_4$. The residue was purified by column chromatography on silica gel with hexane: methylene chloride (90:10) as the eluent to yield =(**AF**)$_2$= (150 mg, 75%) as light yellow solid. ^{1}H NMR (300 MHz, $CDCl_3$) δ8.04 (d, *J* = 6.3 Hz, 4 H), 7.88-7.58 (m, 12 H), 7.17 (d, *J* = 7.8 Hz, 2 H), 5.88-5.75 (m, 2 H), 5.05-4.98 (m, 4 H), 2.89-2.71 (m, 12 H), 2.12 (q, 4 H), 1.90-1.15 (m, 116 H), 0.90-0.81 (m, 12 H). ^{13}C NMR (75 MHz, $CDCl_3$) δ151.3, 141.3, 140.8, 139.2, 138.9, 138.8, 137.4, 131.6, 126.9, 125.8, 125.0, 124.0, 119.2, 119.1, 114.5, 37.8, 37.7, 36.6, 33.8, 32.0, 32.0, 31.4, 30.5, 29.9, 29.7, 29.5, 29.4, 28.6, 28.2, 28.0, 22.8, 14.2.

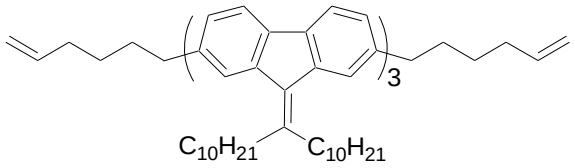

The procedure for the synthesis of =**AF**= was followed to prepare =(**AF**)$_3$=. In a N_2-atmosphere glovebox, a 50 mL flame-dried Schlenk flask was charged with **Br-(AF)$_3$-Br** (250 mg, 0.163 mmol), **9-BBN** (200 mg, 0.98 mmol), $PdCl_2(PPh_3)_2$ (4 mg, 0.006 mmol), and tetrahydrofuran (20 mL). Outside the glovebox, K_2CO_3 (1.6 mL x 2 M, 3.2 mmol) was added by syringe and the reaction mixture was stirred at 45 ℃ for 24 h. After cooling to RT, ethyl ether (20 mL) was added. The organic layer was separated, washed with the brine, and dried over $MgSO_4$. The residue was purified by column chromatography on silica gel with hexane: methylene chloride (90:10) as the eluent to yield =(**AF**)$_3$= (200 mg, 80%) as yellow crystals. ^{1}H NMR (300 MHz, $CDCl_3$) δ 8.04 (d, *J* = 6.3 Hz, 4 H), 7.88-7.58 (m, 12 H), 7.17 (d, *J* = 7.8 Hz, 2 H), 5.88-5.75 (m, 2 H), 5.05-4.98 (m, 4 H), 2.89-2.71 (m, 16 H), 2.12 (q, 4 H), 1.90-1.15 (m, 116

H), 0.90-0.81 (m, 18 H). ^{13}C NMR (75 MHz, $CDCl_3$) δ 151.8, 151.2, 141.3, 141.2, 140.8, 139.7, 139.3, 139.3, 139.0, 138.9, 138.6, 137.6, 131.8, 127.0, 125.9, 125.1, 124.1, 124.0, 119.7, 119.4, 119.2, 114.5, 37.9, 37.8, 36.7, 33.9, 32.1, 31.5, 30.6, 30.4, 30.1, 30.0, 29.7, 29.6, 28.8, 28.3, 28.2, 28.1, 22.9, 14.1.

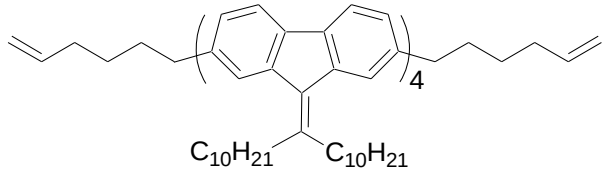

The procedure for the synthesis of **=AF=** was followed to prepare =**(AF)$_4$=**. In a N_2 atmosphere glove box, a 50 mL flame-dried Schlenk flask was charged with **Br-(AF)$_4$-Br** (500 mg, 0.25 mmol), **9-BBN** (310 mg, 1.52 mmol), $PdCl_2(PPh_3)_2$ (5 mg, 0. 007 mmol), tetrahydrofuran (20 mL). Outside the glovebox, K_2CO_3 (3 mL x 2 M, 6 mmol) were added by syringe. The reaction mixture was stirred at 45 ℃ for 24 h. After the mixture was cooled to RT, ethyl ether (20 mL) was added. The organic layer was separated, washed with the brine, and dried over $MgSO_4$. The residue was purified by column chromatography on silica gel with hexane: methylene chloride (90:10) as the eluent to yield =**(AF)$_4$=** (200 mg, 80%) as a yellow solid. ^{1}H NMR (300MHz, $CDCl_3$) δ 8.07-8.03 (m, 6 H), 7.90-7.58 (m, 16 H), 7.17 (d, *J* = 8.4 Hz, 2 H), 5.87-5.78 (m, 2 H), 5.05-4.96 (m, 4 H), 2.89-2.71 (m, 20 H), 2.13 (q, 4 H), 1.82-1.20 (m, 136 H), 0.91-0.82 (m, 24 H). ^{13}C NMR (75 MHz, $CDCl_3$) δ 152.1.93, 151.4, 141.4, 141.3, 141.1, 140.7, 139.54, 139.2, 139.2, 138.8, 138.8, 138.5, 138.4, 137.3, 131.6, 126.9, 125.9, 125.0, 124.1, 119.6, 119.2, 119.1, 114.4, 37.9, 37.8, 36.7, 33.7, 31.9, 31.3, 30.4, 30.3, 29.8, 29.4, 29.4, 28.6, 28.2, 28.1, 22.9, 14.1.

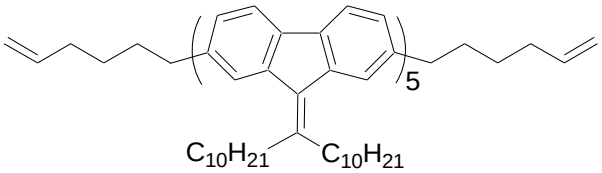

The procedure for the synthesis of **=AF=** was followed to prepare **=(AF)$_5$=**. In a N_2 atmosphere glovebox, a 50 mL flame-dried Schlenk flask was charged with **Br-(AF)$_5$-Br** (350 mg, 0.14 mmol), **9-BBN** (175 mg, 0.84 mmol), $PdCl_2(PPh_3)_2$ (5 mg, 0. 006 mmol), tetrahydrofuran (20 mL). Outside the glovebox, K_2CO_3 (1.4 mL x 2 M, 2.8 mmol) were added by syringe. The reaction mixture was stirred at 45 ℃ for 24 h. After the mixture was cooled to RT, ethyl ether (20 mL) was added. The organic layer was separated, washed with the brine, and dried over $MgSO_4$. The residue was purified by column chromatography on silica gel with hexane: methylene chloride (90:10) as the eluent to yield **=(AF)$_5$=** (300 mg, 86%) as a yellow solid. ^{1}H NMR (300 MHz, $CDCl_3$) δ 8.09-8.04 (m, 8 H), 7.90-7.61 (m, 20 H), 7.17 (d, *J* = 7.5 Hz, 2 H), 5.88-5.77 (m, 2 H), 5.06-4.95 (m, 4 H), 2.90-2.72 (m, 24 H), 2.19-2.10 (q, 4 H), 1.88-1.15 (m, 168 H), 0.91-0.75 (m, 30 H). ^{13}C NMR (100 MHz, $CDCl_3$) δ 152.1, 151.5, 141.4, 141.2, 141.1, 141.1, 140.7, 139.5, 139.2, 139.2, 138.9, 138.8, 138.5, 138.4, 137.3, 131.5, 126.9, 125.9, 125.8, 125.0, 124.1, 119.6, 119.2, 119.1, 114.4, 37.8, 37.7, 36.6, 33.7, 32.0, 31.6, 31.4, 30.5, 30.4, 29.9, 29.7, 29.5, 29.4, 28.6, 28.2, 28.0, 22.7, 14.2.

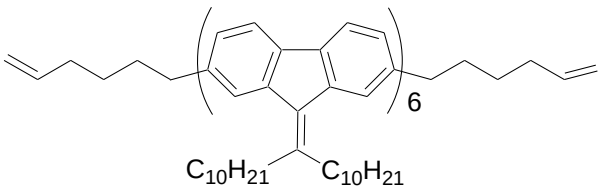

The procedure for the synthesis of **=AF=** was followed to prepare **=(AF)$_6$=**. In a N_2 atmosphere glovebox, a 25 mL flame-dried Schlenk flask was charged with **Br-(AF)$_6$-Br** (200

mg, 0.07 mmol), **9-BBN** (86 mg, 0.42 mmol), $PdCl_2(PPh_3)_2$ (3 mg, 0. 005 mmol), tetrahydrofuran (10 mL). Outside the glovebox, K_2CO_3 (0.7 mL x 2 M, 1.4 mmol) were added by syringe. The reaction mixture was stirred at 45 ℃ for 24 h. After the mixture was cooled to RT, ethyl ether (10 mL) was added. The organic layer was separated, washed with the brine, and dried over $MgSO_4$. The residue was purified by column chromatography on silica gel with hexane: methylene chloride (90:10) as the eluent to yield =**(AF)$_6$=** (180 mg, 90%) as a yellow solid. ^{1}H NMR (300 MHz, $CDCl_3$) δ 8.10-8.05 (m, 10 H), 7.90-7.80 (m, 12 H), 7.73-7.59 (m, 12 H), 7.18 (d, *J* = 7.6 Hz, 2 H), 5.88-5.76 (m, 2 H), 5.06-4.95 (m, 4 H), 2.89-2.71 (m, 28 H), 2.12 (q, 4 H), 1.81-1.22 (m, 200 H), 0.99-0.82 (m, 36 H). ^{13}C NMR (75 MHz, $CDCl_3$) δ 152.2, 152.0, 151.5, 141.4, 141.2, 141.1, 140.7, 139.5, 139.2, 139.1, 138.9, 138.8, 138.5, 138.4, 137.3, 131.5, 125.9, 124.1, 119.6, 114.4, 37.8, 36.6, 34.7, 33.7, 32.0, 31.6, 31.4, 29.8, 29.7, 29.4, 28.6, 28.2, 28.0, 25.3, 22.7, 22.7, 14.2.

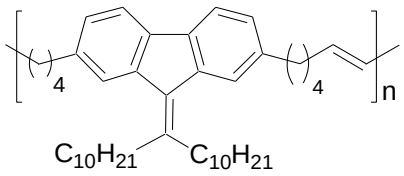

A 5-mL Schlenk flask under N_2 equipped with a condenser was charged with =**AF=** (75 mg, 0.12 mmol) and Grubbs-II catalyst (5 mol%). Methylene chloride (1.5 mL) was added and the reaction was heated to reflux. After 2 d, vinyl ether (1 mL) was added, and the reaction was stirred for 30 min. The reaction mixture was poured into cold methanol (3 x 30 mL) and the precipitate was collected. The crude solid was redissolved and reprecipitated to give **P(AF)$_1$M$_4$=M$_4$** (70 mg) as grey solid in a yield of 93%. ^{1}H NMR (300 MHz, $CDCl_3$) δ 7.62-7.54 (m, 4 H), 7.10 (d, *J* = 6.9 Hz, 2 H), 5.47-5.37 (m, 2 H), 2.74-2.69 (m, 8 H), 2.05 (br-s, 4 H),

1.70-1.29 (m, 44 H), 0.90-0.88 (m, 6 H). ^{13}C NMR (75 MHz, $CDCl_3$) δ 150.7, 141.0, 140.9, 140.8, 138.8, 137.6, 131.5, 130.6, 130.4, 130.3, 130.2, 130.1, 126.7, 124.9, 118.7, 37.6, 36.6, 36.5, 36.1, 32.6, 32.2, 32.0, 31.8, 31.4, 30.4, 29.8, 29.7, 29.7, 29.4, 29.3, 28.0, 22.7, 14.2.

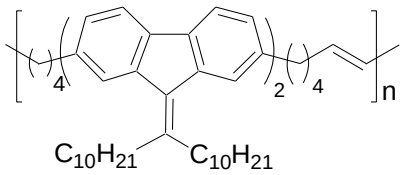

The procedure for the synthesis of **P(AF)$_1$M$_4$=M$_4$** was followed to prepare **P(AF)$_2$M$_4$=M$_4$**. A 5-mL Schlenk flask under N_2 equipped with a condenser was charged with =(**AF)$_2$=** (60 mg, 0.06 mmol) and Grubbs-II catalyst (5 mol%). Methylene chloride (1.5 mL) was added and the reaction was heated to reflux. After 2 d, vinyl ether (1 mL) was added, and the reaction was stirred for 30 min. The reaction mixture was poured into cold methanol (3 x 30 mL) and the precipitate was collected. The crude solid was redissolved and reprecipitated to give **P(AF)$_2$M$_4$=M$_4$** (53 mg) as light yellow solid in a yield of 88%. ^{1}H NMR (300 MHz, $CDCl_3$) δ 8.00-7.33 (m, 10 H), 7.15-7.14 (br-d, 2 H), 5.43 (s, 2 H), 2.80-2.72 (br-d, 12 H), 2.06 (s, 4 H), 1.74-1.20 (m, 116 H), 0.90-0.84 (m, 12 H). ^{13}C NMR (75 MHz, $CDCl_3$) δ 151.3, 141.4, 140.7, 139.1, 138.7, 137.3, 131.5, 130.3, 126.8, 125.7, 125.0, 124.0, 123.0, 119.2, 119.0, 37.8, 37.6, 36.6, 32.6, 32.0, 31.4, 30.4, 29.8, 29.4, 28.1, 27.9, 22.7, 14.2.

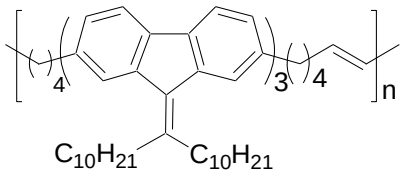

The procedure for the synthesis of **P(AF)$_1$M$_4$=M$_4$** was followed to prepare **P(AF)$_3$M$_4$=M$_4$**. A 5-mL Schlenk flask under N_2 equipped with a condenser was charged with

=**(AF)$_3$=** (100 mg, 0.065 mmol) and Grubbs-II catalyst (5 mol%). Methylene chloride (1.5 mL) was added and the reaction was heated to reflux. After 2 d, vinyl ether (1 mL) was added, and the reaction was stirred for 30 min. The reaction mixture was poured into cold methanol (3 x 30 mL) and the precipitate was collected. The crude solid was redissolved and reprecipitated to give **P(AF)$_3$M$_4$=M$_4$** (70 mg) as yellow sticky solid in a yield of 70 %. ^{1}H NMR (300 MHz, $CDCl_3$) δ 8.01-7.57 (m, 16 H), 7.24-7.15 (br-d, 2 H), 5.43 (br-s, 2H), 2.81-2.72 (br-d, 16 H), 2.06 (br-s, 4 H), 1.73 (br-s, 16H), 1.56-1.12 (m, 100 H), 0.96-0.83 (m, 18H). ^{13}C NMR (75 MHz, $CDCl_3$) δ 151.9, 151.3, 141.5, 141.2, 140.7, 139.6, 139.2,139.2, 139.0, 138.9, 138.5, 138.4, 137.4, 131.6, 130.4, 126.9, 125.9, 125.0, 124.0, 119.4, 119.2, 119.1, 37.8, 32.0, 32.0, 30.5, 29.9, 29.8, 29.7, 29.5, 28.2, 28.0, 22.8, 14.2.

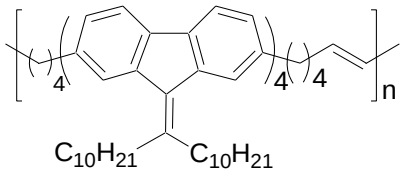

The procedure for the synthesis of **P(AF)$_1$M$_4$=M$_4$** was followed to prepare **P(AF)$_4$M$_4$=M$_4$**. A 5 mL Schlenk flask under N_2 equipped with a condenser was charged with =**(AF)$_4$=** (80 mg, 0.040 mmol) and Grubbs-II catalyst (5 mol%). Methylene chloride (1.5 mL) was added. The reaction was heated to reflux. After 2 d, vinyl ether (1 mL) was added, and the reaction was further stirred for 30 min. The reaction mixture was then poured into cold methanol (3 x 30 mL) and the precipitate was collected. The crude solid was redissolved and reprecipitated to give **P(AF)$_4$M$_4$=M$_4$** (60 m g) as yellow solid in a yield of 75%. ^{1}H NMR (300 MHz, $CDCl_3$) δ 8.02-7.14 (m, 24 H), 5.46-5.40 (m, 2 H), 2.82-2.40 (m, 20 H), 2.31-2.10 (m, 4 H), 1.76-1.21 (136 H), 0.91-0.84 (m, 24 H). ^{13}C NMR (75 MHz, $CDCl_3$) δ152.0, 151.3, 141.1, 140.6, 139.5, 139.2,

138.8, 138.5, 138.4, 137.3, 131.5, 128.5, 126.9, 125.8, 125.0, 124.0, 119.6, 119.2, 119.1, 37.8, 32.0, 30.4, 29.9, 29.5, 28.1, 22.7, 14.2.

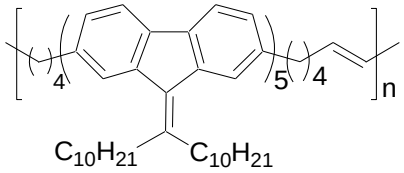

The procedure for the synthesis of **P(AF)$_1$M$_4$=M$_4$** was followed to prepare **P(AF)$_5$M$_4$=M$_4$**. A 5 mL Schlenk flask under N_2 equipped with a condenser was charged with =**(AF)$_5$=** (300 mg, 0.082 mmol) and Grubbs-II catalyst (5 mol%). Methylene chloride (1.5 mL) was added. The reaction was heated to reflux. After 2 d, ethyl vinyl ether (1 mL) was added, and the reaction was further stirred for 30 min. The reaction mixture was then poured into cold methanol (3 x 30 mL) and the precipitate was collected. The collected precipitate solid was redissolved and reprecipitated to give **P(AF)$_5$M$_4$=M$_4$** (250 mg) as yellow powder solid in a yield of 82%. ^{1}H NMR (300 MHz, $CDCl_3$) δ 8.15-7.30 (m, 28 H), 7.10 (br-s, 2H), 5.43 (br-s, 2 H), 2.77 (br-s, 24 H), 2.06 (br-s, 4 H), 1.71-1.20 (m, 168 H), 0.97-0.80 (m, 30 H). ^{13}C NMR (75 MHz, $CDCl_3$) δ 151.9, 151.3, 141.0, 140.6, 139.6, 139.2, 138.8, 138.5, 138.4, 137.3, 131.6, 130.4, 126.8, 125.9, 125.0, 124.0, 119.6, 119.3, 119.1, 37.8, 32.0, 31.4, 30.5, 30.0, 29.7, 29.5, 28.1, 22.8, 14.2.

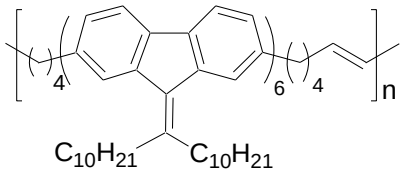

. The procedure for the synthesis of **P(AF)$_1$M$_4$=M$_4$** was followed to prepare **P(AF)$_6$M$_4$=M$_4$**. A 5 mL Schlenk flask under N_2 equipped with a condenser was charged with

=**(AF)$_6$=** (80 mg, 0.04 mmol) and Grubbs-II catalyst (5 mol%). Methylene chloride (1.5 mL) was added. The reaction was heated to reflux. After 2 d, ethyl vinyl ether (1 mL) was added, and the reaction was further stirred for 30 min. The reaction mixture was then poured into cold methanol (3 x 30 mL) and the precipitate was collected. The collected precipitate solid was redissolved and reprecipitated to give **P(AF)$_6$M$_4$=M$_4$** (70 mg) as yellow solid in a yield of 87%. ^{1}H NMR (400 MHz, $CDCl_3$) δ 8.14-7.28 (m, 36 H), 5.47-5.45 (m, 2 H), 2.92-2.82 (m, 28 H), 1.84-1.24 (m, 200 H), 0.95-0.87 (m, 36 H). ^{13}C NMR (100 MHz, $CDCl_3$) δ152.1, 151.9, 141.1, 139.6, 139.2, 138.9, 138.5, 133.7, 131.6, 131.4, 129.8, 125.9, 124.1, 119.6, 37.8, 37.7, 32.0, 30.4, 29.8, 29.7, 29.4, 28.2, 28.0, 22.7, 14.1.

5.2 UV-VIS SPECTROSCOPY

The absorption spectra for the **P(AF)$_x$M$_4$=M$_4$** series of copolymers were obtained in $CHCl_3$ at 10^{-6} M concentration on Perkin-Elmer UV/VIS/NIR Spectrometer Lambda 9 and analyzed using UV Winlab software.

5.3 EMISSION SPECTROSCOPY

All emissions spectra for the **P(AF)$_x$M$_4$=M$_4$** series of copolymers were made on a Varian Cary Eclipse Fluorescence Spectrophotometer. The solution emission spectra were obtained in $CHCl_3$ at 10^{-6} M concentration.

5.4 DIFFERENTIAL SCANNING CALORIMETRY

Differential Scanning Calorimetry (DSC) data were acquired on two seperate instruments, a Perkin-Elmer Pyris 6 and a TA DSC Q200. On the Perkin-Elmer Pyris 6 using ~ 10 mg samples the samples were heated from 0 ℃ to typically 250 ℃ held for 5 min and then cooled back to 0 ℃ at 10 ℃/min. This same heat cycle was repeated and transition data are reported from the both cycles. On the TA DSC Q200 with Refrigerated cooling system 90 using 5-10 mg, the samples were cooled to -40 ℃, and then heated to 160-250 ℃ at 10 ℃/min. This same cooling and heating cycle was repeated. Data were recorded from both cycles.

5.5 POLARIZED OPTICAL MICROSCOPY

The optical detection of the liquid crystal phase transitions were obtained on an Olympus BH-2 microscope with cross polarizers equipped with Mettler FP52 hot stage connected to a Mettler FP5 temperature controller. The samples were prepared by dropcasting the sample from a dilute chloroform solution onto a glass slide.

APPENDIX A

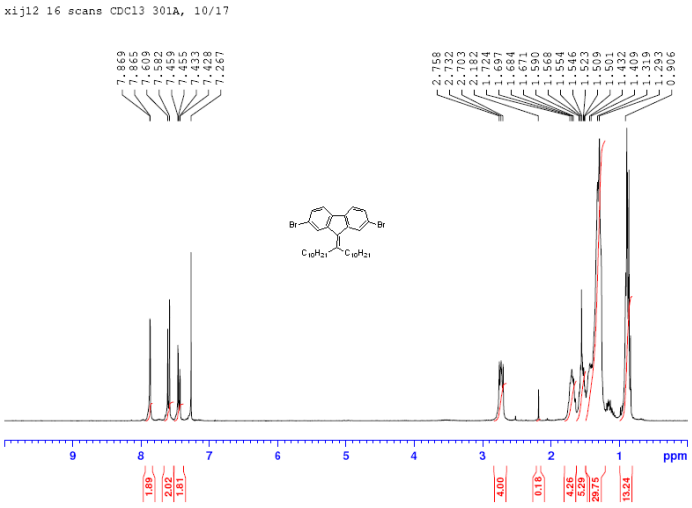

Figure 22. ^{1}H NMR spectrum of Br-AF-Br ($CDCl_3$, 300 MHz).

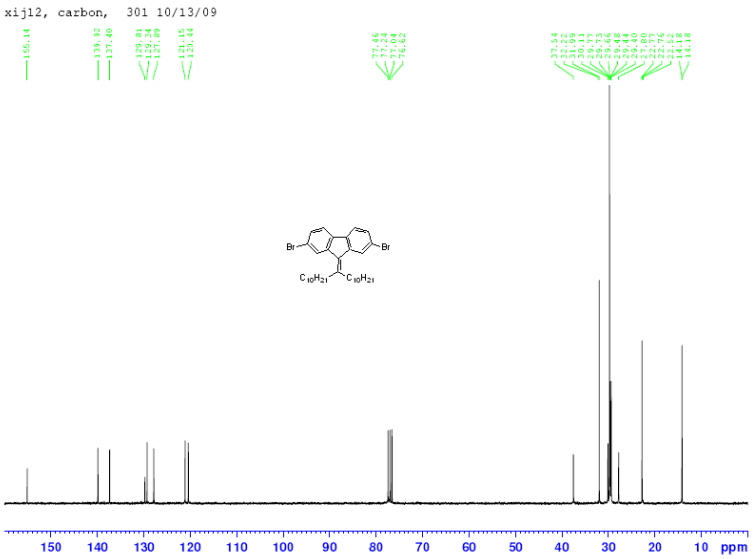

Figure 23. ^{13}C NMR spectrum of Br-AF-Br ($CDCl_3$, 75 MHz).

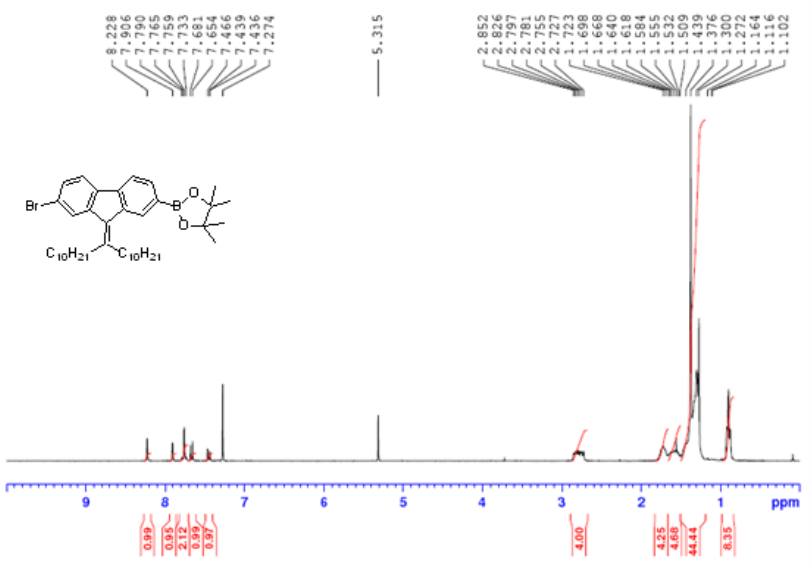

Figure 24. ^{1}H NMR spectrum of B-AF-Br ($CDCl_3$, 300 MHz).

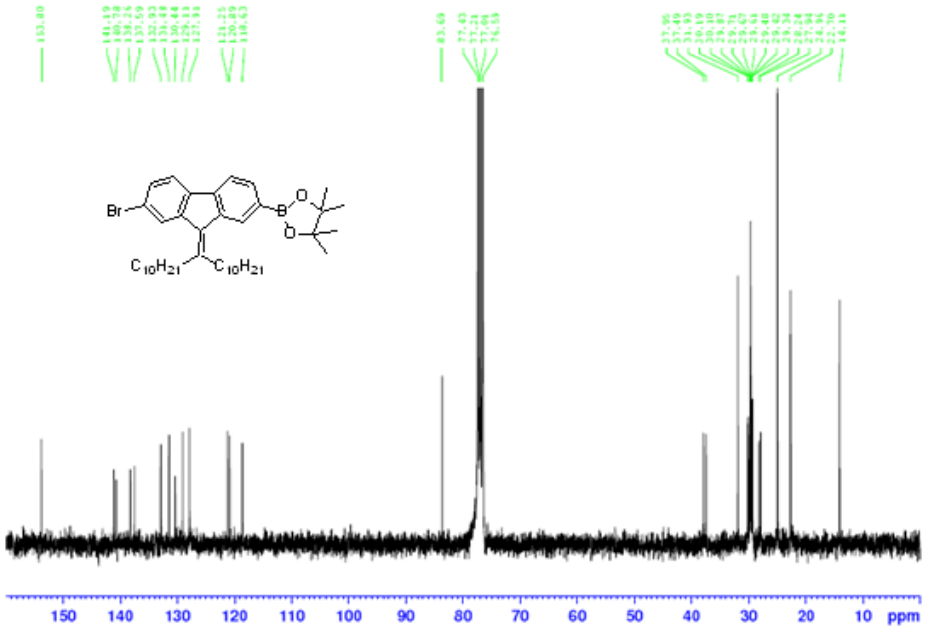

Figure 25. ^{13}C NMR spectrum of Br-AF-B ($CDCl_3$, 75 MHz).

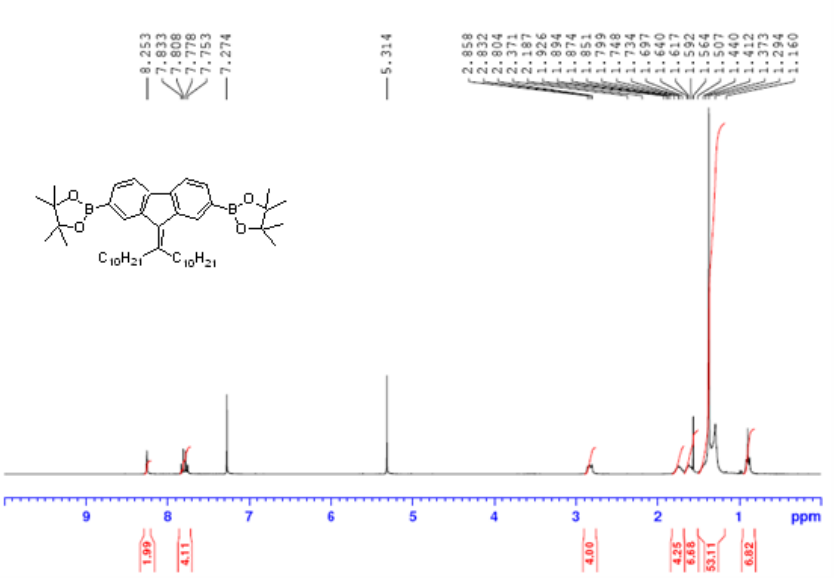

Figure 26. ^{1}H NMR spectrum of B-AF-B ($CDCl_3$, 300 MHz).

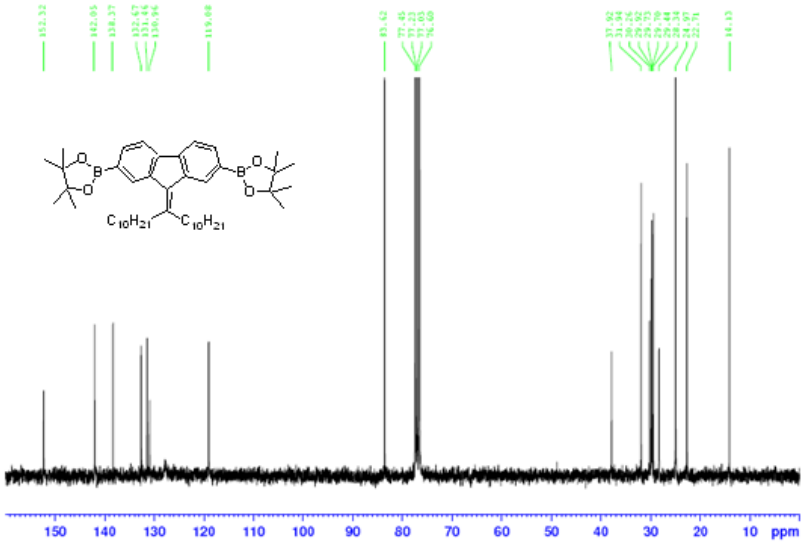

Figure 27. ^{13}C NMR spectrum of B-AF-B ($CDCl_3$,75 MHz).

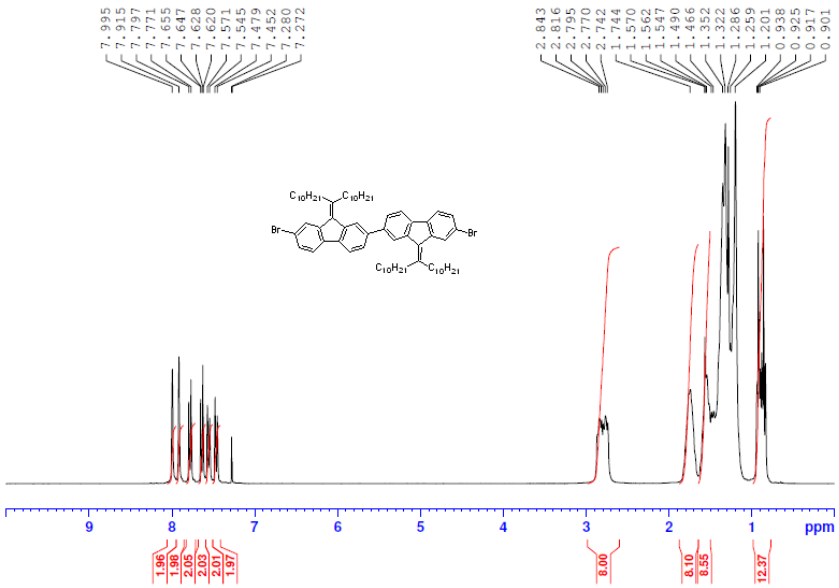

Figure 28. ^{1}H NMR spectrum of Br-(AF)$_2$-Br ($CDCl_3$, 300 MHz).

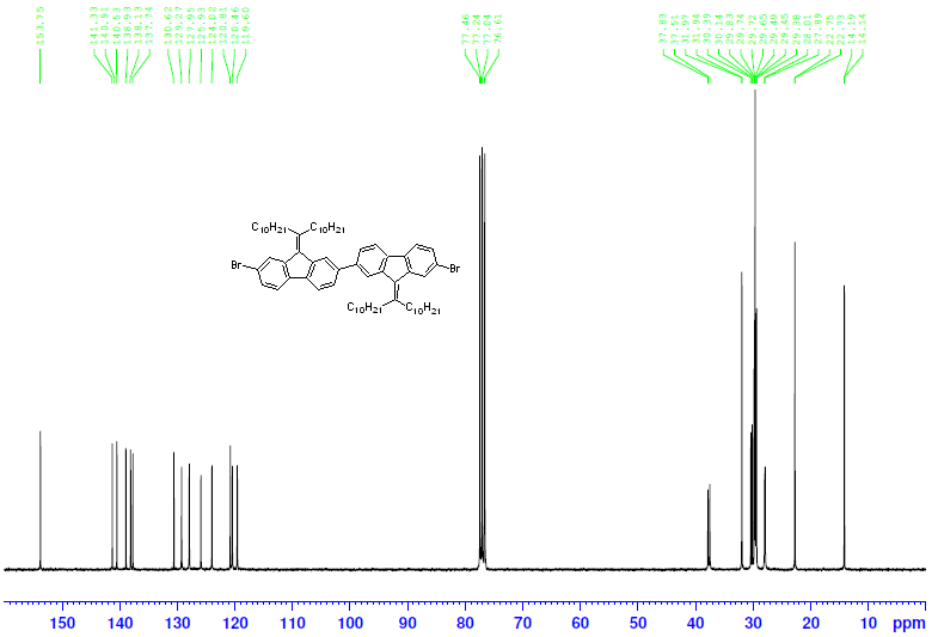

Figure 29. ^{13}C NMR spectrum of Br-(AF)$_2$-Br ($CDCl_3$, 75 MHz).

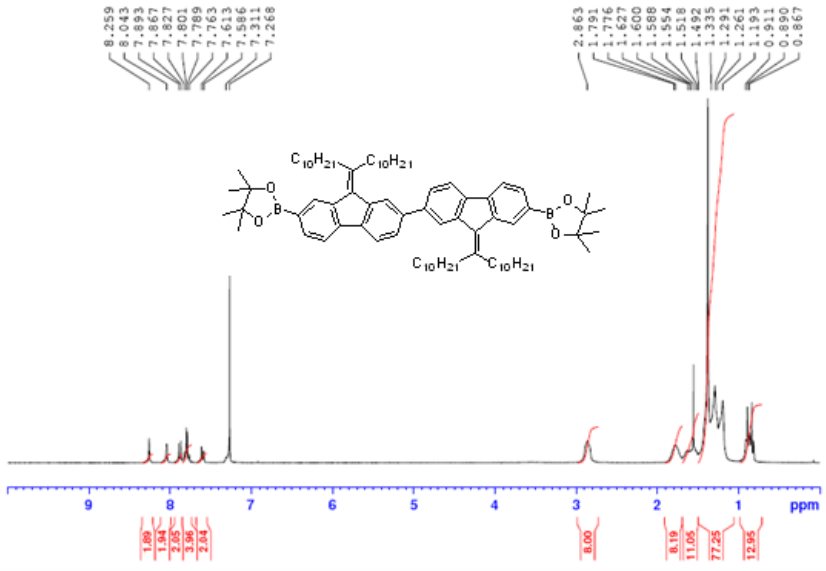

Figure 30. ^{1}H NMR spectrum of B-(AF)$_2$-B (CDCl$_3$, 300 MHz).

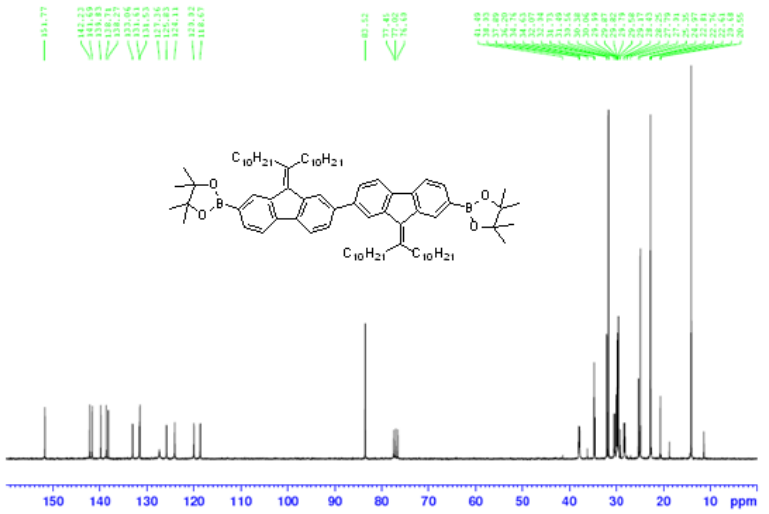

Figure 31. ^{13}C NMR spectrum of B-(AF)$_2$-B (CDCl$_3$, 75 MHz).

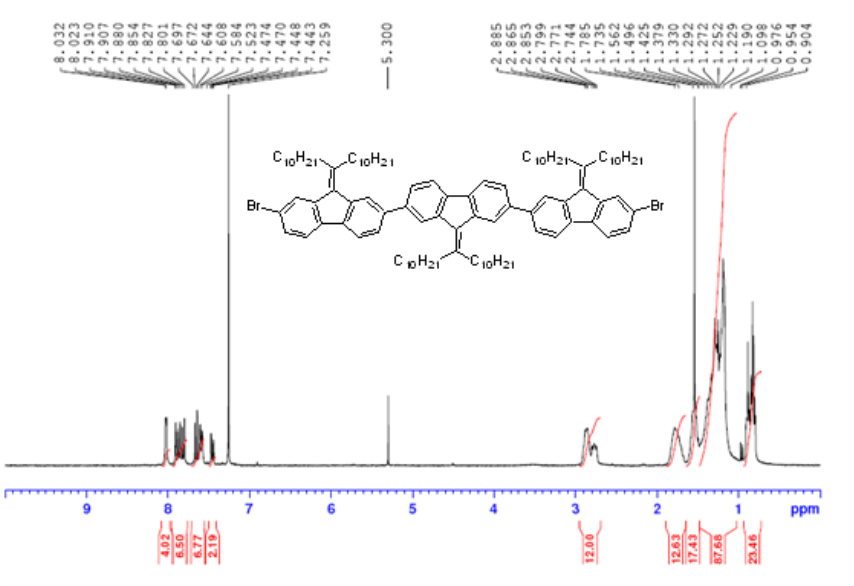

Figure 32. ^{1}H NMR spectrum of Br-(AF)$_3$-Br (CDCl$_3$, 300 MHz).

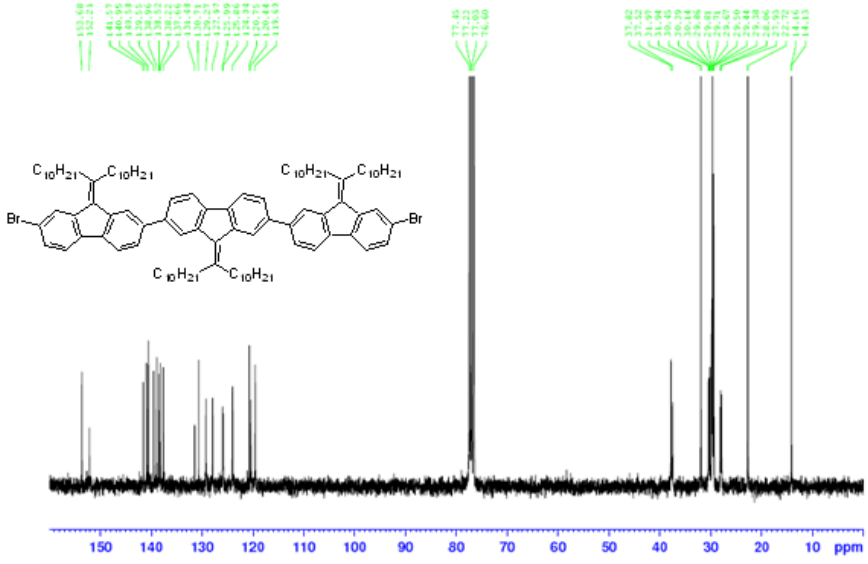

Figure 33. ^{13}C NMR spectrum of Br-(AF)$_3$-Br (CDCl$_3$, 75 MHz).

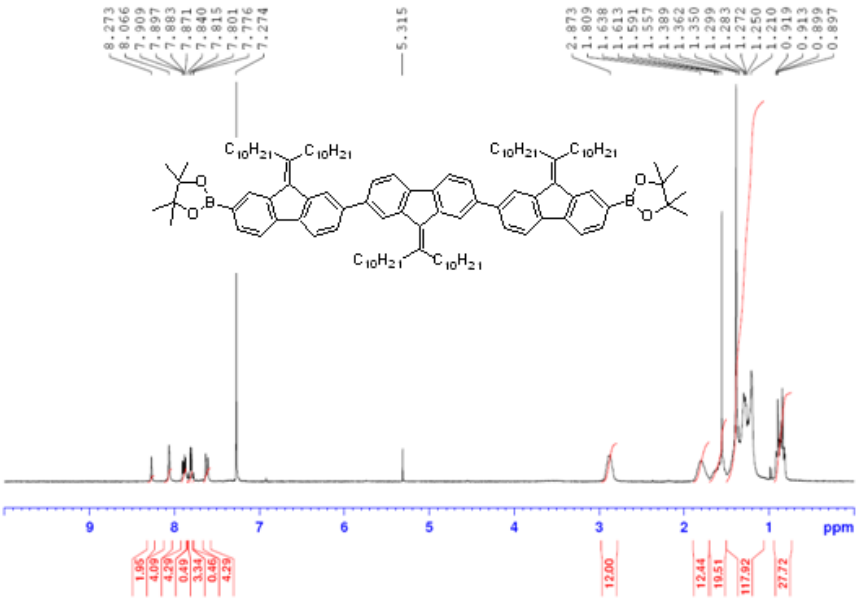

Figure 34. ^{1}H NMR spectrum of B-(AF)$_3$-B (CDCl$_3$, 300 MHz).

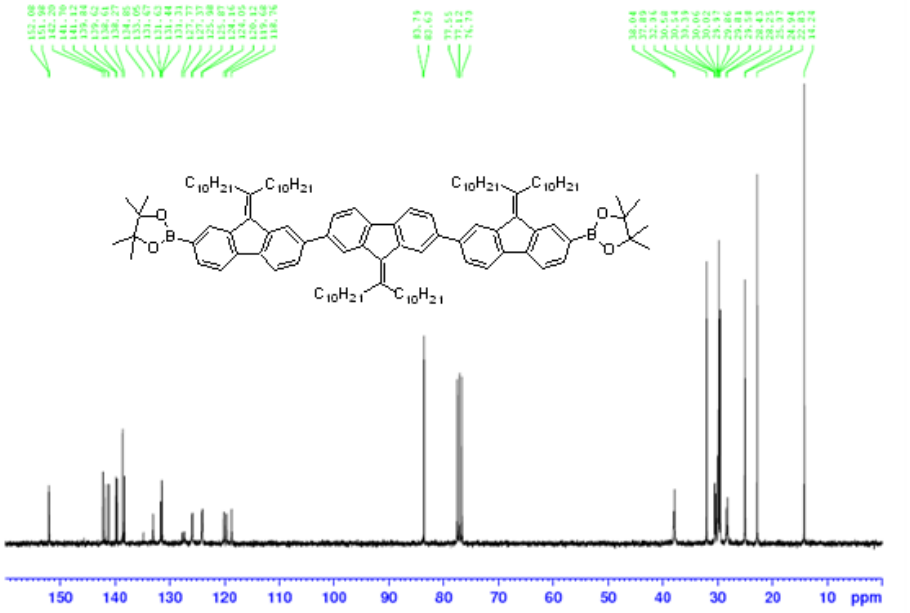

Figure 35. ^{13}C NMR spectrum of B-(AF)$_3$-B(CDCl$_3$,75 MHz).

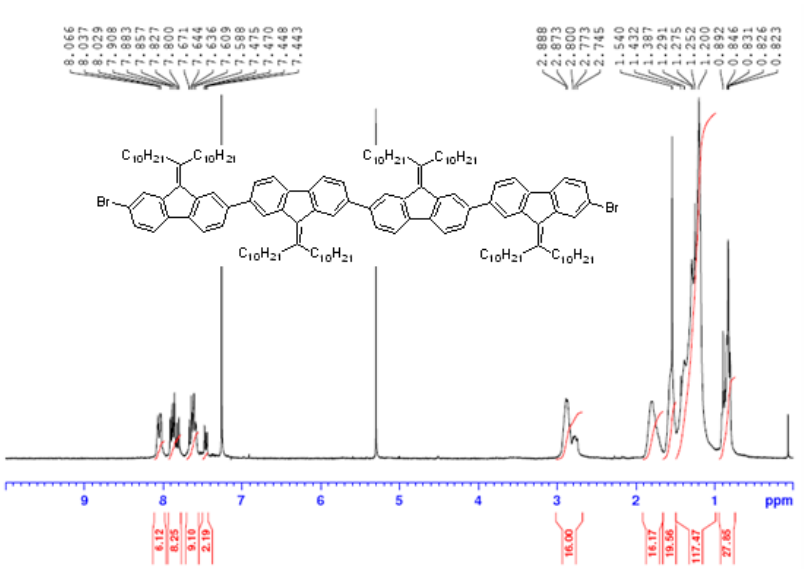

Figure 36. ^{1}H NMR spectrum of Br-(AF)$_4$-Br ($CDCl_3$, 300 MHz).

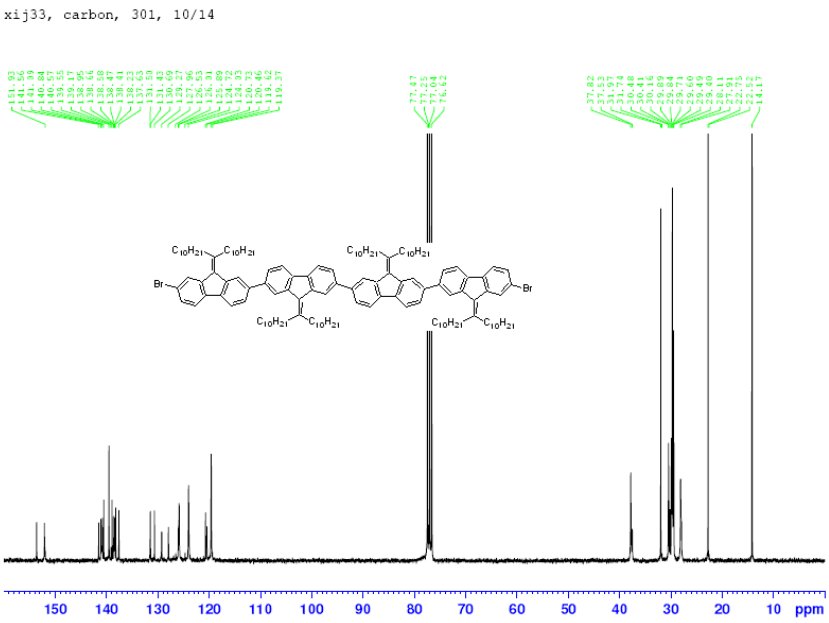

Figure 37. ^{13}C NMR spectrum of Br-(AF)$_4$-Br ($CDCl_3$, 75 MHz).

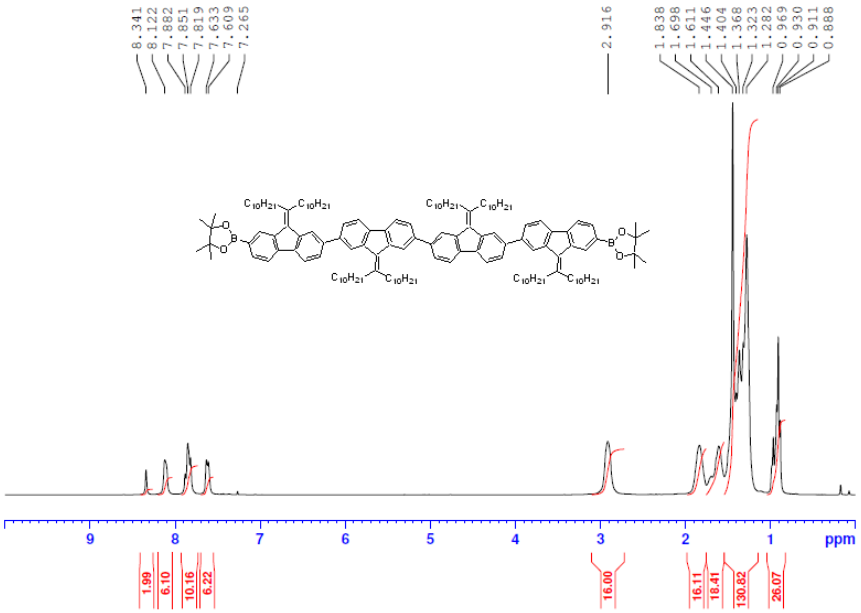

Figure 38. ^{1}H NMR spectrum of B-(AF)$_4$-B ($CDCl_3$, 300 MHz).

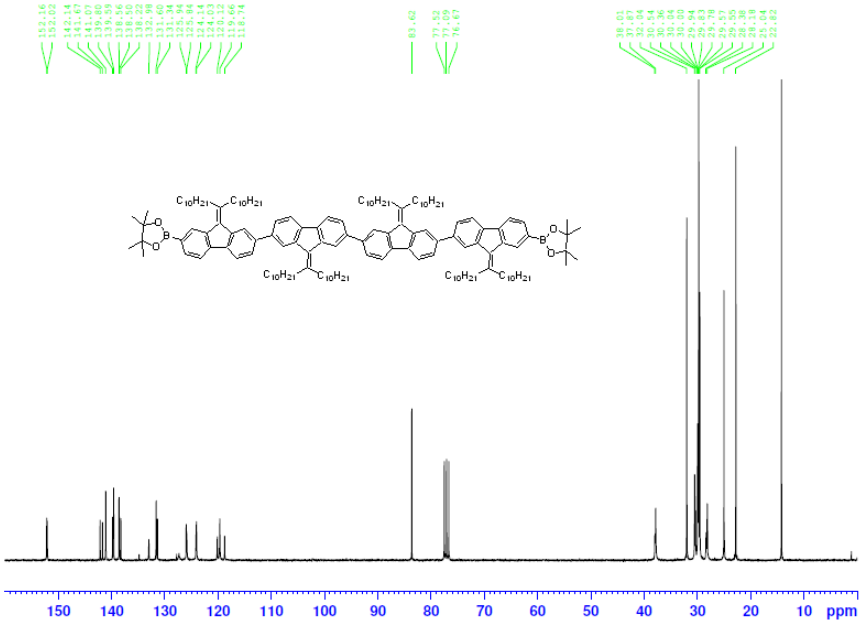

Figure 39. ^{13}C NMR spectrum of B-(AF)$_4$-B ($CDCl_3$, 75 MHz).

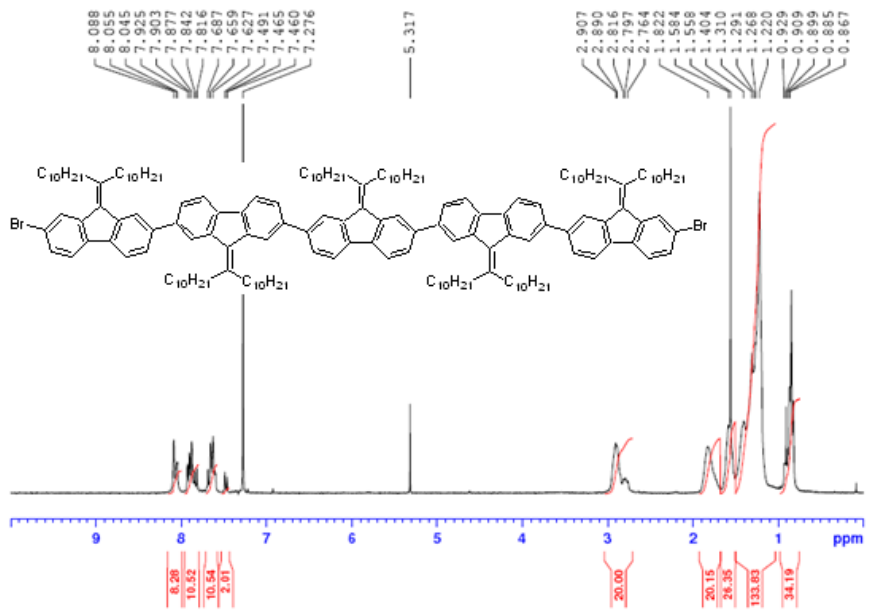

Figure 40. ^{1}H NMR spectrum of Br-(AF)$_5$-Br ($CDCl_3$, 300 MHz).

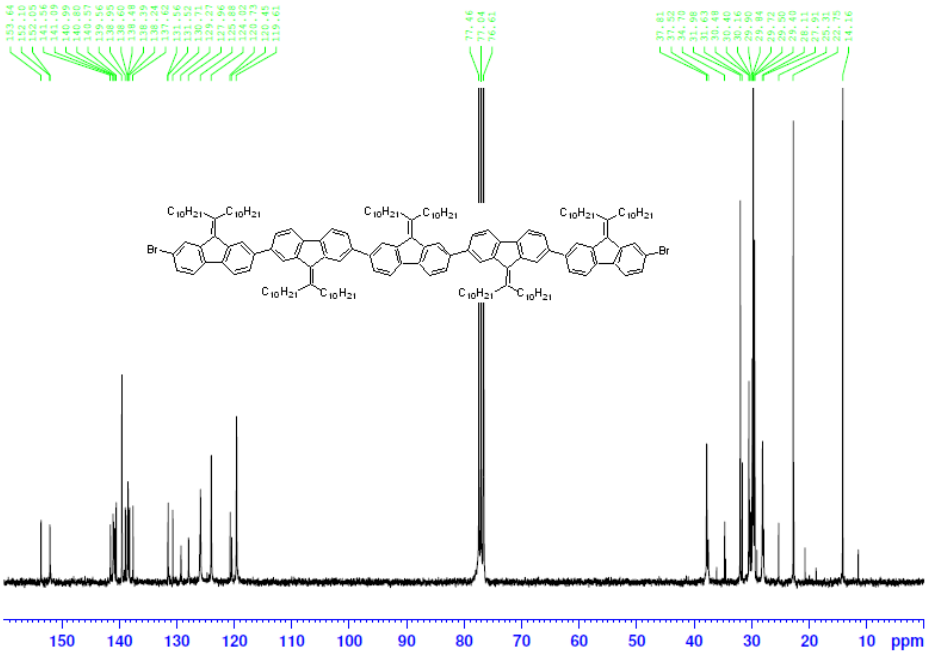

Figure 41. ^{13}C NMR spectrum of Br-(AF)$_5$-Br ($CDCl_3$, 75 MHz).

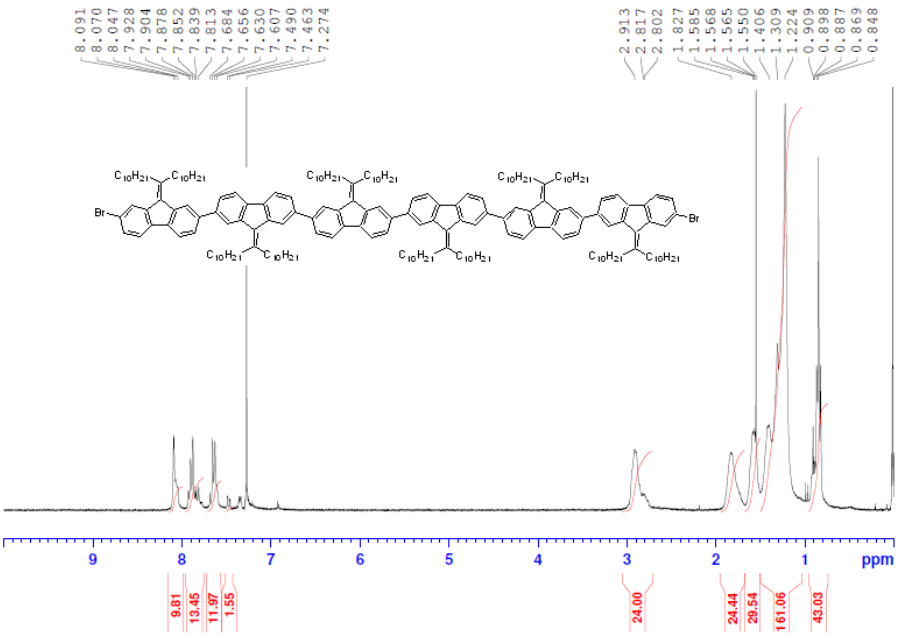

Figure 42. ^{1}H NMR spectrum of Br-(AF)$_6$-Br ($CDCl_3$, 300 MHz).

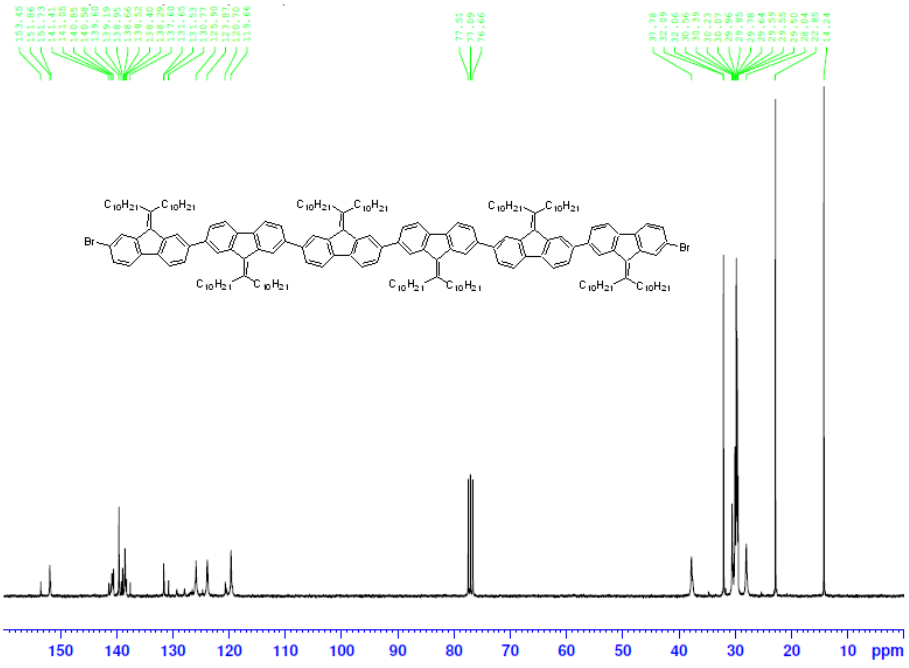

Figure 43. ^{13}C NMR spectrum of Br-(AF)$_6$-Br ($CDCl_3$, 75 MHz).

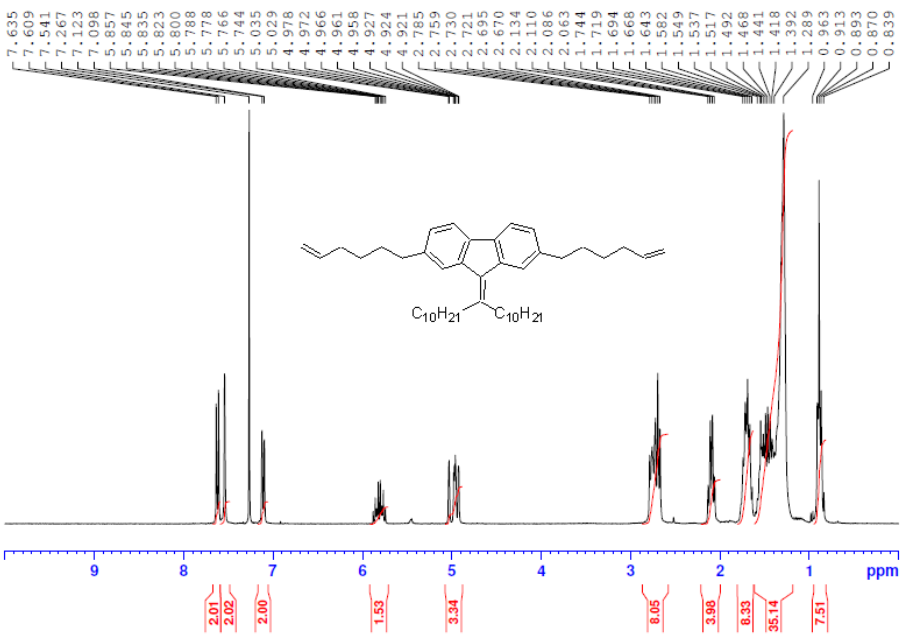

Figure 44. ^{1}H NMR spectrum of =(AF)$_1$= ($CDCl_3$, 300 MHz).

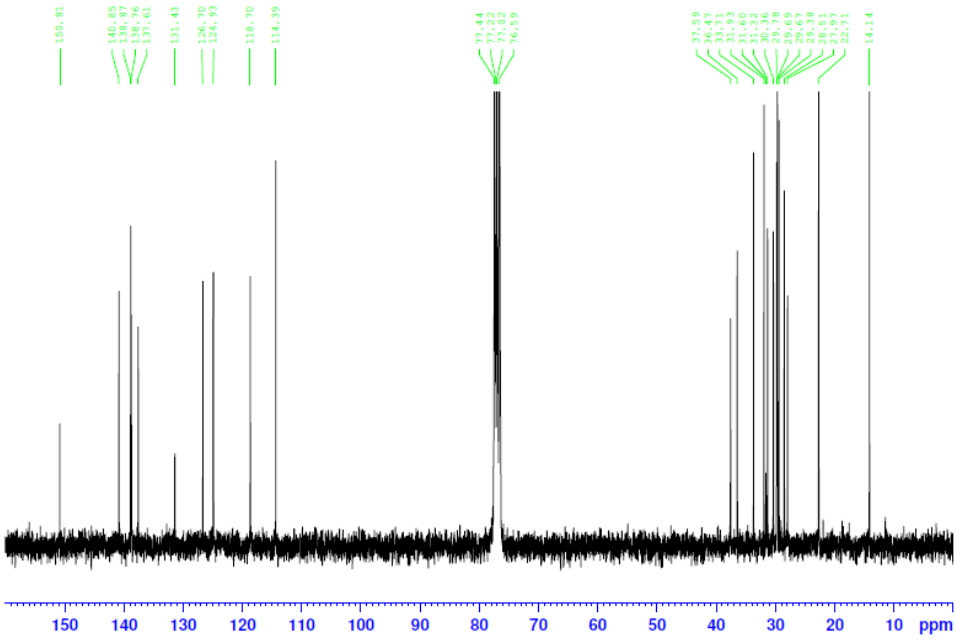

Figure 45. ^{13}C NMR spectrum of =(AF)$_1$= ($CDCl_3$, 75 MHz).

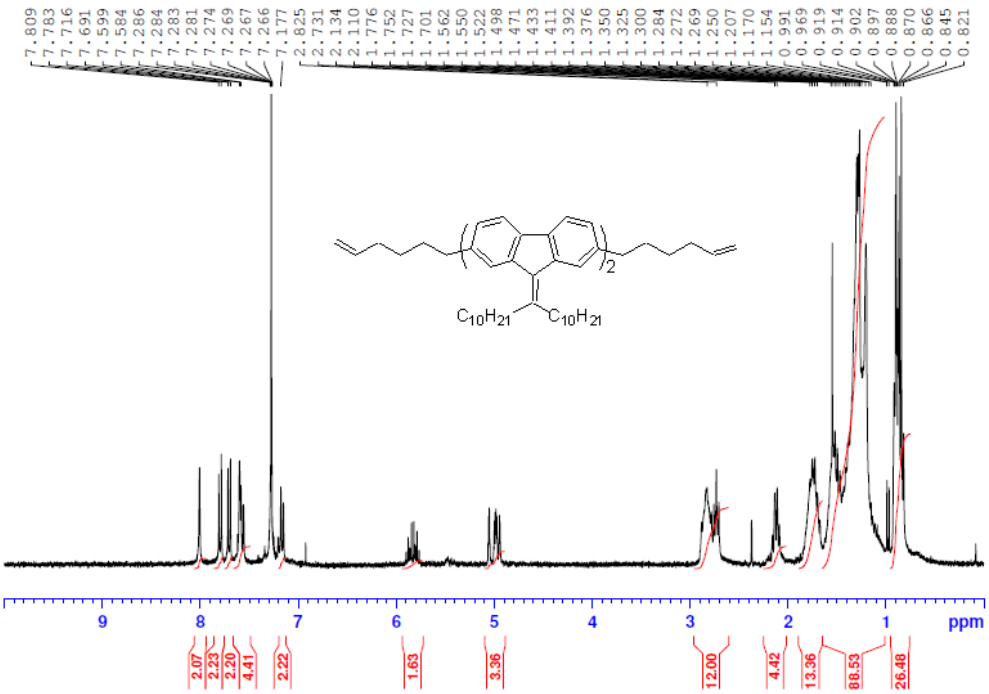

Figure 46. ^{1}H NMR spectrum of =(AF)$_2$= (CDCl$_3$, 300 MHz).

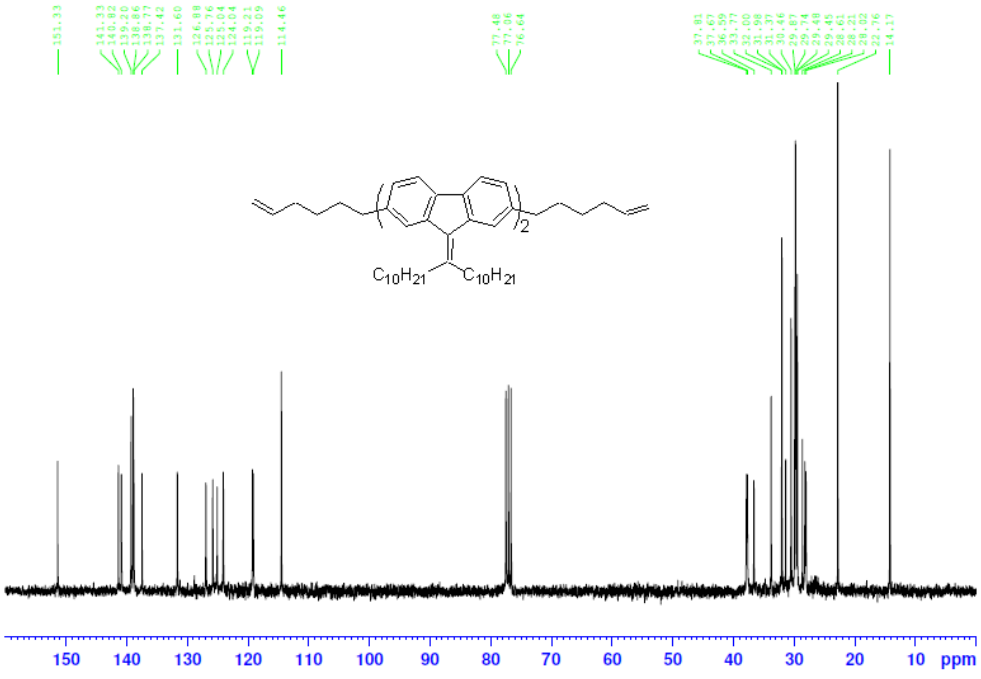

Figure 47. ^{13}C NMR spectrum of =(AF)$_2$= (CDCl$_3$, 75 MHz).

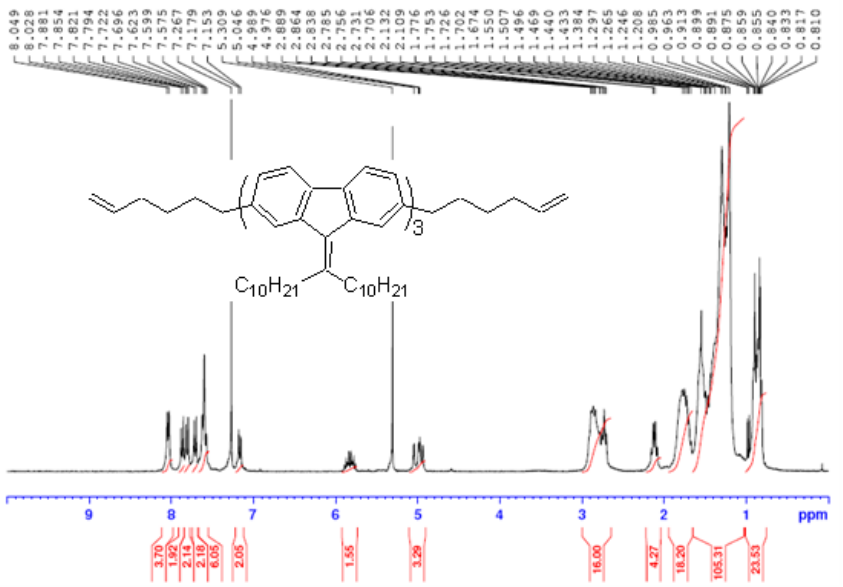

Figure 48. ^{1}H NMR spectrum of =(AF)$_3$= ($CDCl_3$, 300 MHz).

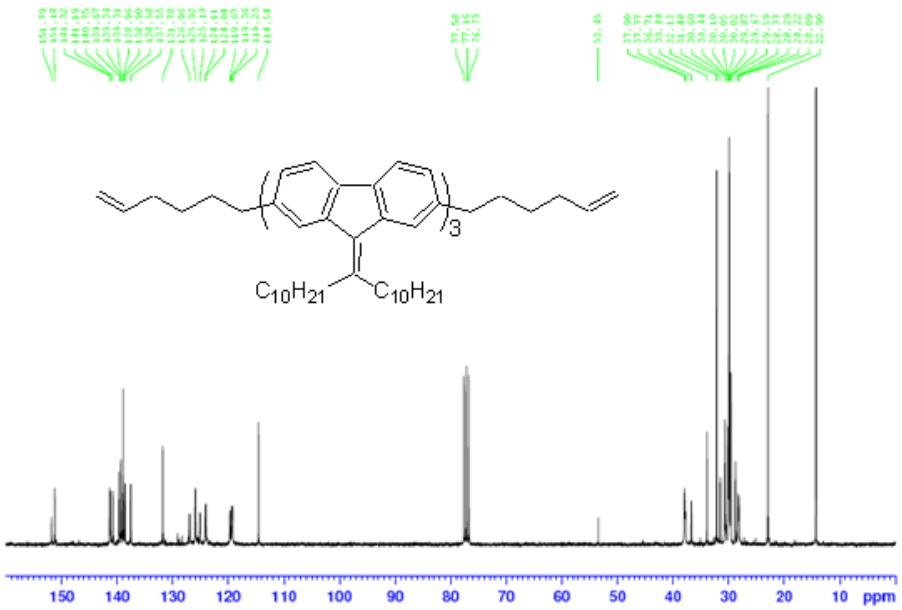

Figure 49. ^{13}C NMR spectrum of =(AF)$_3$= ($CDCl_3$, 75 MHz).

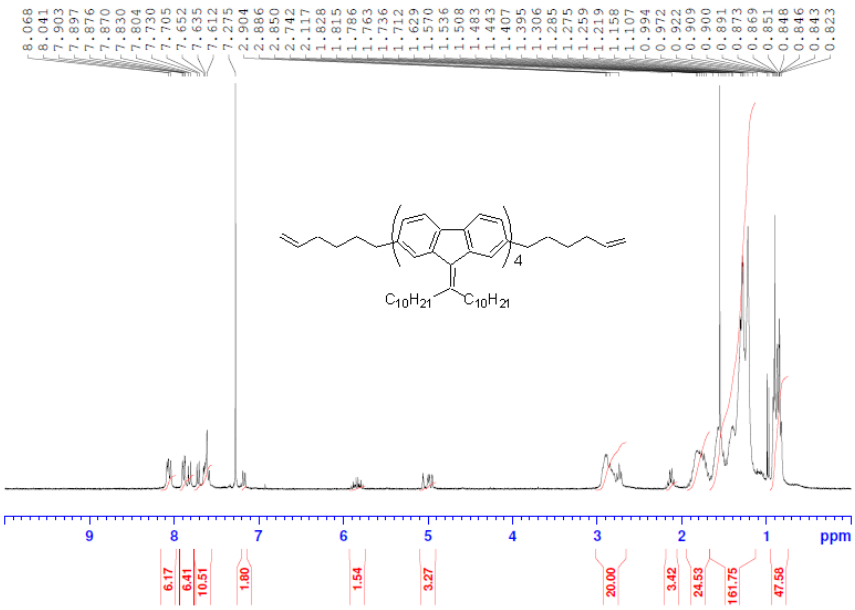

Figure 50. ^{1}H NMR spectrum of =(AF)$_4$= ($CDCl_3$, 300 MHz).

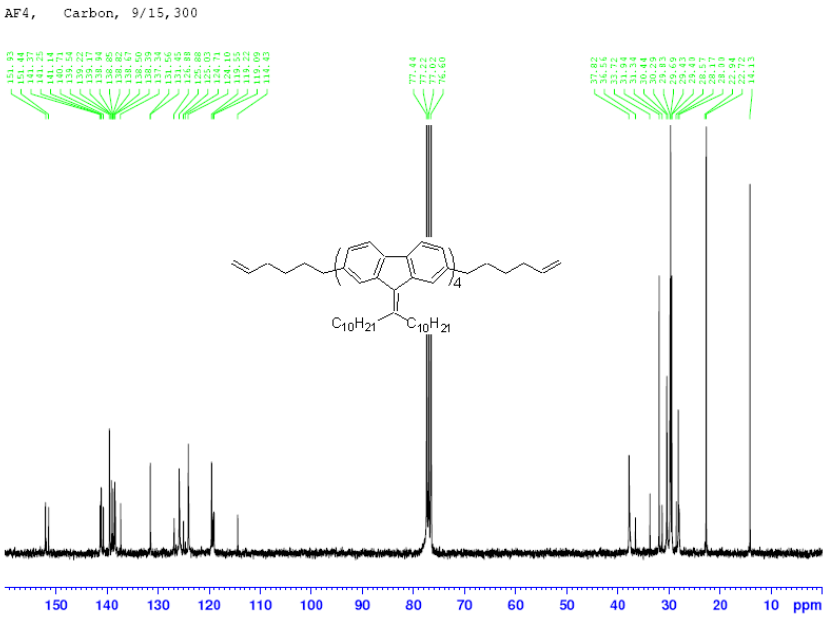

Figure 51. ^{13}C NMR spectrum of =(AF)$_4$= ($CDCl_3$,75 MHz).

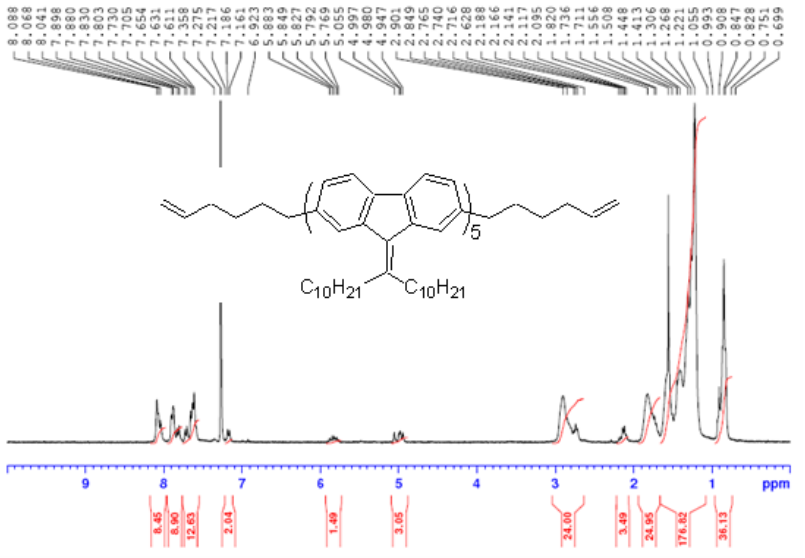

Figure 52. ^{1}H NMR spectrum of =(AF)$_5$= (CDCl$_3$, 300 MHz).

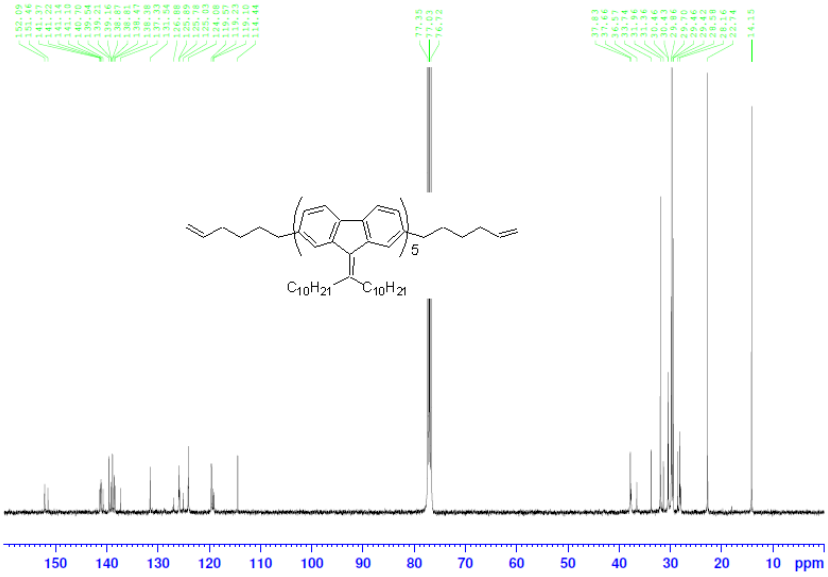

Figure 53. ^{13}C NMR spectrum of =(AF)$_5$= (CDCl$_3$, 300 MHz).

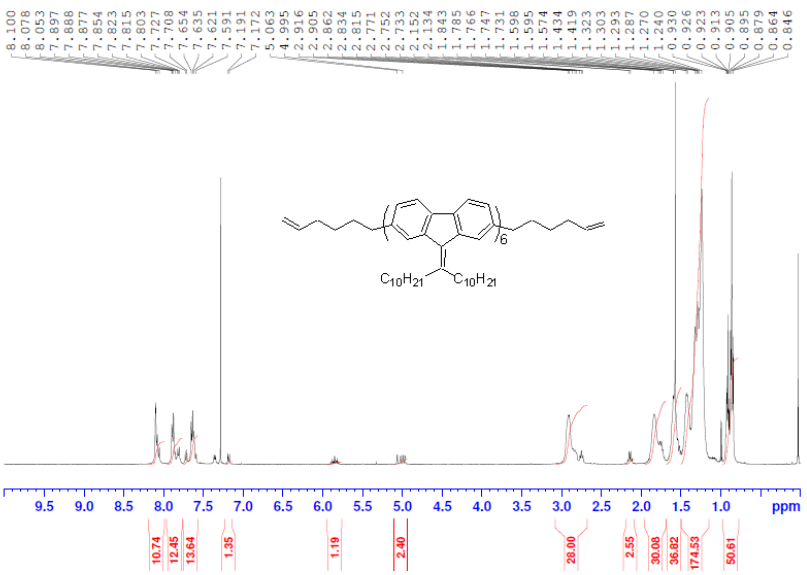

Figure 54. ^{1}H NMR spectrum of =(AF)$_6$= ($CDCl_3$, 300 MHz).

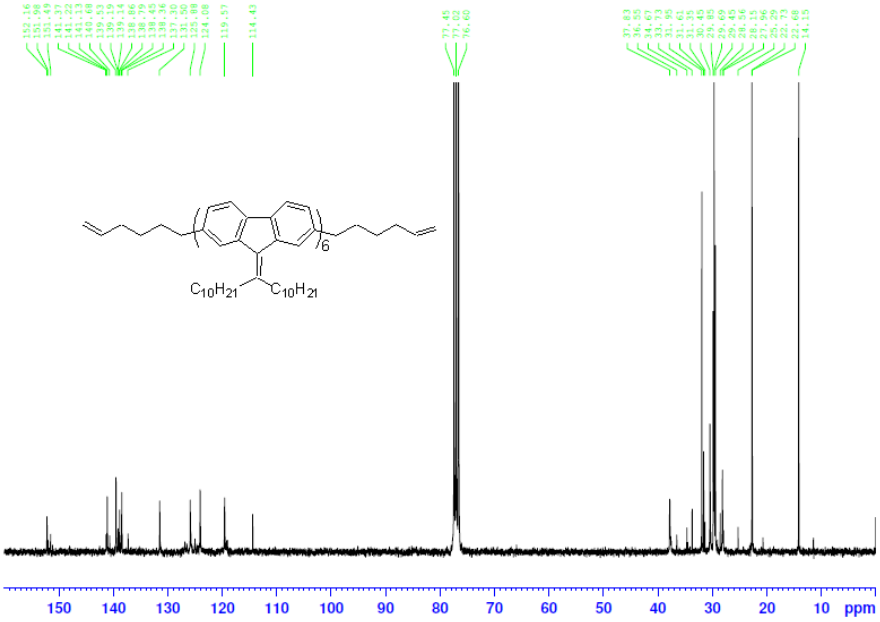

Figure 55. ^{13}C NMR spectrum of =(AF)$_6$= ($CDCl_3$, 75 MHz).

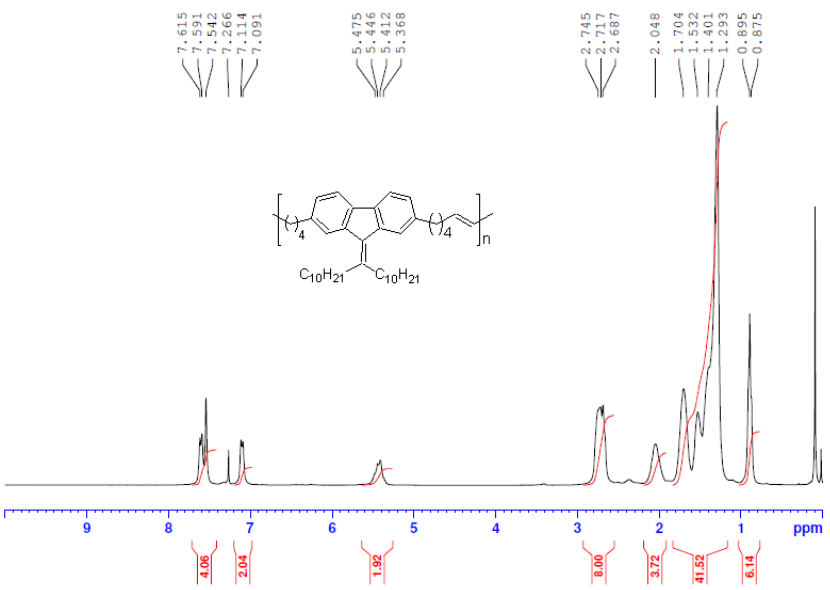

Figure 56. ^{1}H NMR spectrum of P(AF)$_1$M$_4$=M$_4$ (CDCl$_3$, 300 MHz).

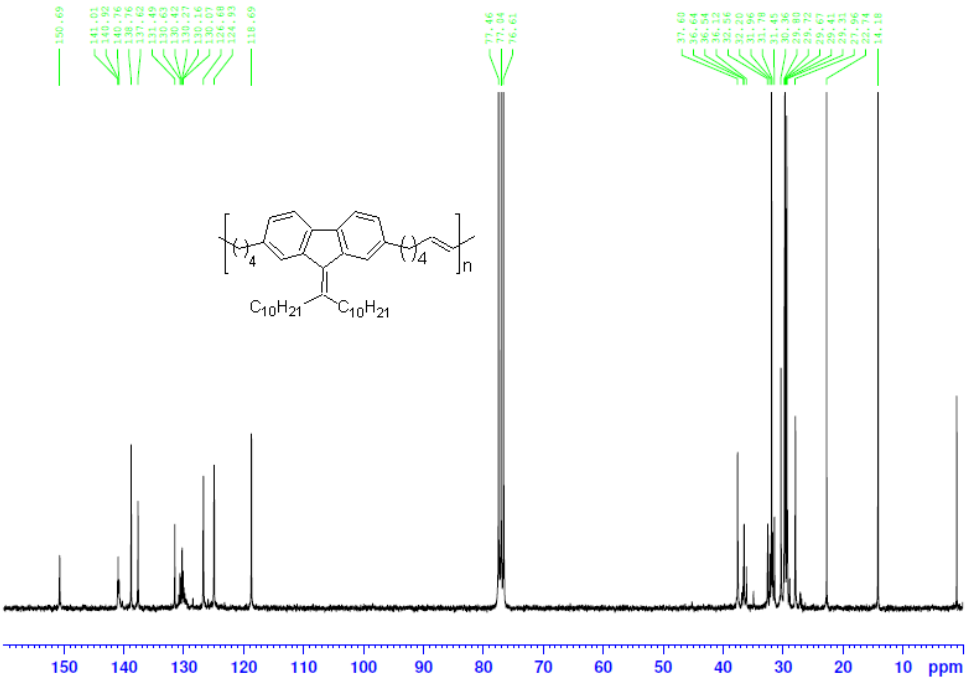

Figure 57. ^{13}C NMR spectrum of P(AF)$_1$M$_4$=M$_4$ (CDCl$_3$, 75 MHz).

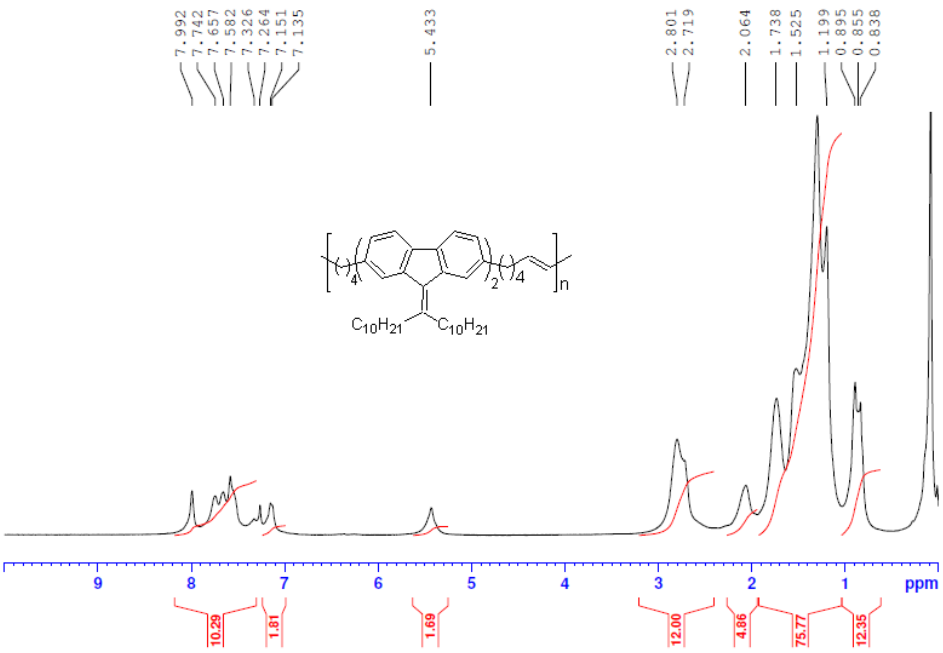

Figure 58. ^{1}H NMR spectrum of P(AF)$_2$M$_4$=M$_4$ (CDCl$_3$, 300 MHz).

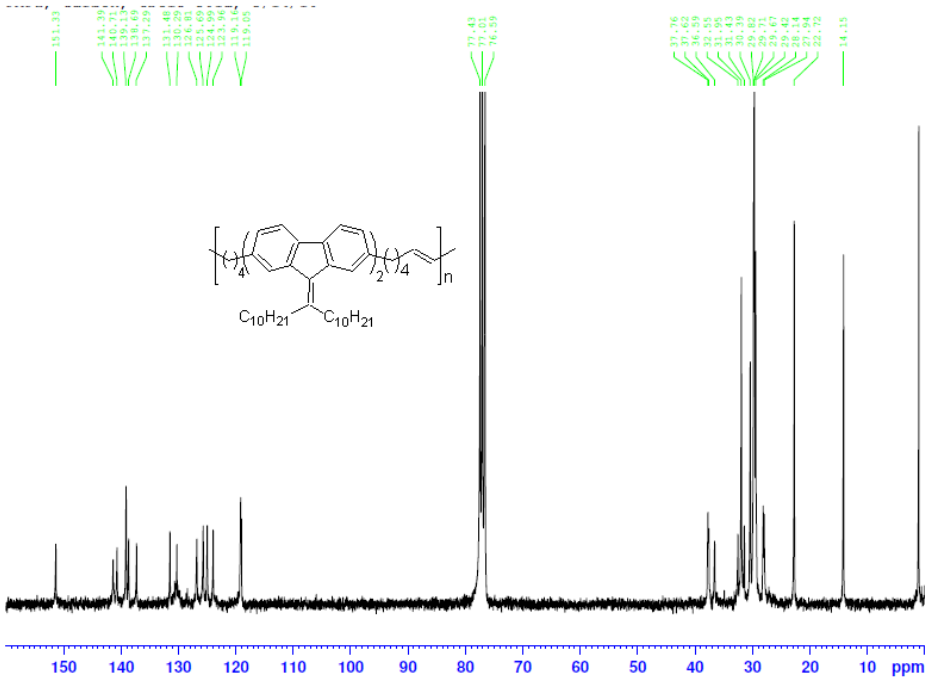

Figure 59. ^{13}C NMR spectrum of P(AF)$_2$M$_4$=M$_4$ (CDCl$_3$, 75 MHz).

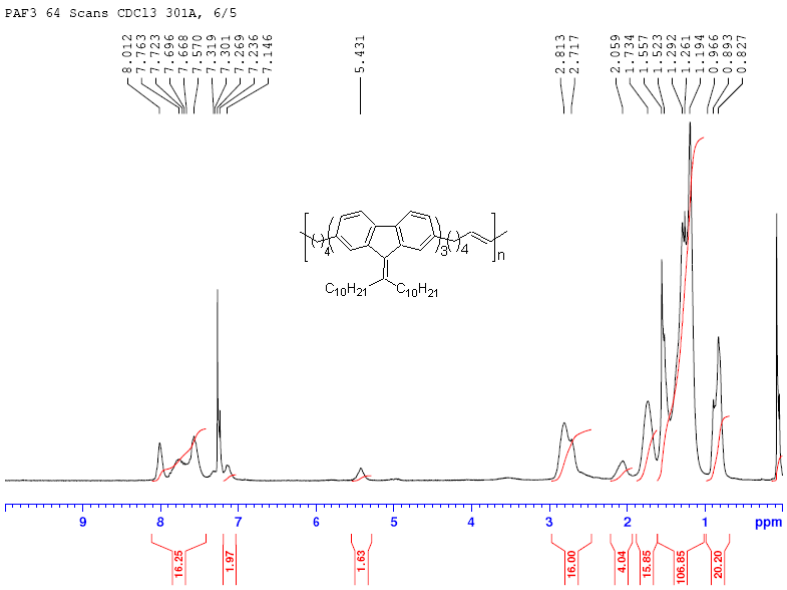

Figure 60. ^{1}H NMR spectrum of P(AF)$_3$M$_4$=M$_4$ (CDCl$_3$, 300 MHz).

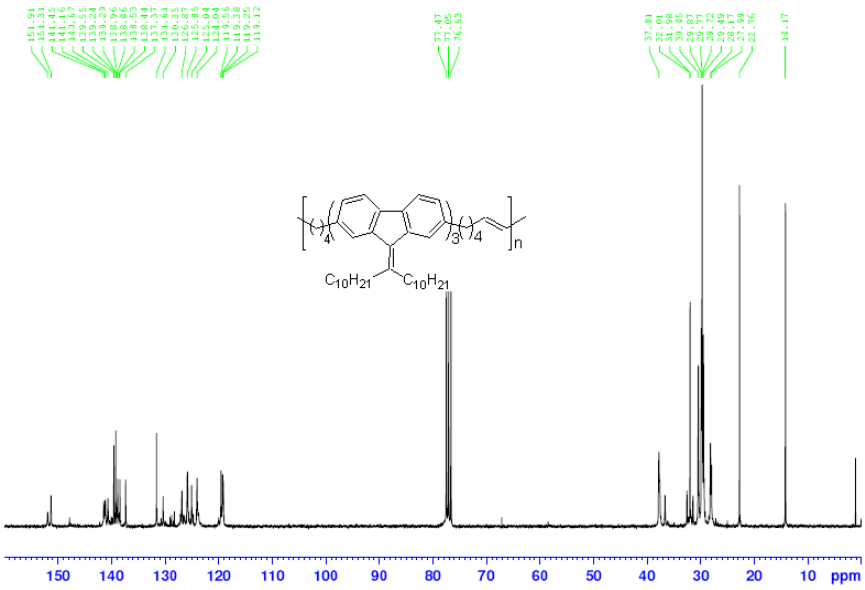

Figure 61. ^{13}C NMR spectrum of P(AF)$_3$M$_4$=M$_4$ (CDCl$_3$, 75 MHz).

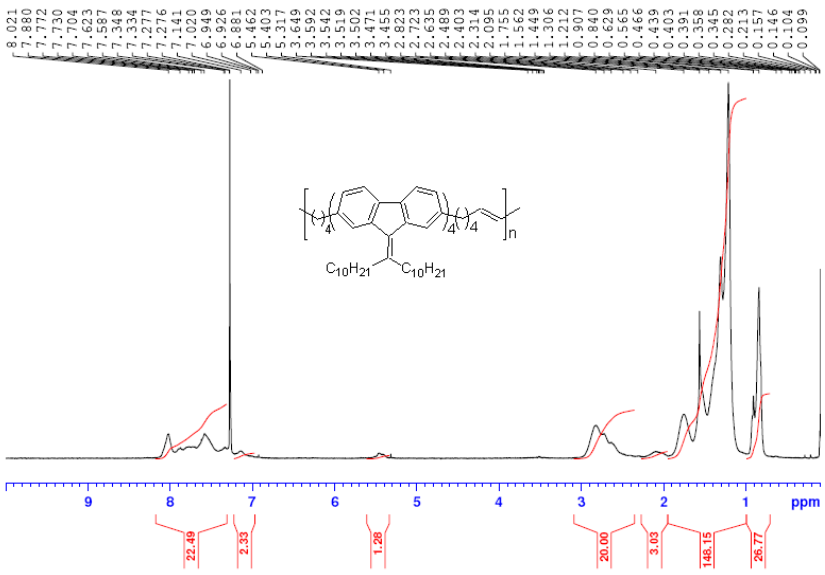

Figure 62. ^{1}H NMR spectrum of P(AF)$_4$M$_4$=M$_4$ (CDCl$_3$, 300 MHz).

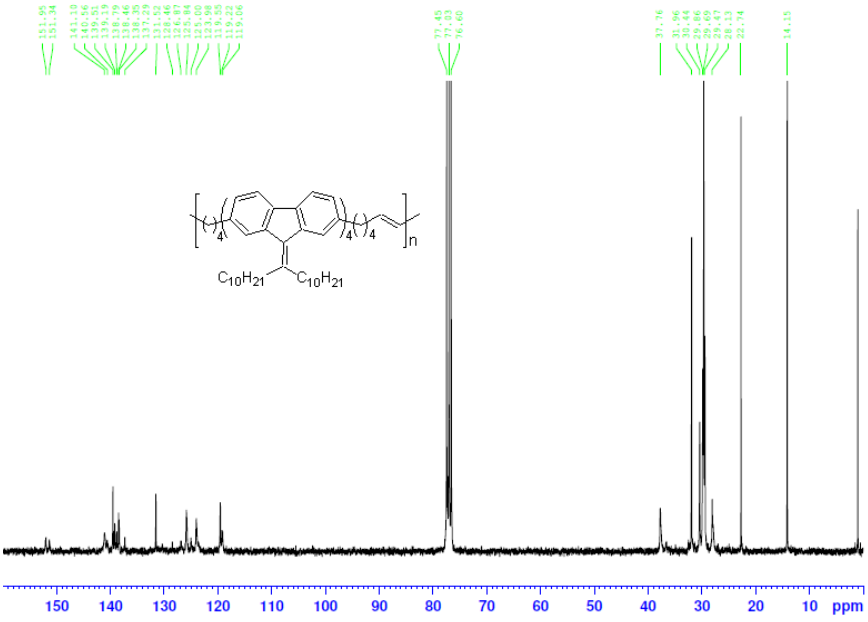

Figure 63. ^{13}C NMR spectrum of P(AF)$_4$M$_4$=M$_4$ (CDCl$_3$, 75 MHz).

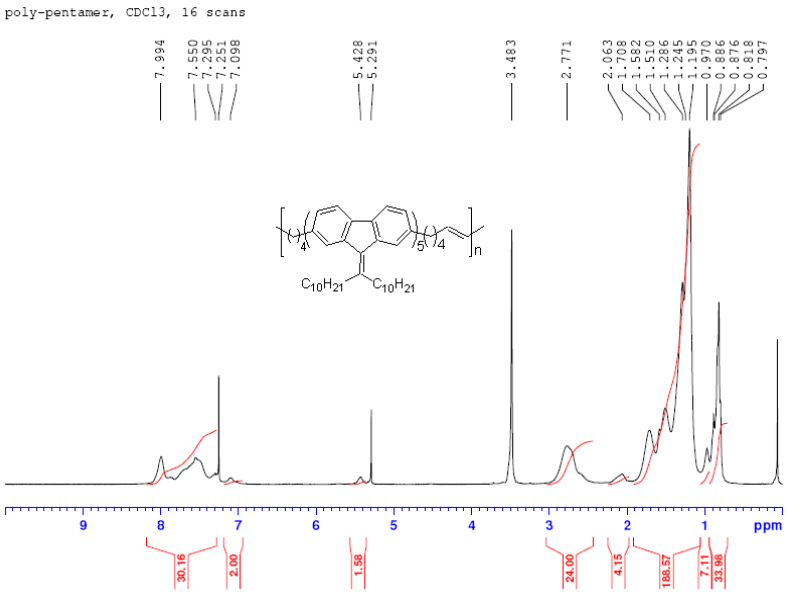

Figure 64. ^{1}H NMR spectrum of P(AF)$_5$M$_4$=M$_4$ (CDCl$_3$, 300 MHz).

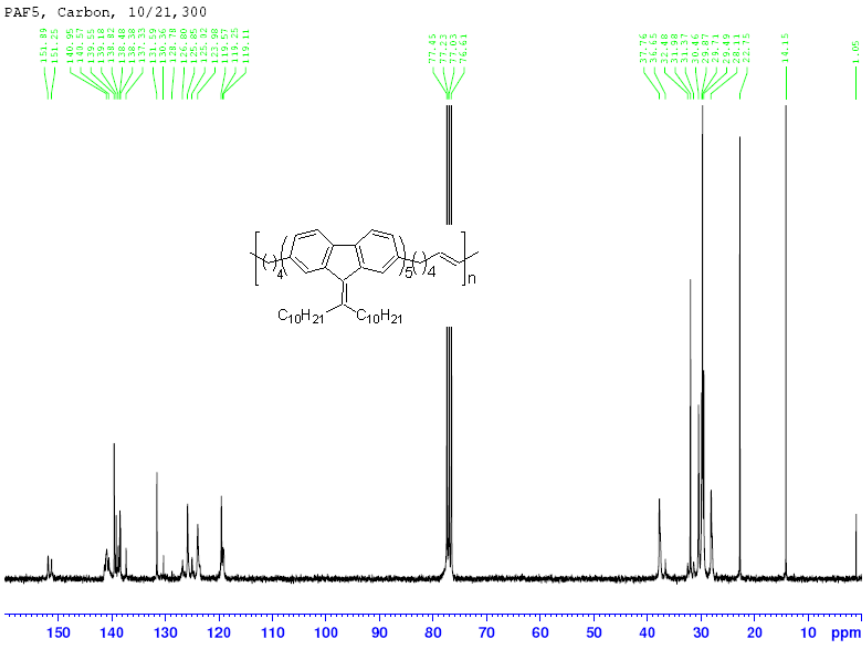

Figure 65. ^{13}C NMR spectrum of P(AF)$_5$M$_4$=M$_4$ (CDCl$_3$, 75 MHz).

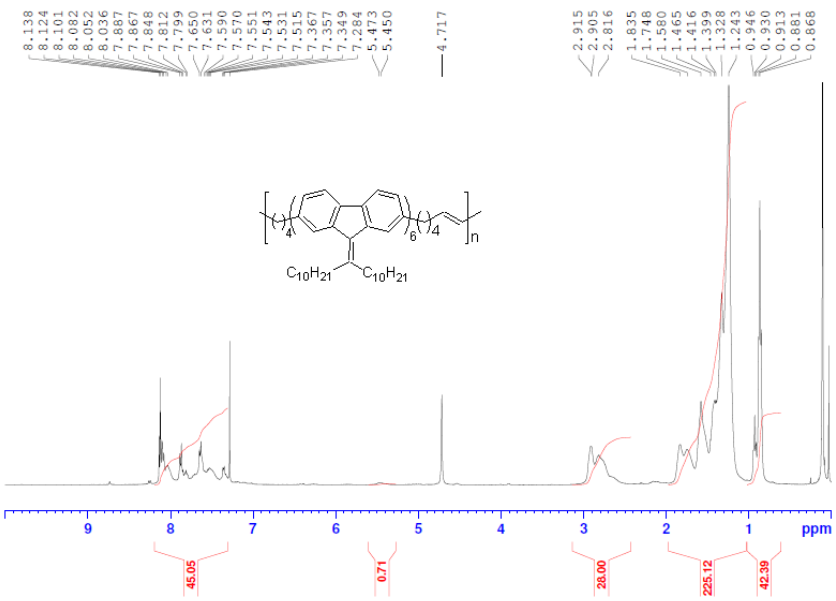

Figure 66. ^{1}H NMR spectrum of P(AF)$_6$M$_4$=M$_4$ (CDCl$_3$, 400 MHz).

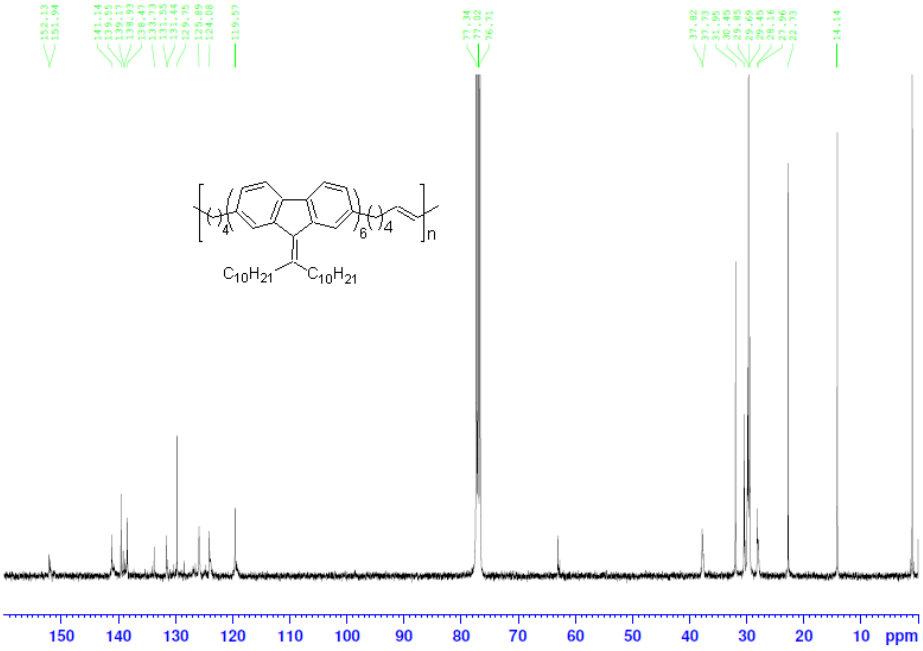

Figure 67. ^{13}C NMR spectrum of P(AF)$_6$M$_4$=M$_4$ (CDCl$_3$, 100 MHz).

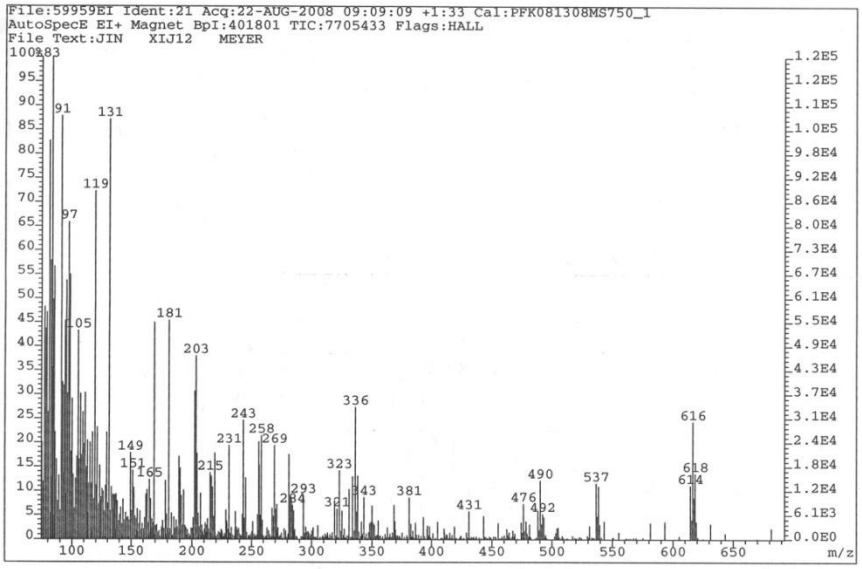

Figure 68. Mass spectrum of Br-AF-Br.

APPENDIX B

GPC TRACES OF $P(AF)_xM_4=M_4$

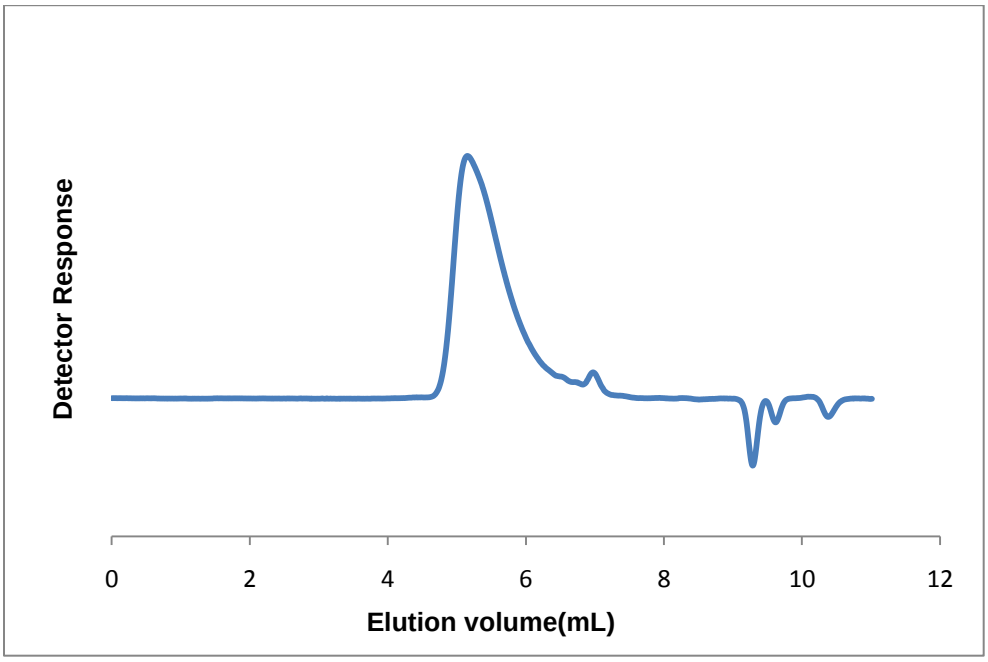

Figure 69. GPC chromatograph of $P(AF)_1M_4=M_4$ performed in chloroform at RT.

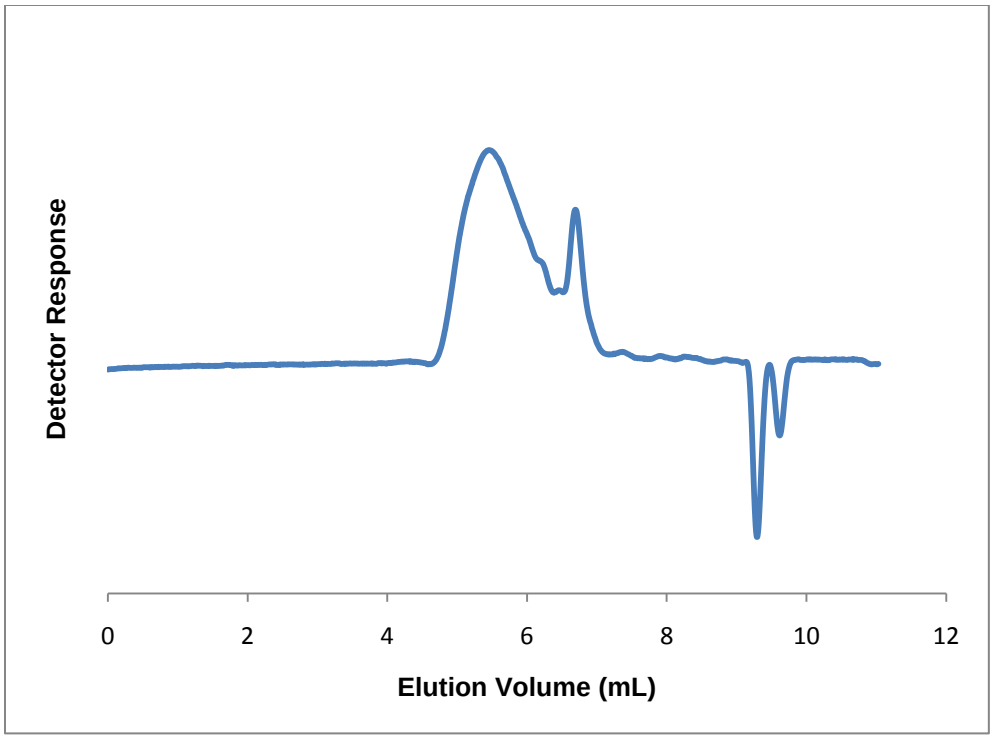

Figure 70. GPC chromatograph of $P(AF)_2M_4{=}M_4$ performed in chloroform at RT.

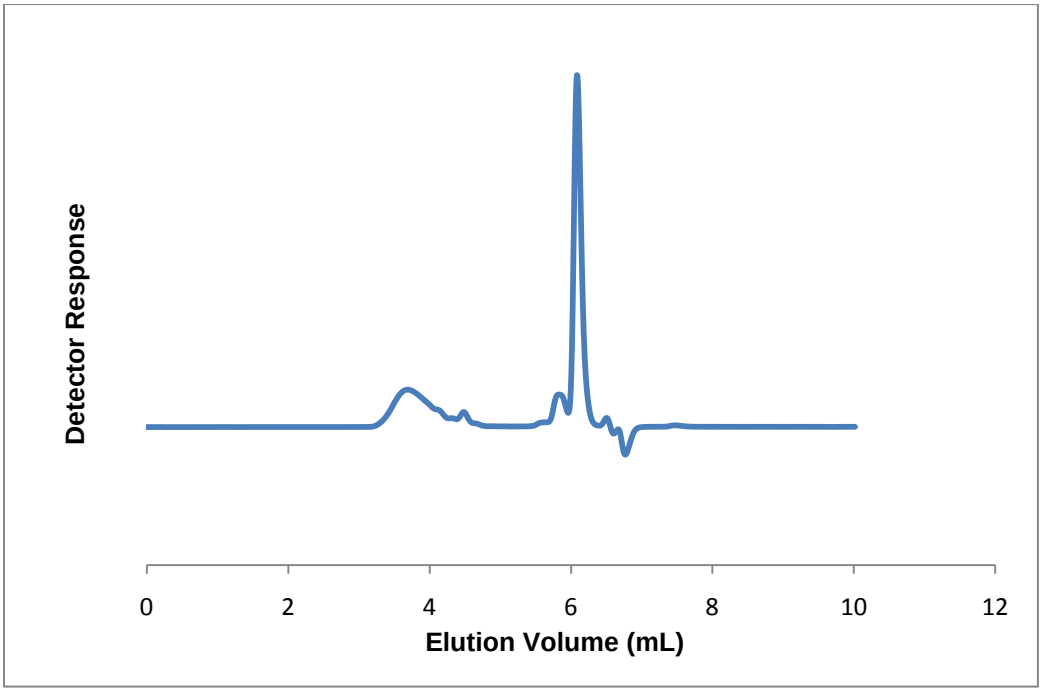

Figure 71. GPC chromatograph of $P(AF)_3M_4{=}M_4$ performed in THF at RT.

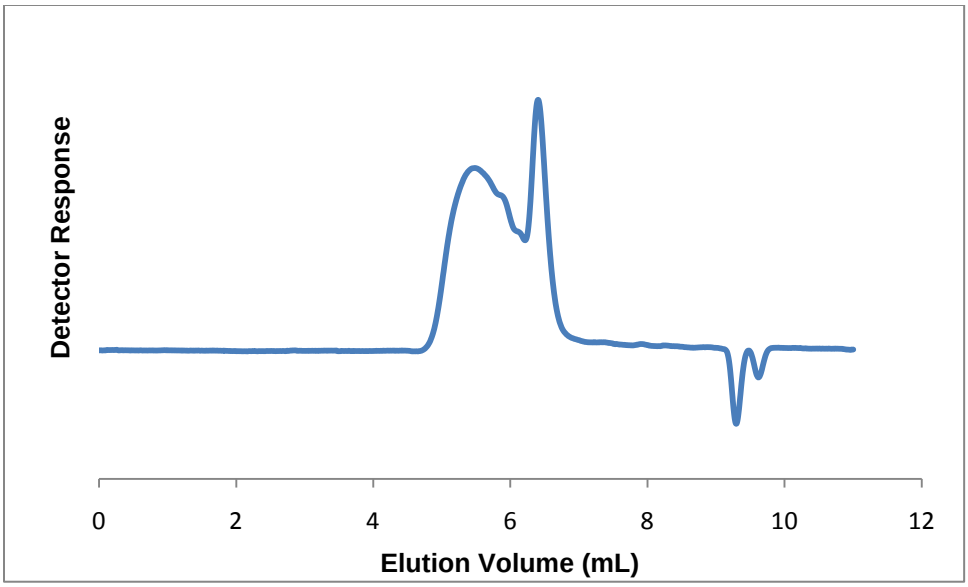

Figure 72. GPC chromatograph of $P(AF)_4M_4=M_4$ performed in chloroform at RT.

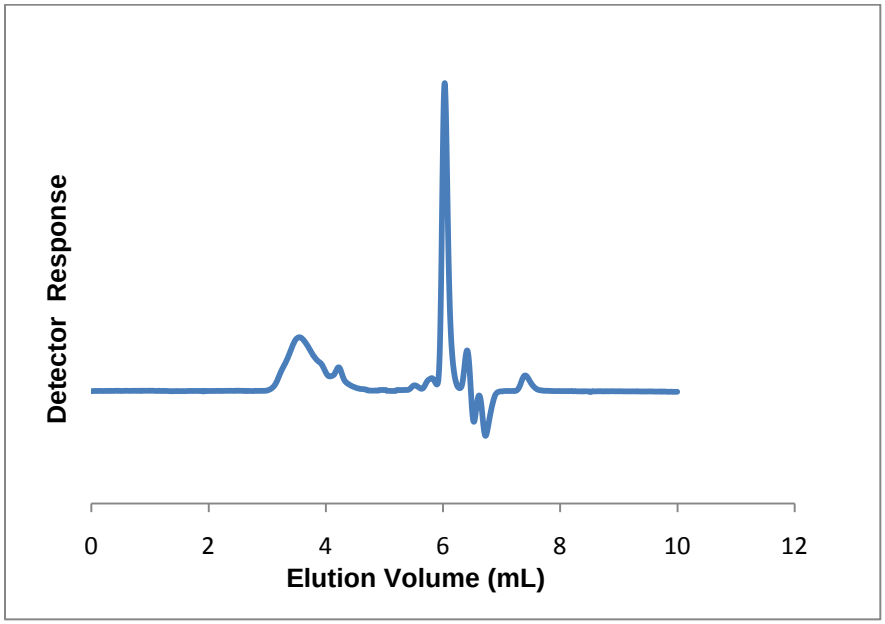

Figure 73. GPC chromatograph of $P(AF)_5M_4=M_4$ performed in THF at RT.

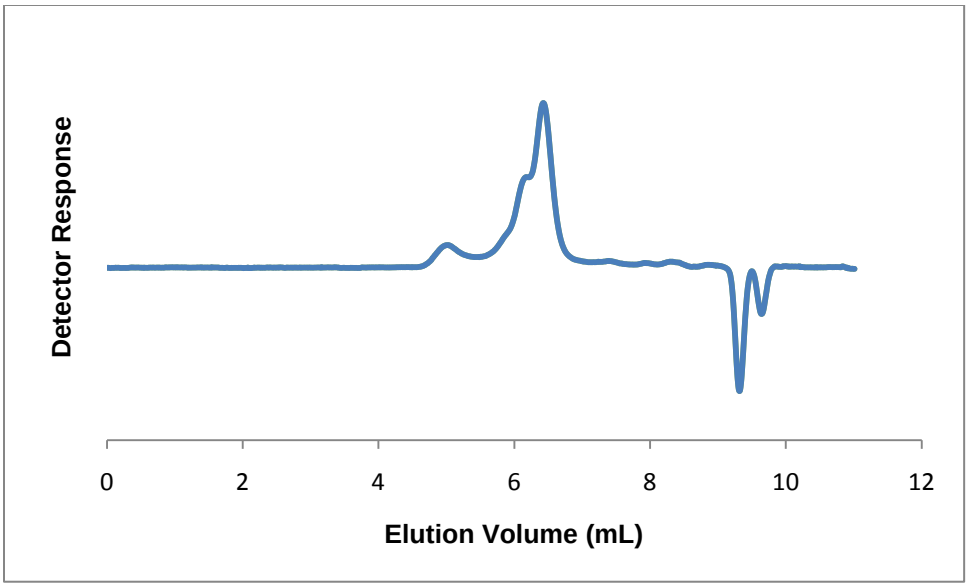

Figure 74. GPC chromatograph of $P(AF)_6M_4=M_4$ performed in chloroform at RT.

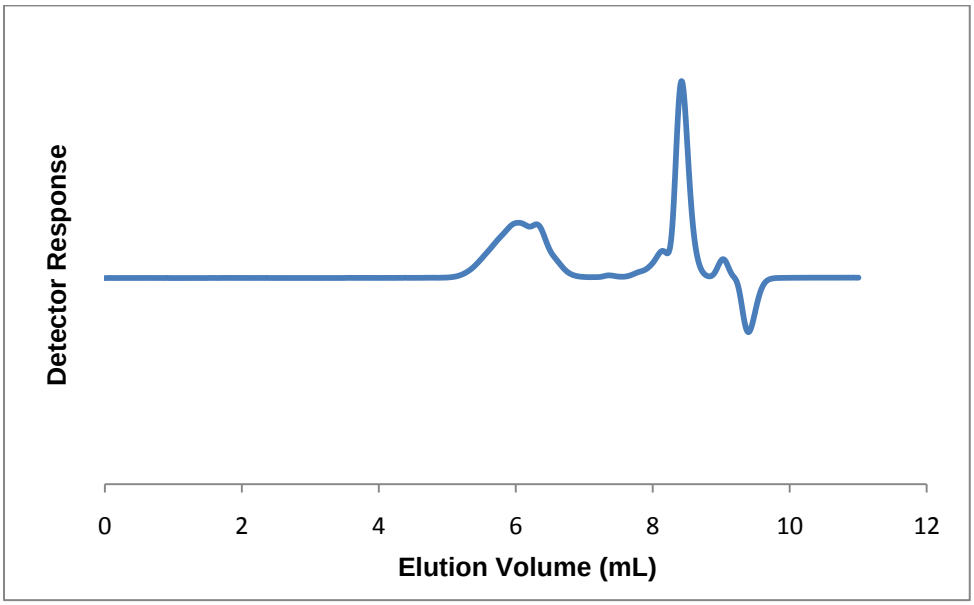

Figure 75. GPC chromatograph of P(25% AF3 : 75% AF5) performed in THF at RT.

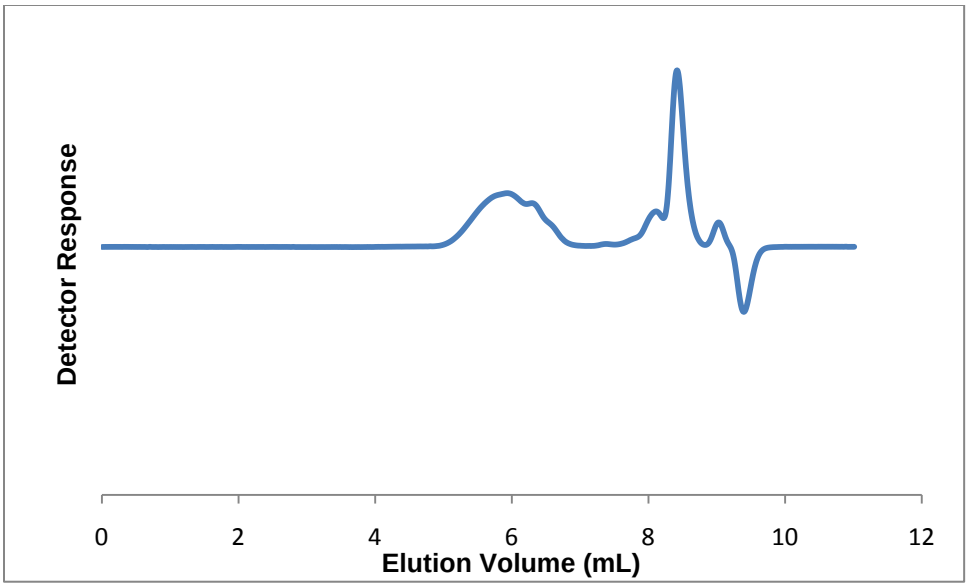

Figure 76. GPC chromatograph of P(50% AF3 : 50% AF5) performed in THF at RT.

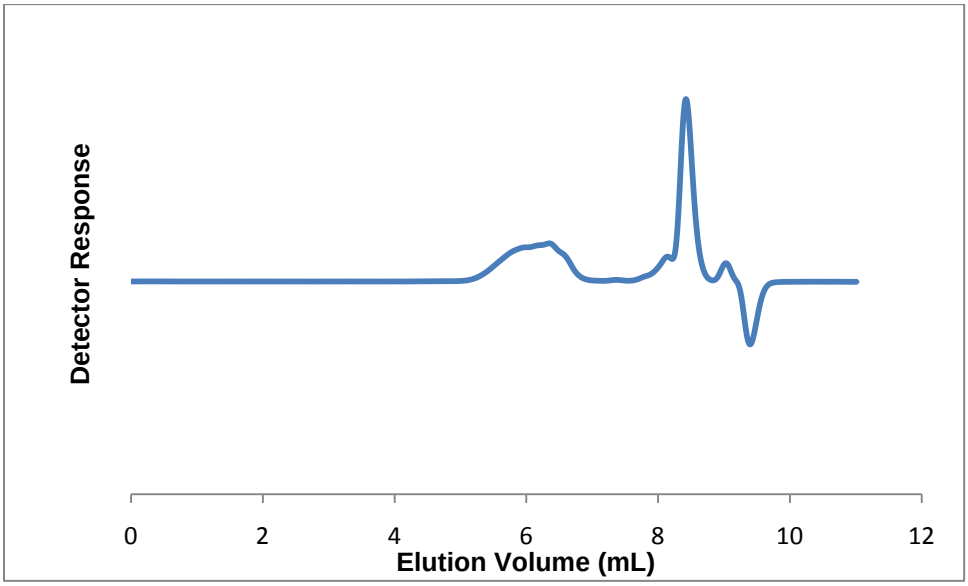

Figure 77. GPC chromatograph of P(75% AF3 : 25% AF5) performed in THF at RT.

APPENDIX C

DSC TRACES OF $P(AF)_xM_4=M_4$

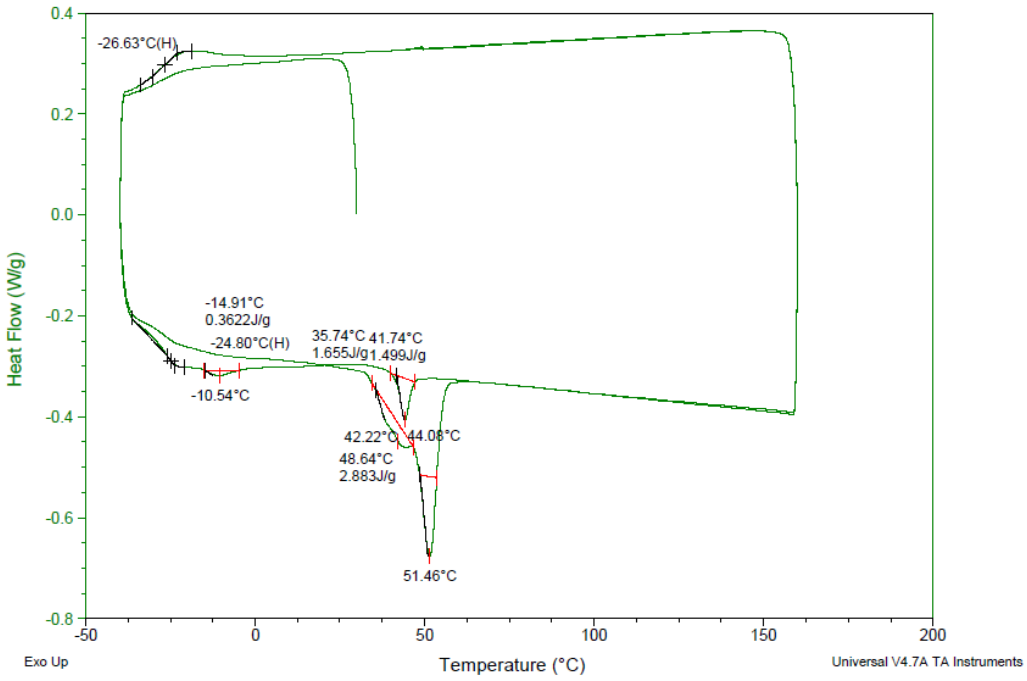

Figure 78. DSC trace of $P(AF)_1M_4=M_4$ with a scan rate of 10 ℃/min performed by TA DSC Q200.

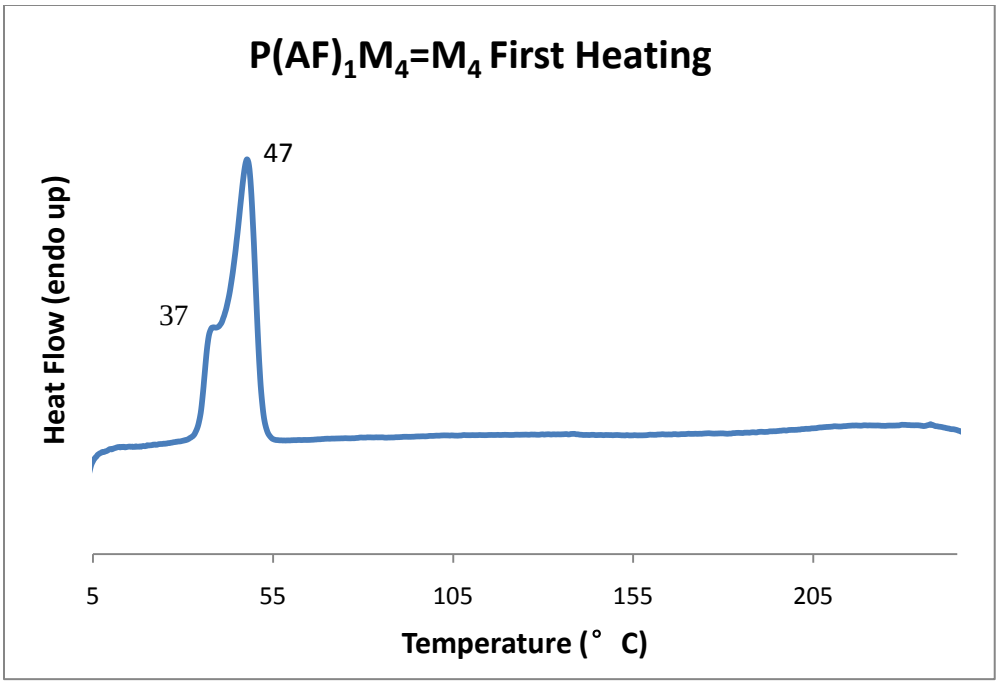

Figure 79. The first heating DSC trace of $P(AF)_1M_4=M_4$ with a scan rate of 10 ℃/min performed by Perkin-Elmer Pyris 6 (2nd heating and both cooling scans were not well behaved).

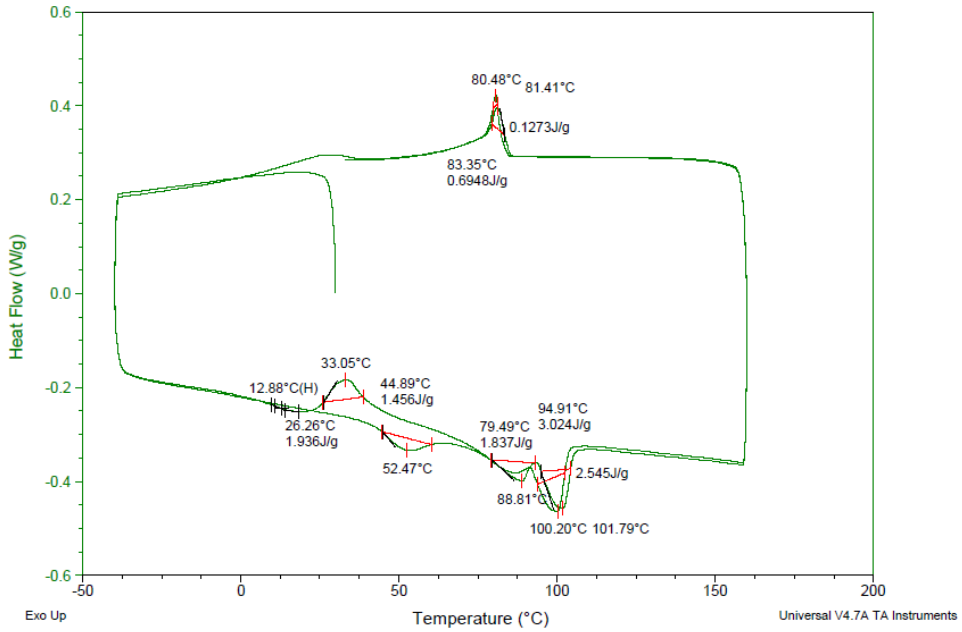

Figure 80. DSC trace of $P(AF)_2M_4=M_4$ with a scan rate of 10 ℃/min performed by TA DSC Q200.

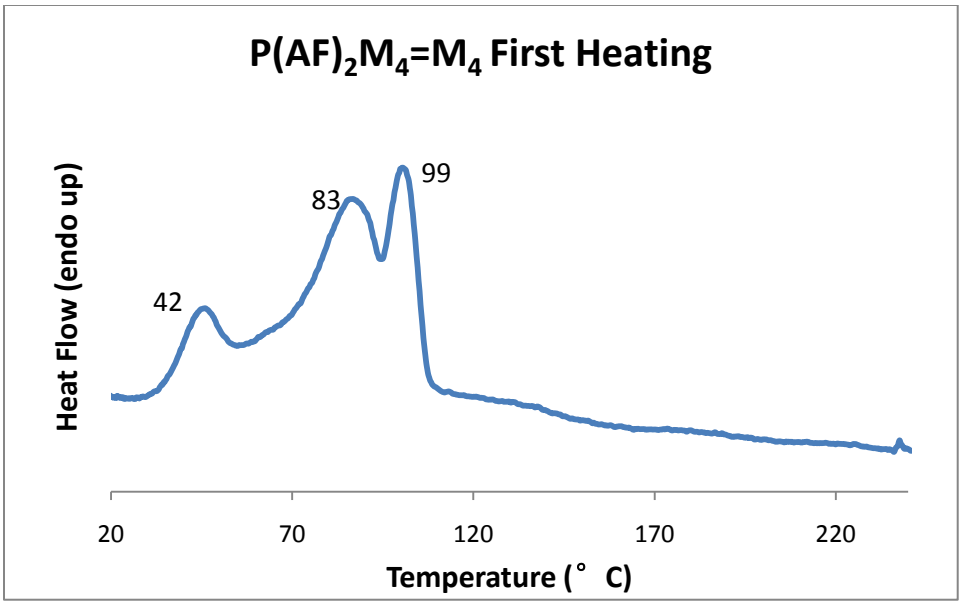

Figure 81. The first heating DSC trace of $P(AF)_2M_4=M_4$ with a scan rate of 10 ℃/min performed by Perkin-Elmer Pyris 6.

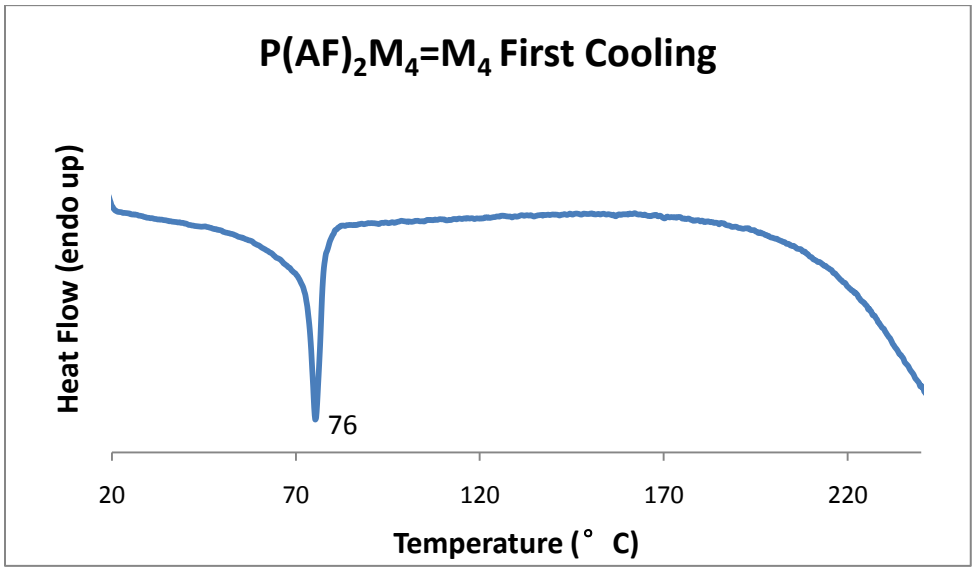

Figure 82. The first cooling DSC trace of $P(AF)_2M_4=M_4$ with a scan rate of 10 ℃/min performed by Perkin-Elmer Pyris 6.

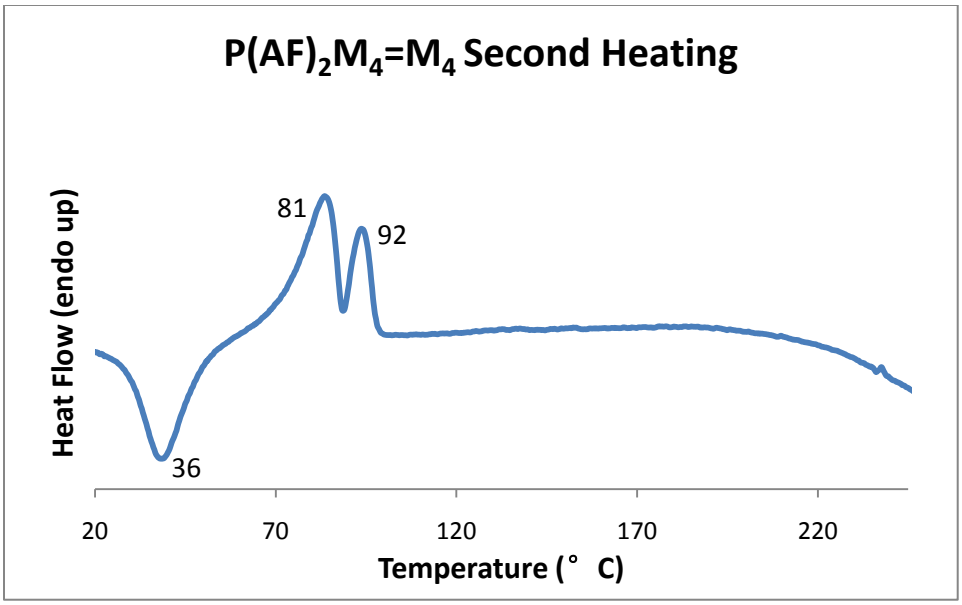

Figure 83. The second heating DSC trace of $P(AF)_2M_4=M_4$ with a scan rate of 10 ℃/min performed by Perkin-Elmer Pyris 6.

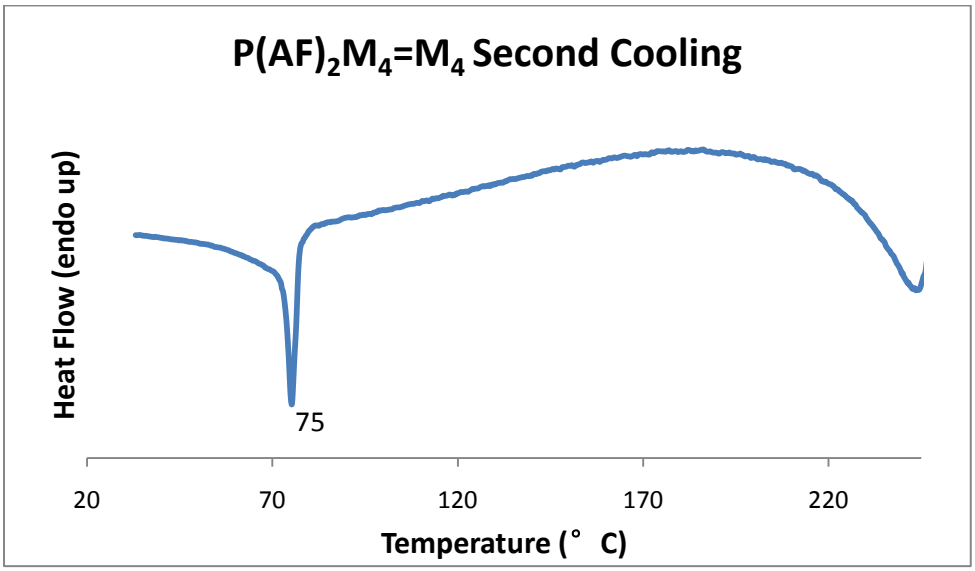

Figure 84. The first cooling DSC trace of $P(AF)_2M_4=M_4$ with a scan rate of 10 ℃/min performed by Perkin-Elmer Pyris 6.

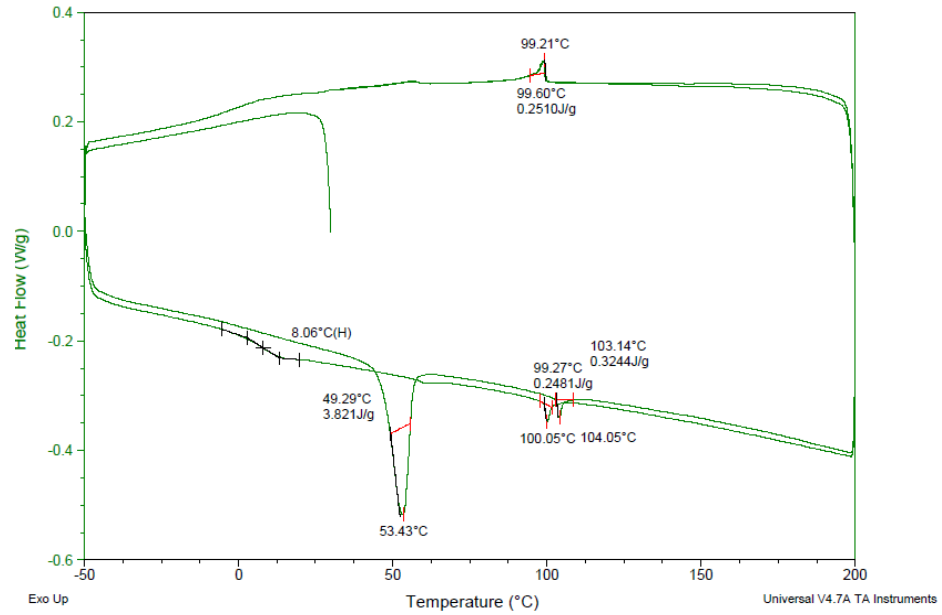

Figure 85. DSC trace of $P(AF)_3M_4=M_4$ with a scan rate of 10 ℃/min performed by TA DSC Q200.

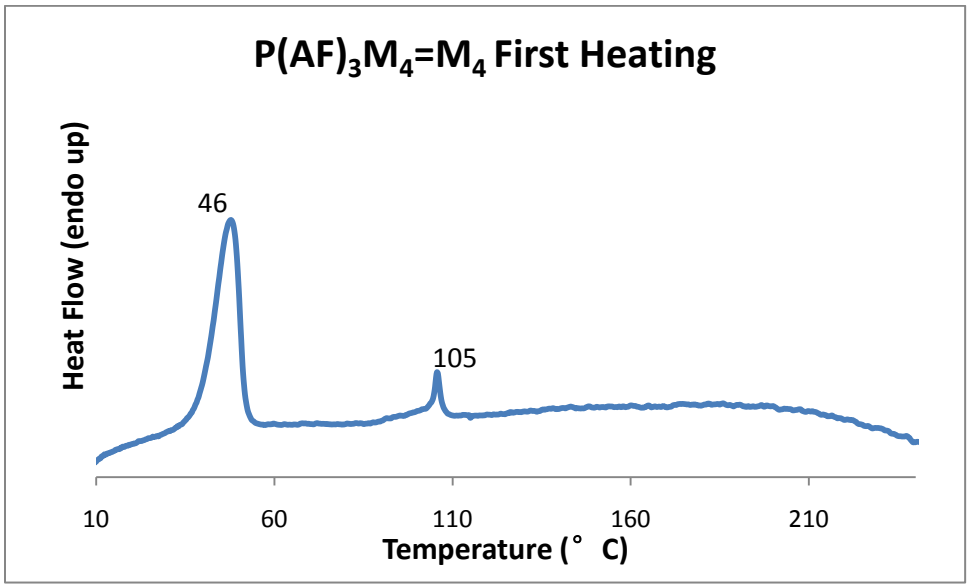

Figure 86. The first heating DSC trace of $P(AF)_3M_4=M_4$ with a scan rate of 10 ℃/min performed by Perkin-Elmer Pyris 6 (2nd heating and both cooling scans were not well behaved).

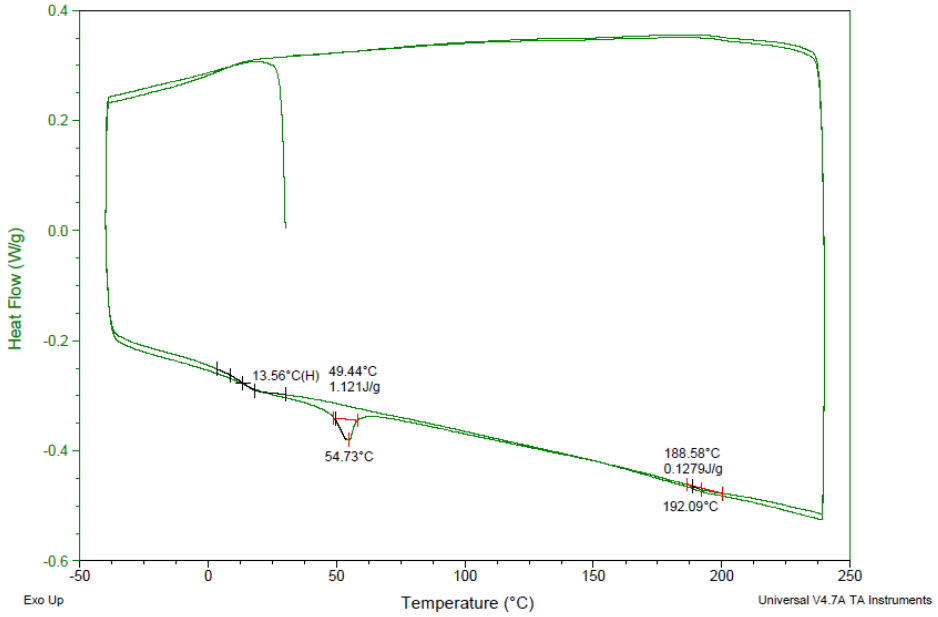

Figure 87. DSC trace of $P(AF)_4M_4=M_4$ with a scan rate of 10 ℃/min performed byTA DSC Q200 (Both heating and cooling scans performed by Perkin-Elmer Pyris 6 were not well behaved).

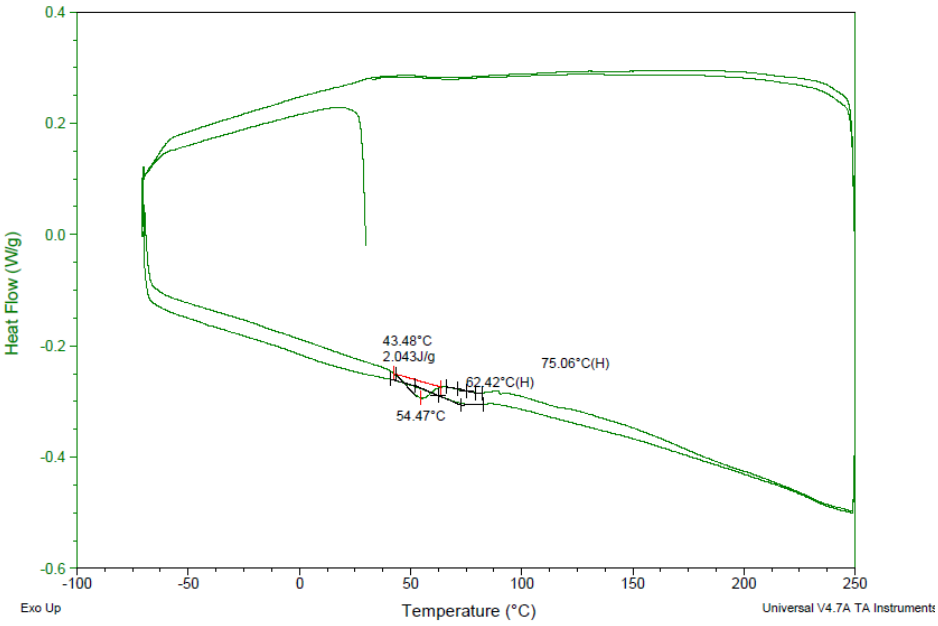

Figure 88. DSC trace of $P(AF)_5M_4=M_4$ with a scan rate of 10 ℃/min performed by TA DSC Q200.

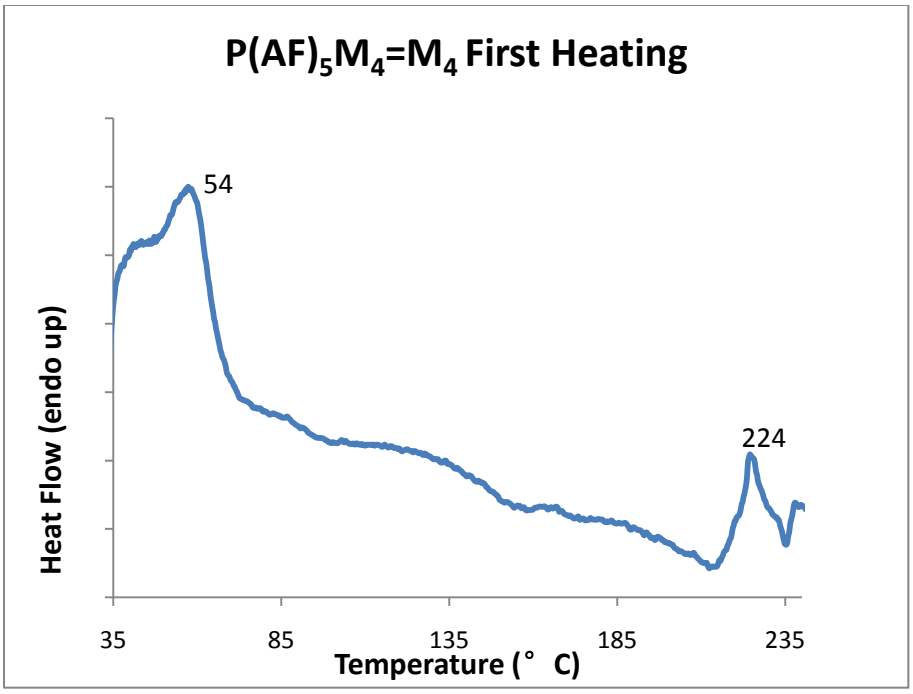

Figure 89. The first heating DSC trace of $P(AF)_5M_4=M_4$ with a scan rate of 10 ℃/min performed by Perkin-Elmer Pyris 6 (2nd heating scan was not well behaved).

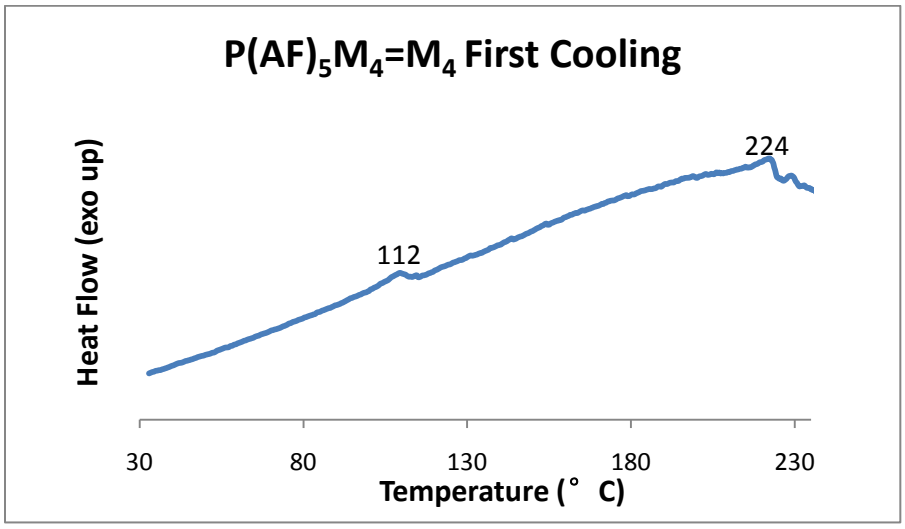

Figure 90. The first cooling DSC trace of $P(AF)_5M_4=M_4$ with a scan rate of 10 ℃/min performed by Perkin-Elmer Pyris 6 (2nd cooling scan was not well behaved).

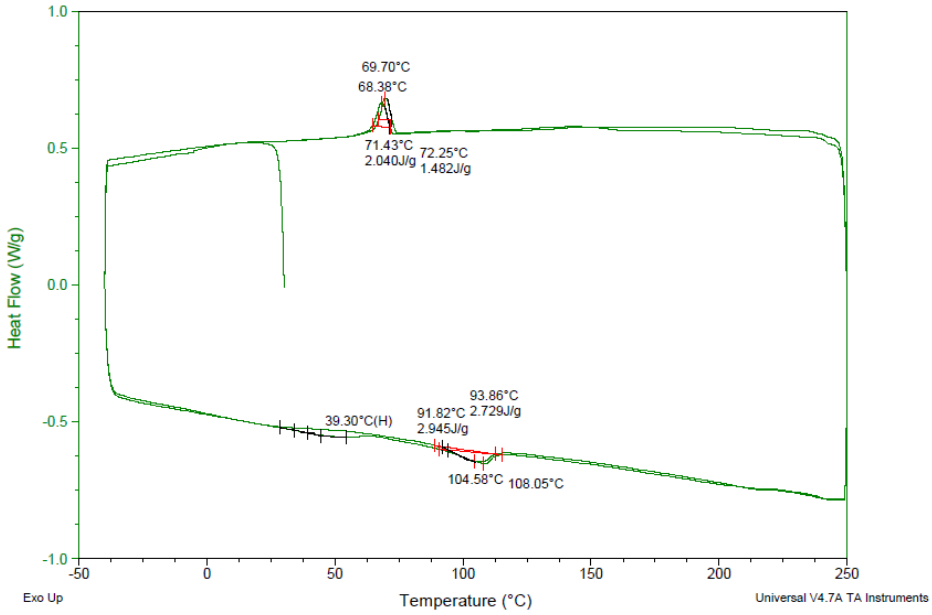

Figure 91. DSC trace of $P(AF)_6M_4=M_4$ with a scan rate of 10 ℃/min performed byTA DSC Q200.

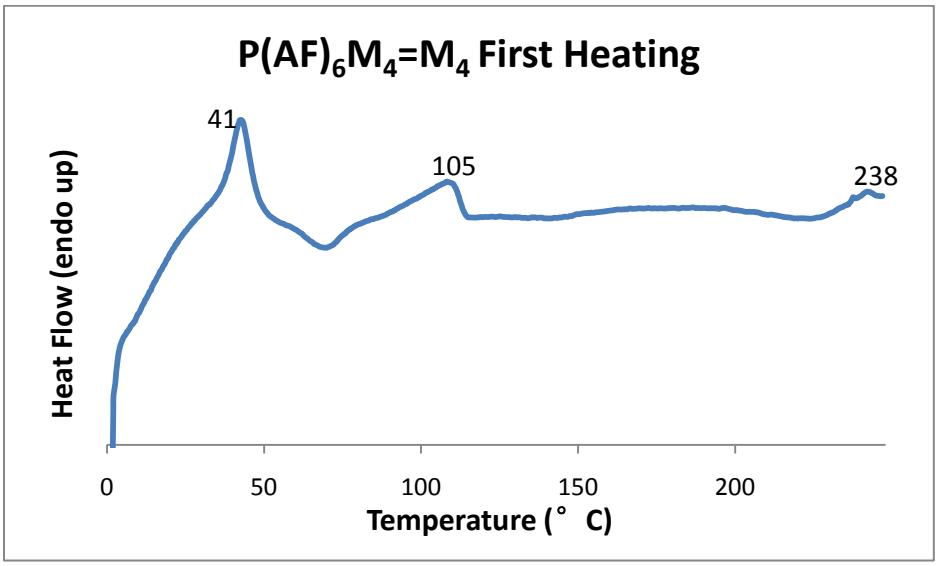

Figure 92. The first heating DSC trace of $P(AF)_6M_4=M_4$ with a scan rate of 10 ℃/min performed by Perkin-Elmer Pyris 6.

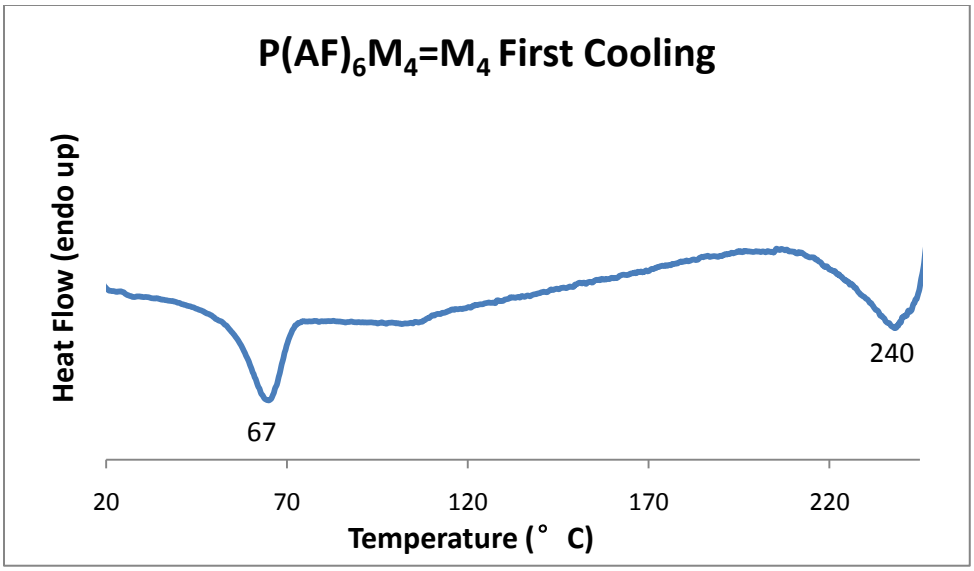

Figure 93. The first cooling DSC trace of $P(AF)_6M_4=M_4$ with a scan rate of 10 ℃/min performed by Perkin-Elmer Pyris 6.

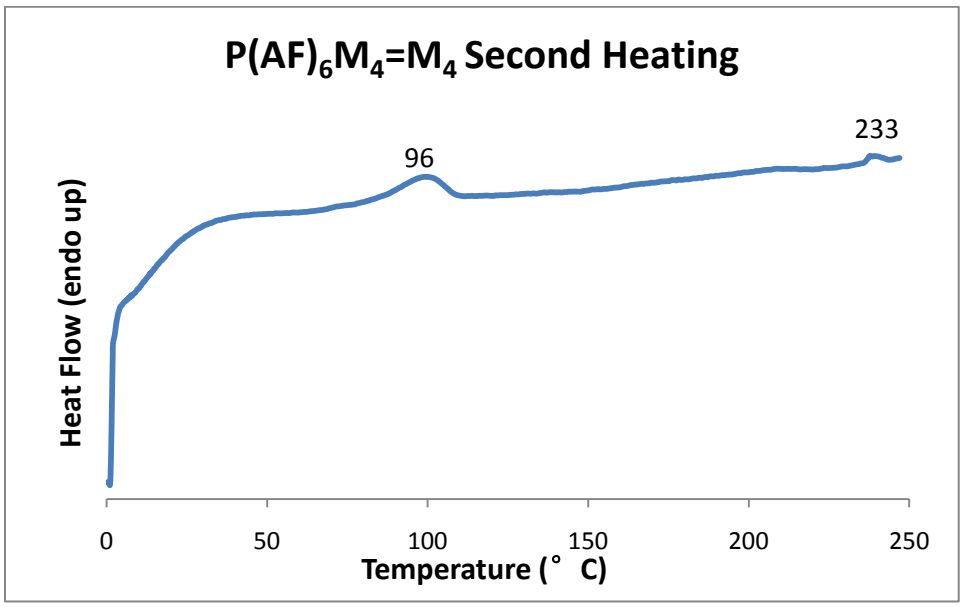

Figure 94. The second heating DSC trace of $P(AF)_6M_4=M_4$ with a scan rate of 10 ℃/min performed by Perkin-Elmer Pyris 6.

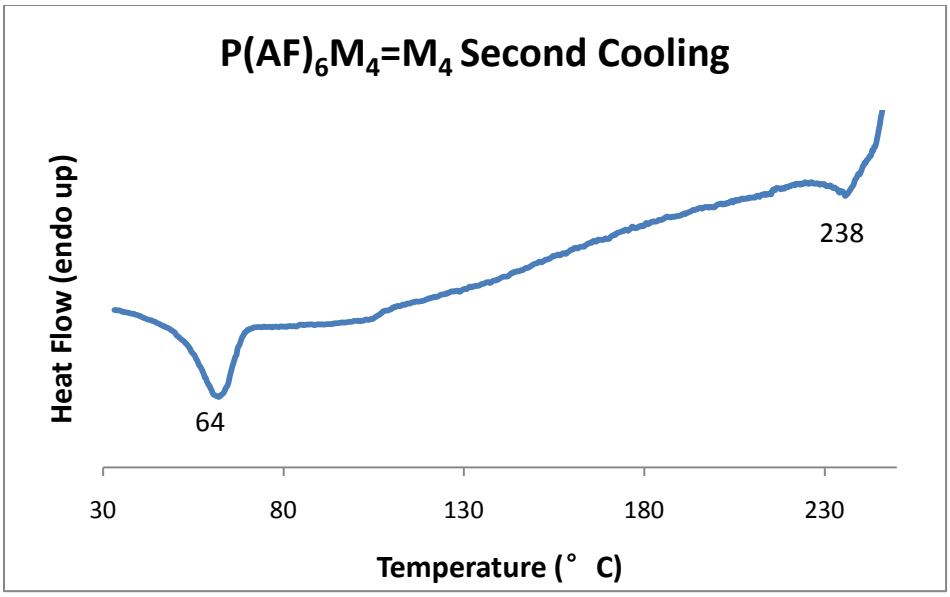

Figure 95. The second cooling DSC trace of $P(AF)_6M_4=M_4$ with a scan rate of 10 ℃/min performed by Perkin-Elmer Pyris 6.

BIBLIOGRAPHY

[1] Copenhafer, J. E.; Walters, R. W.; Meyer, T. Y., Synthesis and Characterization of Repeating Sequence Copolymers of Fluorene and Methylene Monomers. *Macromolecules* **2008,** 41, (1), 31-35.

[2] Walters, R.W. Dissertation Repeat Sequence Fluorene-Co-Methylene Polymers and Phosphorescent Mercury Sensors.

[3] Knnapila, M.; Winokur, M. J., Structure and Morphology of Polyfluorenes in Solutions and the Solid State. *Adv. Polym. Sci* **2008**, 212, 227-272.

[4] Heeney, M.; Bailey, C.; Giles, M.; Shkunov, M.; Sparrowe, D.; Tierney, S.; Zhang, W.; McCulloch, I., Alkylidene Fluorene Liquid Crystalline Semiconducting Polymers for Organic Field Effect Transistor Devices. *Macromolecules* **2004,** 37, (14), 5250-5256.

[5] Grisorio, R.; Mastrorilli, P.; Ciccarella, G.; Suranna, G. P.; Nobile, C. F., Synthesis and optical behaviour of monodispersed oligo(fluorenylidene)s. *Tetrahedron Letters* **2008,** 49, (13), 2078-2082.

[6] Yamamoto, T.; Morita, A.; Miyazaki, Y.; Maruyama, T.; Wakayama, H.; Zhou, Z. H.; Nakamura, Y.; Kanbara, T.; Sasaki, S.; Kubota, K., Preparation of pi-conjugated poly(thiophene-2,5-diyl), poly(p-phenylene), and related polymers using zerovalent nickel complexes. Linear structure and properties of the pi-conjugated polymers. *Macromolecules* **1992,** 25, (4), 1214-23.

[7] Miyaura, N.; Suzuki, A. *Chem. Rev.* **1995**, 95, 2457-2483.

[8] Wallace, J. U.; Chen, S. H., Fluorene-based conjugated oligomers for organic

photonics and electronics. *Adv. Polym. Sci.* **2008,** 212, (Polyfluorenes), 145-186.

[9] Scherf, U.; List, E. J. W., Semiconducting polyfluorenes - towards reliable structure-property relationships. *Adv. Mater.* **2002,** 14, (7), 477-487.

[10] Forrest, S. R.; Thompson, M. E., Introduction: Organic Electronics and Optoelectronics. *Chem. Rev.* **2007,** 107, (4), 923-925.

[11] Grimsdale, A. C.; Leok Chan, K.; Martin, R. E.; Jokisz, P. G.; Holmes, A. B., Synthesis of Light-Emitting Conjugated Polymers for Applications in Electroluminescent Devices. *Chem. Rev.* **2009,** 109, (3), 897-1091.

[12] Tang, C. W.; van Slyke, S. A. Appl. Phys. Lett. 1987, 51, 913.

[13] Tang, C. W. Appl. Phys. Lett. 1986, 48, 183.

[14] Allard, S.; Forster, M.; Souharce, B.; Thiem, H.; Scherf, U., Organic semiconductors for solution-processable field-effect transistors (OFETs). *Angew. Chem., Int. Ed.* **2008,** 47, (22), 4070-4098.

[15] Murphy, A. R.; Frechet, J. M. J., Organic Semiconducting Oligomers for Use in Thin Film Transistors. *Chem. Rev.* **2007,** 107, (4), 1066-1096.

[16] Collings, P.,Hird, M. (1997) Introduction to Liquid Crystals Chemistry and Physics (Taylor&Francis)

[17] Watson, M. D.; Wagener, K. B., Ethylene/Vinyl Acetate Copolymers via Acyclic Diene Metathesis Polymerization. Examining the Effect of "Long" Precise Ethylene Run Lengths. *Macromolecules* **2000,** 33, (15), 5411-5417.

[18] Tindall, D.; Wagener, K. B., Acyclic Diene Metathesis (ADMET) Segmented Copolymers. *Macromolecules* **2004,** 37, (9), 3328-3336.

[19] Schwendeman, J. E.; Church, A. C.; Wagener, K. B., Synthesis and catalyst issues associated with ADMET polymerization. *Adv. Synth. Catal.* **2002,** 344, (6+7), 597-613.

[20] Chung, T. C., Synthesis of polyalcohols via Ziegler-Natta polymerization. *Macromolecules* **1988,** 21, (4), 865-9.

[21] Pankaj, S., Beiner, M. Side chain crystallization and non-equilibrium phenomena in nanophase seperated by poly(3-alkyl thiophenes). *Vth International Conference on Times of Polymers (TOP) and Composites.*